

UNCLASSIFIED

AD 284 082

*Reproduced
by the*

**ARMED SERVICES TECHNICAL INFORMATION AGENCY
ARLINGTON HALL STATION
ARLINGTON 12, VIRGINIA**



UNCLASSIFIED

NOTICE: When government or other drawings, specifications or other data are used for any purpose other than in connection with a definitely related government procurement operation, the U. S. Government thereby incurs no responsibility, nor any obligation whatsoever; and the fact that the Government may have formulated, furnished, or in any way supplied the said drawings, specifications, or other data is not to be regarded by implication or otherwise as in any manner licensing the holder or any other person or corporation, or conveying any rights or permission to manufacture, use or sell any patented invention that may in any way be related thereto.

62-500

40

AD No. 284 082

ASTIA FILE COPY

TRANSACTIONS OF THE A. I. VOYEKOVA MAIN
GEOPHYSICAL OBSERVATORY

By

Various Authors

40

AD No. 284 082
ASTIA FILE COPY

TRANSACTIONS OF THE A. I. VOYEKOVA MAIN
GEOPHYSICAL OBSERVATORY

By

Various Authors

ASTIA
RECEIVED
SEP 21 1962
RECEIVED
TISIA C

28 4082

UNEDITED ROUGH DRAFT TRANSLATION

TRANSACTIONS OF THE A.I. VOYEKOVA MAIN
GEOPHYSICAL OBSERVATORY

BY: Various Authors

English Pages: 133

SOURCE: Trudy Glavnoy Geofizicheskoy Observatorii
imeni A. I. Voyekova, No. 101, Gidrometeoizdat,
Leningrad, 1959, 75 pp.

THIS TRANSLATION IS A RENDITION OF THE ORIGINAL FOREIGN TEXT WITHOUT ANY ANALYTICAL OR EDITORIAL COMMENT. STATEMENTS OR THEORIES ADVOCATED OR IMPLIED ARE THOSE OF THE SOURCE AND DO NOT NECESSARILY REFLECT THE POSITION OR OPINION OF THE FOREIGN TECHNOLOGY DIVISION.

PREPARED BY:

TRANSLATION SERVICES BRANCH
FOREIGN TECHNOLOGY DIVISION
WP-AFB, OHIO.

TABLE OF CONTENTS

	PAGE
1. Experimental Application of the Method of Mathematical Statistics to Microstructural Fog and Cloud Research, by P. V. Dyachenko.....	1
2. Results of an Analysis of a Wind Tunnel Used in a Main Geophysical Observatory, by P. V. D'yachenko and A. I. Kameneva.....	79
3. Testing of Hand Anemometers at the Plant, by A. I. Kameneva.....	104
4. Errors of Thermoelectric Balancometer Testing, by A. I. Pokrovskaya.....	110

ANNOTATION.

This symposium contains materials on improved verification techniques for individual meteorological instruments, more precise definition of their parameters, and also on methods of increasing the accuracy and precision of certain meteorological investigations.

The symposium is intended for use by specialists engaged in precision tool engineering and meteorological research.

FTD-TT-62-500/1+2

EXPERIMENTAL APPLICATION OF THE METHOD OF MATHEMATICAL
STATISTICS TO MICROSTRUCTURAL FOG AND CLOUD RESEARCH.

by P.V. Dyachenko.

This paper describes the results of an inquiry into the problem of fog and cloud particle size determination from the viewpoint of statistical probability.

The materials contained in the paper make it possible to improve considerably the accuracy and precision of investigations relating to the microstructure of fog and clouds.

Polydispersity is a general and integral property of natural fogs and clouds. So far this fact has never been questioned in any modern work devoted to the microphysics of fog and clouds. Only the positions taken by I.P. Smirnov in his article reviewed in detail by this author on an earlier occasion present an isolated exception.

The unquestionable polydispersity of natural fog and clouds entails the requirement for a consistent approach to the problem of size determination of ^{the} particles which form them from the positions of statistical probability.

The statistical inconsistency manifested by some authors engaged in microphysical studies of clouds is responsible for a considerable number of inaccuracies and errors.

Houghton /31/, for example, has introduced a new method for plotting experimental distribution curves, different from the method which is considered classical and is employed in Europe and the USSR. This has caused not only Houghton himself, but also a number of other investigators who have accepted his conclusions without a critical analysis, to develop erroneous theories /2, 16, 27/.

A physically well substantiated selection of one or another mean size suited for a given problem is essential for microphysical investigations of fog and clouds. Analysis of ^{the practiced} application of the mean sizes in fog and cloud microphysics shows that with a rare exception /10/ the mean sizes are improperly used.

FTD-TT-62-500/1+2

1

Of no lesser importance is the matter of determining ^{those} values for the width of the interval (^{class}) and the volume of the sample of the investigated set of particles which could assure a given statistical accuracy of the measurement results. The absence of this type of criteria has lead in several cases to the appearance of statistically inadequate data (27), (28).

Special attention was devoted by us to H. Köhler's ideas on the relationship of masses (33). It is well known that on the basis of a statistical analysis of the results of his observations Köhler has formulated a hypothesis ^{about} the predominant coalescence of equal-size drops. From the statistical viewpoint this hypothesis did not seem to give rise to any objections. It is known that in his work Köhler has thanked the famous English statistician, K. Pearson, for his assistance in dealing with problems of mathematical statistics arising in the development of Köhler's ideas. Köhler's theory has found a large number of supporters; it was presented in many textbooks, and was given further substantiation in certain scientific papers (16), (22) in the form of "the law of multiple masses".

In our work we were oriented by the guiding ideas of Prof. P.N. Tverskoy, which are, possibly, unique in our own and foreign literature (19). He doubted the correctness of Köhler's hypothesis and wrote thus about the multiple relationship of masses: "Hence, it is necessary to look for some other possible explanation of the indicated observed fact, or -- in questioning its realism -- to expose it to verification by means of new observations with the aid of more accurate methods than those employed until now" (page 29).

In the light of the results obtained by us, it became clear that Köhler has made his basic errors precisely in dealing with the statistical problem where his views remained unchallenged.

An important connection between the character of experimental distribution and the form of the investigated cloudiness was repeatedly established in the papers published by several authors (1,7,15,16,22, 28, and others). It is obvious that more precise data in this respect will be forthcoming only after the accuracy of measurements has been subsequently improved. This, on the other hand, calls for higher standards in the technique of observation and the treatment of the results. In fact, the objective of this work is to provide the technique for experimental ^{particle size}/determination [REDACTED] in a polydisperse system with such statistical substantiation as would contribute to further development of sampling methods for observation of natural fog and cloud particles.

Along with the solution of this principal problem, it became possible for us to subject to critical analysis a number of ideas, familiar in fog and cloud microphysics, which are actually wrong.

In addition to the generally known positions of mathematical statistics, we have utilized in our work and developed in application to the requirements of the problem at hand the ideas of A.K. Mitropol'skiy (12) on the envelopes of errors, on the character of experimental distributions, the requirements they are supposed to meet, and so on, and also the ideas formulated by V.I. Romanovski (13) on the mean values and their meaning.

The dimensionless method was used in presenting all the materials in this paper. As a result of this we have succeeded without too much of a difficulty in introducing a few considerations a more precise defining of which proves to be rather cumbersome in terms of conventional treatment.

The present article reports the results of a thesis study /5/ prepared under the guidance of Professor P.N. Tverskoy and defended in 1950.

1. Method of Experimental Distribution Curve Construction.

Whereas in the USSR and in Europe it is customary to construct size distribution curves for fog and cloud particles, the standard practice in the U.S. is to deal in terms of the, so called, "volume

distribution". The latter method is developed mainly in Houghton's works (31). Initially (in 1932) he also used to plot size distribution curves, and it^{is} only later (in 1938), and without sufficient substantiation of his reasons^{over} [redacted], that he has switched to the new method of curve construction. This fact was duly registered by Ye.S. Selezneva (16) and B.V. Kiryukhin (9) in their papers. However, erroneous ideas still continue to appear in the studies of some European authors. These ideas are similar to those revealed by Ye.S. Selezneva (16) in M. Diem's writings (27) wherein the author assumed that the American fogs consist of larger particles. In Gertner's book (2) one finds the following lines: "It is difficult to understand from Houghton's works why is it that in his more recent fog investigations he has found the predominant size of drops to be about $\rho = 25$ microns, while in his first paper the highest maxima were registered at $\rho = 3.1, 6.2, 9.3$ microns. Whereas his earlier measurements are in agreement with the measurement results of other investigators, no such correspondence is to be recorded with respect to his new measurements" (page 63).

A comparison of the two mentioned methods to determine their characteristics, merits, and disadvantages, no doubt, appears to be interesting. Before considering the differences between the two methods of experimental curve construction, we shall dwell for awhile on certain possible methods of distribution curve plotting for a certain set of real particles.

For this purpose we shall first analyse a unimodal distribution of particles described by a given generalized variate τ .

For a ^{discrete} [redacted] variate τ , which is numerically equal to

$$\tau = \frac{t}{t_0}, \quad (1)$$

where ^{continuous} t - [redacted] variate, and t_0 - its most probable dimensional value, a distribution takes place which for a set of N particles may

in a general case be written as

$$\frac{dN}{N} = n(\tau) d\tau, \quad (2)$$

where $\frac{dN}{N}$ is the ^{occurrence} probability of a particle with the variate value ranging from τ to $\tau + d\tau$; $n(\tau)$ being an arbitrary function satisfying the following conditions:

- a) $\int_0^{\infty} n(\tau) d\tau = 1;$ (2^a)
- b) the single solution of equation $\frac{dn(\tau)}{d(\tau)} = 0$ is root $\tau = 1$ corresponding to the most probable value of t_0 ;
- c) function $n(\tau)$ is continuous, single-valued, and positive over the interval $0 < \tau < \infty$.

Ratio (2) is a differential expression of the law governing the distribution of the analyzed variate in the investigated set of particles. On drawing a random sample of finite volume comprising N_k particles from such a set, we shall obtain N_k values of the variate which form an experimental distribution. From the physical point of view this distribution may be considered as continuous since with increasing volume of the sample it may be as near to such a distribution as desired. In dividing this distribution into intervals of finite width, it is possible for the distribution of the variate to obtain frequencies n_1 or relative frequencies $\frac{n_1}{\sum n_1}$, which correspond to the mid-points of the intervals. An experimental distribution obtained in this manner is usually represented graphically in the form of a stepped curve (or frequency polygon). Plotted along the X-axis are the variate values, and along the Y-axis - the frequencies and relative frequencies. The distributions which satisfy (2), if graphically represented, appear to be centered, i.e. their modes are being reduced to the unit value of the ^{discrete} variate. All the means and the sizes of the intervals may be measured in fractions of the most probable variate value for a given population.

A dimensionless presentation, therefore, considerably simplifies the possible comparison of individual distributions regardless of the method of their assignment. Henceforward we shall use the method of dimensionless presentation and resort to dimensional statements only when necessary, mainly with respect to the final results.

The basic mean values which interest us may be calculated from the following formulas:

the arithmetic mean value of the variate

$$\bar{\tau}_1 = \int_0^{\infty} n(\tau) \tau d\tau \cong \frac{\sum n_i t_i}{t_0 \sum n_i}, \quad (3)$$

the mean square value

$$\bar{\tau}_2 = \sqrt{\int_0^{\infty} n(\tau) \tau^2 d\tau} \cong \frac{1}{t_0} \sqrt{\frac{\sum n_i t_i^2}{\sum n_i}}, \quad (4)$$

the mean cubic value

$$\bar{\tau}_3 = \sqrt[3]{\int_0^{\infty} n(\tau) \tau^3 d\tau} \cong \frac{1}{t_0} \sqrt[3]{\frac{\sum n_i t_i^3}{\sum n_i}}. \quad (5)$$

In restricting ourselves to the above mean values, we shall pass on directly to an analysis of the main possible methods of constructing experimental curves which may be plotted in investigating a set of real particles.

Distribution of Sizes.

If in formula (1) we assume

$$\tau = \rho = \frac{r}{r_0}, \quad (6)$$

where r is the radius of the particles in a set, r_0 - the most probable radius, we obtain a size distribution

$$\frac{dN}{N} = n(\rho) d\rho. \quad (7)$$

Function $n(\rho)$ in (7) will continue to satisfy the conditions (2). The method of experimental curve construction adopted in the Soviet Union and in Europe corresponds to such a distribution. Here the pure variate values -- the particle radii r (or diameters) -- are plotted against the X-axis, while the frequencies or relative frequencies for the experimental curves, and the probabilities for the distributions given in the differential form, are plotted against the Y-axis.

Expressions for the size distribution means may be obtained from (3), (4), and (5), by replacing in them τ ~~by~~ ρ . They assume the form:

the arithmetic mean size distribution radius

$$\bar{\rho}_1 = \int_0^{\infty} n(\rho) \rho d\rho \cong \frac{\sum n_i r_i}{r_0 \sum n_i} \quad (8)$$

the mean square radius

$$\bar{\rho}_2 = \sqrt{\int_0^{\infty} n(\rho) \rho^2 d\rho} \cong \frac{1}{r_0} \sqrt{\frac{\sum n_i r_i^2}{\sum n_i}} \quad (9)$$

the mean cubic radius

$$\bar{\rho}_3 = \sqrt[3]{\int_0^{\infty} n(\rho) \rho^3 d\rho} \cong \frac{1}{r_0} \sqrt[3]{\frac{\sum n_i r_i^3}{\sum n_i}} \quad (10)$$

More detailed information on ~~size~~ size distribution based on the method of experimental curve construction resulting from this distribution, as well as the data on the ~~size means~~ of distribution (7) will be discussed below in the corresponding sections devoted to this problem. Here we shall only state that the mean values (8), (9), and (10) have an entirely definite physical meaning and constitute important physical characteristics of distribution (7).

Distribution of Surface Areas.

In passing over to a new ~~discrete~~ discrete variate s , numerically equal to the ratio of the particle surface (sectional area) to the most probable value of this surface s_0 , we shall obtain a distribution of surface areas:

$$\frac{dN}{N} = n(s) ds. \quad (11)$$

The experimental curve for this distribution may also be represented in the form of a stepped curve or frequency polygon. As in the previous case the frequencies and relative frequencies are plotted against the Y-axis. Distribution (11) has its own system of mean values.

The arithmetic mean particle surface is equal to

$$\bar{s}_1 = \int_0^{\infty} n(s) s ds \cong \frac{4\pi \sum n_i r_i^2}{s_0 \sum n_i} \quad (11^a)$$

and coincides numerically, as it is easy to see, with the surface area of a particle having mean quadratic size distribution radius (9).

The mean square surface are^a of the particle

$$\bar{s}_2 = \sqrt{\int_0^{\infty} n(s) s^2 ds} \cong \frac{4\pi}{s_0} \sqrt{\frac{\sum n_i r_i^4}{\sum n_i}} \quad (11^b)$$

and the mean cubic surface area

$$\bar{s}_3 = \sqrt[3]{\int_0^{\infty} n(s) s^3 ds} \cong \frac{4\pi}{s_0} \sqrt[3]{\frac{\sum n_i r_i^6}{\sum n_i}} \quad (11^c)$$

have no simple and obvious physical meaning, so that their use as physical characteristics presents no interest. The mode of surface area distribution and the only mean s_1 , which has an obvious physical meaning for skewed distributions, do not coincide. The method of experimental curve construction based on the utilization of surface area distributions has found no application, mainly due to the absence of an obvious physical meaning of the means.

Distribution of Volumes.

In a similar way, through replacement of v for τ (dimensionless volume), it is possible to obtain a volume distribution for a given set of particles from ratio (2):

$$\frac{dN}{N} = n(v) dv \quad (12)$$

with the same conditions for $n(v)$, as in (2). By analogy with the preceding cases the dimensionless volume v is equal to the ratio of the volume of particle $\frac{4\pi r^3}{3}$ to its most probable value v_0 .

The volume distribution means of (12) turn out to be equal to

$$\bar{v}_1 = \int_0^{\infty} n(v) v dv \cong \frac{4\pi \sum n_i r_i^3}{3v_0 \sum n_i} \quad (13)$$

for the arithmetic mean of the particle volume;

$$\bar{v}_2 = \sqrt{\int_0^{\infty} n(v) v^2 dv} \cong \frac{4\pi}{3v_0} \sqrt{\frac{\sum n_i r_i^6}{\sum n_i}} \quad (13^a)$$

for the mean square volume, and

$$\bar{v}_3 = \sqrt[3]{\int_0^{\infty} n(v) v^3 dv} \cong \frac{4\pi}{3v_0} \sqrt[3]{\frac{\sum n_i r_i^9}{\sum n_i}} \quad (13^b)$$

for the mean cubic volume of particle.

The arithmetic mean volume \bar{v}_1 is numerically equal to the volume of a particle having the mean cubic size distribution radius (10). The remaining means, as in the preceding case, have no obvious physical meaning and are, therefore, of no practical interest. The ^{sole} meaningful mean volume \bar{v}_1 may be obtained only through computations from

formulae (10) and (13) and in a general case does not coincide with mode v_0 of volume distribution. Plotting of experimental curves according to this, and the preceding, methods is, for obvious reasons, of no practical research interest, since there is no advantage in producing a distribution with only one mean value which is present in size distribution.

In conclusion we shall revert to the method of experimental curve construction adopted in Houghton's papers.

Houghton's experimental curves differ from the volume distribution curves analyzed above mainly in that he plots the linear particle dimensions (diameters) along the X-axis, and not the volumes. This fact does not essentially affect the matter since it is the volume that functions as the variate in Houghton's distribution. An experimental curve constructed by Houghton's method represents a ^{empirical} distribution in which the values of the volume as the variate are divided into intervals whose width (in terms of volume) is not constant. This can be readily seen if along with a linear size scale, one should plot against the X-axis of Houghton's curve also a scale of volumes which will prove to be non-uniform.

According to statistical requirements the width of the X-axis intervals (classes) must be the same in any ^{given} distribution. The values of the distribution variate plotted along this axis must be of equal magnitude. In his method Houghton has violated this important condition.

Quantities which have the dimensionality of the ^{variate} (volume) may be plotted against the Y-axis of Houghton's curves, this is wrong. In speaking of statistical distributions A.K. Mitropol'skiy (12) makes this quite definite statement: "The values of a statistical quantity represented along the X-axis are as a general rule concrete numbers, for example, centimeters of growth, kilograms of weight, and so on. And by contrast, the frequencies represented along the Y-axis are always abstract numbers indicating how many times that or another value of

of the statistical quantity was encountered". In Houghton's curves, whenever one turns to the frequencies, the Y-axis becomes dimensional and this cannot be considered correct.

Therefore, strictly spoken, Houghton's curves cannot be regarded as experimental from a statistical point of view. Furthermore, the system of the means, as it logically follows from the above discussion, is absent in Houghton's method.

Instead of mean volume \bar{v}_1 , or the corresponding radius \bar{r}_3 , Houghton utilized a mean size which, as it will be shown later on, is the mean size of distribution (7) having no direct bearing on the distribution of volumes.

In the light of the aforesaid we arrive at the obvious conclusion that the method of experimental curve construction in the form in which it is presented in Houghton's papers /31/ is in its very essence statistically inconsistent. At the same time, the method adopted in the USSR and Europe, and known to be classical, does not contradict the basic principles of mathematical statistics. This is the reason why only problems related to research in size distribution will be discussed further in this text.

2. Peakedness and Height of the Distribution Curves.

The character of experimental distributions produced as a result of natural fog and cloud particle size measurements is, as a rule, described (also in discussing the peakedness of curves in which we are interested) mainly from the qualitative point of view /16/. We know only of one attempt at quantitative estimate made by Houghton /31/. He was determining the proportion of the total amount of liquid water represented by drops contained in a 10-micron band centered about the peak of a relative-volume distribution curve. The width of the band consisting of two adjacent intervals -- one of which is situated to the left, the other to the right of the curve maximum -- was made arbitrarily without any substantiation whatever. Most of the measurements were carried out

by Houghton in subdividing the volume distribution into 5-micron intervals (^{in terms of} diameter). Moreover, he has found that the "sharpness" estimated in this manner in terms of percentages varies from 16 to 47, i.e. increasing 3 times, with the most frequently encountered value being 30%.

One might in a similar way estimate the sharpness of ~~th~~ a distribution curve constructed by the method of plotting experimental curves as adopted in the USSR. It would seem sufficient for this purpose to determine the proportion of the particles comprized in the band of fixed size.

Our investigations show that Houghton's test has no direct bearing on the evaluation of the distribution curve peakedness. The discussions in this section actually represent an attempt at developing a new peakedness test suited both for distributions given in a differential form, and for experimental distributions expressed in the form of finite differences.

In accordance with the method adopted in the Soviet Union and Europe for constructing emperic distributions, we shall take the most probable radius r_0 of size distribution (7) as the basic initial size. All other sizes, including thereby any means, we shall measure in units of the most probable radius.

Expression (7) will from now on be considered as the distribution law of a population consisting of an infinite number of particles from which a random sample of limited volume is being taken. With the exception of specially qualified cases, distribution (7) will be assumed as unimodal. Consequently function $n(\rho)$ will have one maximum at $\rho = 1$.

Let it be mentioned in passing that function $n(\rho)$, and only it, may in full determine the character of distribution (7). The distributions with different r_{0A} ^{values} described by one and the same function $n(\rho)$ must have a common peakedness. There can be no inverse effect, i.e. distributions with ^{peaks of} equal height may be described by different functions. This

is the reason for the bounded character of the peakedness characteristic applicable only for purposes of distribution curve comparison in terms of the curve ^{altitude} at the maximum.

It is easy to see that in (7) ratio $\frac{dN}{N}$ represents the probability, while $\frac{dN}{Nd\rho}$ is the probability density at a given point in the distribution curve. The probability density at a given point is understood to mean the probability value related to the unit value of variate ρ . In our case, it turns out to be equal to $n(\rho)$ for distribution (7).

For unimodal distributions which interest us, probability density $n(\rho)$ in accordance with (6) has its own single maximum at point $\rho = 1$ corresponding to the peak of distribution (7). For a characteristic providing a single-valued determination of distribution (7) peakedness we shall use the numerical value of the probability density maximum at the maximum point $\rho = 1$. This value then will be the ^{altitude} of the distribution curve equal to

$$H = n(\rho)|_{\rho=1} = \frac{dN_m}{Nd\rho} \quad (14)$$

or, respectively, in dimensional form when $d\rho = \frac{dr}{r_0}$, in accordance with (6)

$$H = \frac{dN_m r_0}{N dr} \quad (15)$$

where dN_m is the number of particles with sizes ranging from $\rho = 1$ to $\rho = 1 + d\rho$, or (which is the same) from $r = r_0$ to $r = r_0 + dr$.

Expressions (14) and (15) hold only for the case when the distribution is given in a differential form. If we have to deal with an experimental distribution in which the subdivision interval is not infinitesimal, but finite, then formula (15) may be written as

$$\bar{H} = \frac{n_m}{N_k \Delta\rho} \quad (16)$$

where \bar{H} is the value of the curve altitude averaged for an interval of finite width $\Delta\rho$ and is numerically equal to the relative frequency density maximum at this interval; n_m - number of particles measured in the region of interval $\Delta\rho$ maximum; N_k - total number of particles

in k intervals, or the sample volume numerically equal to

$$N_k = \sum_{i=1}^k n_i. \quad (16a)$$

In passing over to dimensional presentation, we obtain a final expression suitable for empiric distribution curve altitude determination, when this distribution has been measured ~~xx~~ over finite intervals $\Delta r = r_i - r_{i-1}$,

$$\bar{H} = \frac{n_m r_0}{N_k \Delta r}. \quad (17)$$

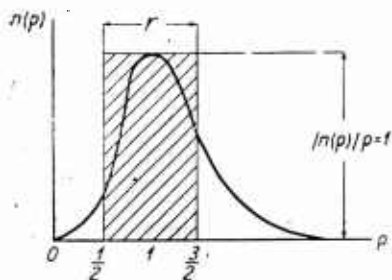


Fig. 1 Curve altitude

Further on we shall analyze the errors arising in consequence of the finiteness of Δp and N_k . In the meantime we shall note only that if the sample volumes are sufficiently large and the intervals small, formula (17) in comparison with the ~~explicit~~ relationship (14) yields such results the inaccuracies of which may be conveniently disregarded.

Thus the numerical value of the curve altitude may be determined from formula (14) for distributions given in differential form, and from (17) for experimental distributions.

In the first case we calculate the probability density maximum, in the second that of the relative frequency density:

$$\frac{n_i}{\Delta p \sum n_i}. \quad (17a)$$

If we construct a rectangle the height of which is equal to the distribution curve maximum (Fig.1), and whose width is assumed to be equal to the most probable radius r_0 , then the ~~ratio of the area~~ of the thus constructed rectangle to that of the curve (the area enclosed between the curve and the X-axis will, for brevity sake, be referred to by us as the curve area) actually characterizes the pointedness of the distribution from the geometrical point of view. This is understandable, when one considers the fact that the probability density in any point of the distribution curve is numerically equal to the area with unit base and an altitude equal to the curve ordinate at a given point, provided the area of the entire curve is regarded as unit area.

One may define $H = \infty$ for distributions with the maximum possible peakedness (monodisperse fog) and $H = 0$ for distributions with minimum peakedness as the limit values for curve altitude to serve as parameters of peakedness. In somewhat forestalling the discussion, we would like to note that, according to the materials covering a large number of experimental distributions relating to fogs and clouds, the most probable curve altitude value turned out to be equal to unity, with deviations rarely exceeding 30% in one or another direction.

A comparison of our criterion with that of Houghton's shows that the method of peakedness evaluation based on the measurement of the proportion of particles, or the percentage of water content, available within a band of fixed width is wrong. The resulting quantity in this case turns out to be dependent on the most probable size, and the size, ¹⁰/₁₁ as it is well known, is subject to much greater changes than the peakedness which interested Houghton. The dependence of Houghton's characteristic on the drop sizes is obvious. Indeed, the area of the entire distribution curve numerically expresses a quantity which is dimensionless. Portions of this area may be estimated only by means of integrals of the following form

$$\int_{p_1}^{p_2} n(\rho) d\rho, \quad (17^b)$$

where p_1 and p_2 are the finite integration limits.

So long as the integration limits p_1 and p_2 are dimensionless, the portions of the distribution curve area will also be dimensionless, but as soon as p_1 and p_2 are replaced by dimensional limits, the curve area portions also assume a dimensionality.

If we should use a dimensional ratio

$$\frac{H}{r_0} = \frac{n_m}{N_k \Delta r} \quad (17^c)$$

to estimate the distribution curve peakedness, we would obtain a criterion possessing all the defects of the ratio used by Houghton. The latter ratio also appears to be varying over a larger range than H , in view of the changing most probable size.

Let us now pass to the relationship between the width of the curve and the height as introduced by us.

For the characteristic of a single peak curve it is customary in mathematics to use the curve's width numerically equal to the difference of abscissae $\rho'' - \rho'$ in which function $n(\rho)$ succeeds in diminishing e times as compared to the maximum value (Fig.2). A comparison of parameter

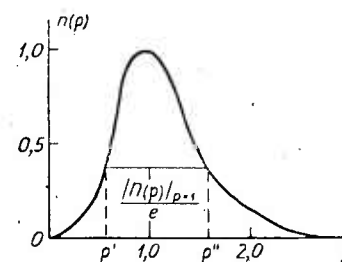


Fig. 2. Width of curve.

H introduced by us and the width of curve $\rho'' - \rho'$ presents an obvious interest. For this purpose we shall revert to the class of distributions originally proposed and used by us (5) in 1950. Its form is

$$\frac{dN}{N} = n(\rho) d\rho = C \rho^m e^{-\frac{m}{n} \rho^n} d\rho, \quad (18)$$

where C is the normalizing distribution constant, and m and n are the parameters of distribution.

It is easy to show that the normalizing constant C is itself a function only of two parameters m and n .

In introducing a new variable

$$z^n = \frac{m}{n} \rho^n, \quad (18^a)$$

it is possible to reduce (18) to

$$C \left(\frac{n}{m} \right)^{\frac{m+1}{n}} \int_0^\infty z^m e^{-z^n} dz = 1, \quad (18^b)$$

but

$$\int_0^\infty z^m e^{-z^n} dz = \frac{1}{n} \Gamma\left(\frac{m+1}{n}\right), \quad (18^c)$$

where $\Gamma\left(\frac{m+1}{n}\right)$ is a known gamma-function.

Consequently,

$$C \left(\frac{n}{m} \right)^{\frac{m+1}{n}} \frac{\Gamma\left(\frac{m+1}{n}\right)}{n} = 1, \quad (18^d)$$

whence

$$C = \frac{n}{\Gamma\left(\frac{m+1}{n}\right)} \left(\frac{m}{n} \right)^{\frac{m+1}{n}}. \quad (18^e)$$

Then the expression for CLASS (18) DISTRIBUTION as a function of only two positive parameters m and n may be presented in the final form as:

$$\frac{dN}{N} = \frac{n}{\Gamma\left(\frac{m+1}{n}\right)} \left(\frac{m}{n}\right)^{\frac{m+1}{n}} \rho^m e^{-\frac{m}{n}\rho^n} d\rho. \quad (19)$$

In accordance with the definition for the
THE CURVE ALTITUDE
class of distributions (19) will appear to be equal to

$$H = \frac{ne^{-\frac{m}{n}}}{\Gamma\left(\frac{m+1}{n}\right)} \left(\frac{m}{n}\right)^{\frac{m+1}{n}} \quad (20)$$

curve

In order to find the width of class (19) we shall write a ratio of the probability density maximum to that value of probability density which is e times smaller than the maximum. On the basis of (19) and (20) this ratio is equal to

$$\frac{e^{-\frac{m}{n}}}{\rho^m e^{-\frac{m}{n}\rho^n}} = e. \quad (21)$$

In transforming (21), we arrive at an equation relative to ρ

$$\rho = e^{\frac{1}{n}\left(\rho^n - \frac{m+n}{m}\right)}. \quad (22)$$

Equation (22) is transcendental with respect to the independent variable ρ and it becomes, therefore, impossible to establish an accurate relation between H and $\rho'' - \rho'$ in a general form. Important for us is the fact that for class (19) curves with curve altitude close to unity (and they are the object of our greatest interest) the product $(\rho'' - \rho')H$ turns out to be a practically invariable quantity. Graphically this fact is demonstrated in Table 1 data calculated for distributions with varying m and n from formulae (14) and (22).

T a b l e 1

№ п/п	$n(\rho)$	ρ'	ρ''	$\rho'' - \rho'$	H	$(\rho'' - \rho')H$
1	$\rho^2 e^{-\rho^3}$	0,398	1,775	1,377	0,83	1,14
2	$\rho^2 e^{-\frac{2}{3}\rho^3}$	0,45	1,566	1,116	1,025	1,15
3	$\rho e^{-2\rho^3}$	0,551	1,537	0,986	1,16	1,14
4	$\rho^5 e^{-\frac{5}{2}\rho^3}$	0,594	1,481	0,887	1,28	1,14
5	$\rho^6 e^{-6\rho}$	0,53	1,69	1,16	0,972	1,13
6	$\rho^3 e^{-3\rho}$	0,39	2,05	1,66	0,675	1,12
7	$\rho^2 e^{-2\rho}$	0,30	2,36	2,06	0,541	1,11

It follows from Table 1 data that the following relationship

$$(\rho'' - \rho') H \cong 1.13, \quad (23)$$

takes place for class (19) distributions if the peakedness is moderate and varies around unity. The meaning of this relationship, as it will be easily perceived, consists in that the unimodal distribution curve area is proportional to the product of the curve's width by its height in the domain of the maximum. We shall note in passing that for a normal Gaussian distribution this product does not differ from that determined by us and is equal to 1.13.

The curve altitude as a parameter of distribution curves, including also the experimental ones, is more convenient for natural fog and cloud particle size investigation than the curve width. This is so, because in the case of experimental distributions the height of the curve may be measured with a considerably lesser number of errors owing to the greater concentration of particles about the maximum.

For the analytically defined distributions the altitude of the curve may also be determined in a simpler way and more precisely than its width.

Should the investigator be interested in the width of the curve, then it would appear to us more effective for him to determine it by method of calculation from the approximate formula:

$$\rho'' - \rho' \cong \frac{1.13}{H} \cong \frac{1.13 N_k \Delta r}{n_m r_0}, \quad (23^a)$$

ensuing from (17) and (23). In general, however, it is far better to deal directly with the altitude of the curve.

In conclusion we shall estimate the peakedness of experimental curves. We have utilized the distributions produced by A.M. Borovikov (1) to serve as experimental material. These curves were plotted by him on the basis of observations carried out in different forms of clouds. Shown in

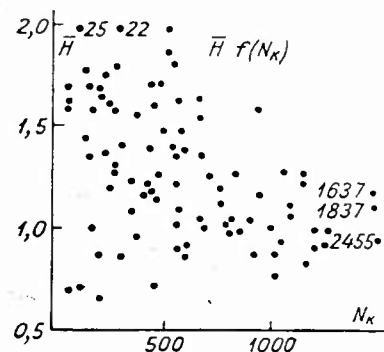


Fig.3. Peakedness of experimental curves

Fig. 3 is a graph illustrating the effect of the sample volume N_k on the magnitude of the factor calculated from formula (17). From the graph's data it appears that the most probable value is that of $\bar{H} = 1$ with deviations practically not exceeding $\pm 30\%$ for distributions with a large sample volume. No substantial effect of the cloud particle size was to be registered.

Thus, the height of the curve is a characteristic which is constant for natural fog and cloud particle size distributions, provided the volume of the experimental distribution sample is sufficiently large.

This characteristic is auxiliary and will be repeatedly utilized in the further development of the discussion.

3. Effect of the Finiteness of the Interval Width.

It is well known that any large population consisting of an infinite number of particles, whose sizes may interest us, may be characterized by an experimental curve (stepped curve or frequency polygon) ^{REFLECTING THE DISTRIBUTION} with any pre-assigned accuracy, if the size measurements effected in the form of random sampling are carried out for a sufficiently large number of particles, with the width of the interval being sufficiently small. In spite of a considerable progress achieved in the practice of natural fog and cloud particle size measurement, both these requirements are not always satisfied to a sufficient degree. There occur measurements in which the total number of particles $N_k = \sum n_i$ is too small (27), (28), and the width of the interval is unnecessarily large (29). This leads to appreciable errors which were not studied with respect to cloud and fog particle distributions.

An investigation of the ^{problem of how the/} finiteness of the interval width ^{affects} ~~the~~ ^{as a whole} construction of an experimental distribution curve ~~does not appear to us to be fundamentally possible. Hence we shall restrict ourselves to an analysis of a distribution curve peak statistically so~~ ^{filled} ~~that the limitedness of the sample volume may be totally disregarded.~~

We shall consider the curve altitude (the concept of which was defined in the preceding section) as the investigated characteristic whose magnitude depends substantially on the width of the interval.

If we denote by $\bar{H}_{\Delta p}$ the height of distribution (7) investigated on the basis of the data resulting from an infinite sample by way of dividing it into intervals of finite width Δp , then, obviously,

$$\bar{H}_{\Delta p} < H, \quad (24)$$

where H is the height of the curve of the same distribution calculated from the ^{precision} formula (14) in the assumption that the width of the interval is infinitesimal.

Inequality (24) turns into equation

$$\bar{H}_{\Delta p} = H \quad (25)$$

only with vanishing Δp .

This means that in particle size measurement involving any unimodal distribution (7) by subdividing it into intervals of finite width Δp , no matter how large the sample volume, there occurs a distortion or deformation of the experimental curve as compared to the curve of a distribution given in differential form and corresponding to the population distribution. The immediate objective of this section actually is to determine the magnitude of this deformation which in the main boils down to the lowering of the maximum depending on the width of the interval. This problem is equivalent to an evaluation of the error arising from the utilization of equation (25) instead of inequality (24).

Remembering that n_m is the number of particles measured in the vicinity of the maximum in interval Δp , we shall find the expression for n_m for the case of distribution (7). Pursuant to the definition

$$n_m = N \int_1^{1+\Delta p} n(p) dp. \quad (26)$$

Then formula (7), with consideration of (26), may be rewritten in the form of

$$\bar{H}_{\Delta p} = \frac{\int_1^{1+\Delta p} n(p) dp}{\Delta p}, \quad (27)$$

where $\bar{H}_{\Delta p}$ is the curve altitude of a distribution distorted owing to the finiteness of the interval width.

In utilizing (14) for H and (27) for $\bar{H}_{\Delta p}$ we shall compose an expression for the maximum possible relative error in determining the curve altitude:

$$\frac{\Delta H}{H} = \frac{H - \bar{H}_{\Delta p}}{H} = 1 - \frac{\int_1^{1+\Delta p} n(\rho) d\rho}{\Delta p |n(\rho)|_{\rho=1}} \quad (28)$$

THE MAGNITUDE OF ERROR $\frac{\Delta H}{H}$ On the basis of quite obvious considerations, depends on the position occupied by the ordinate of the distribution (7) maximum (the distribution mode) in the arbitrarily selected, and, therefore, also arbitrarily superimposed, interval of Δp width. The integration limits in (26) are so selected as to assure that formula (28) should correspond to the case of maximum possible error which takes place when the mode of distribution (7) coincides with the boundary of two adjacent intervals.

Of the two possible intervals we select the right-hand one, since measurements of the fine particles in the left-hand interval are not always reliable. Moreover, it is interesting to investigate the case involving intervals the width of which is comparable to r_0 and larger than it. This, however, is possible only for intervals situated to the right from the mode.

With reference to the character of experimental distributions Ye.S. Selezneva (16) writes: "Most cloud forms are characterized by distribution curves with single distinct maximum. The structural distinctions are manifested in the sharpness of the maximum and the nature of ^{skewness} ~~skewness~~: sometimes these curves are narrow, almost symmetrical; in other cases the maximum is smoothed out and the curve shows a sharp ^{skewness} ~~skewness~~ in the direction of large drops" (page 36). To obtain a dependence $\frac{\Delta H}{H} = f(\Delta p)$ it is necessary to apply ^a concrete distribution law to (28) and then such one of them which corresponds to the most symmetrical experimental distributions. In the capacity of such a law we have utilized the size ~~size~~

distribution

$$\frac{dN}{N} = 2\rho^2 e^{-\frac{2}{3}\rho^3} d\rho, \quad (29)$$

which constitutes a particular case of class (19) for $m = 2$ and $n = 3$. It has already been used for some theoretical calculations by N.S. Shishkin (23) in the form of volume distribution and compared with experimental data. This distribution in terms of peakedness ($\bar{H} = 1.025$) and the absence of distinctly expressed ~~skewness~~ is quite suitable for our purposes.

In substituting the expression for probability density from distribution (29) into (28)

$$n(\rho) = 2\rho^2 e^{-\frac{2}{3}\rho^3}, \quad (29^a)$$

as well as the maximum probability density value

$$|n(\rho)|_{\rho=1} = 2e^{-\frac{2}{3}}. \quad (29^b)$$

After integration and transformation we obtain

$$\frac{\Delta H}{H} = \frac{2\Delta\rho - 1 + e^{-2\Delta\rho \left(1 + \Delta\rho + \frac{\Delta\rho^2}{3}\right)}}{2\Delta\rho}. \quad (30)$$

Formula (30) gives the expression for the maximum possible relative error in the determination of the curve altitude, which arises as a result of the finiteness of the interval width. This formula holds only for distributions similar to the model distribution (29) in terms of peakedness. Given below in Table 2 is the dependence of the experimental distribution curve compression on the magnitude of interval $\Delta\rho$, where $\frac{\Delta H}{H}$ values are calculated from formula (30).

The results of the first half of the table for the case when $0.1 \leq \Delta\rho \leq 0.5$ are represented in Fig. 4 in the form of a curve of relative errors accompanied by experimental data (points) obtained from the experimental curves produced by A.M. Borovikov (1).

As it may be seen from the graph, measurement of fog and cloud particle sizes with utilization of intervals comparable in width with the magnitude of the most probable radius may lead in individual cases to considerable errors in the region of the maximum. On the contrary, if $\Delta\rho \approx 0.2 - 0.25$ the errors do not exceed 4 - 7%. Findeisen (29)

has plotted experimental curves in which the interval width exceeds the magnitude of the most probable size r_0 . For some of his curves $\Delta p \approx 2$, and they, therefore, have no peaks at all.

In selecting the width of the interval $\Delta p = \frac{\Delta r}{r_0}$ ^{one} should be guided by the data from Table 2 or the graph in Fig. 4 to make sure that the chosen interval ^{is} not be too large. But there exists a circumstance which should induce the observer to resist being carried away in selecting overly small intervals. Indeed, if the experimental distribution is represented, as this is usually the case, in the form of a stepped curve or frequency polygon, then the smaller the interval, the more precise is the position of the maximum if the sample volume is sufficiently large so that the error resulting from the insufficient statistical ^{filling} of the interval becomes negligibly small at least for the intervals near the experimental curve maximum. Under these conditions the position of the maximum cannot be, in principle, defined with an accuracy exceeding one-half of the interval width. However, whenever the n_1 values in the vicinity of the experimental curve maximum are small -- and this is possible at any arbitrarily selected large $N_k = \sum n_1$ so long as the width of the interval is sufficiently small -- the advantage in ~~the~~ determining the maximum's position resulting from the reduced interval width turns out to be but apparent. This is so because with a decrease of the interval width, the insufficient statistical ^{filling} of the maximum and its environment begins to manifest itself and reduces to nought the effect resulting from the reduction of the interval width. In the next section we shall consider the problem concerning the error in n_1 determination ^{due to} the insufficient statistical ^{filling} , or (which is the same) to the finiteness of the sample volume.

Consequently, the width of the interval cannot be selected arbitrarily, and must be comensurate to the value of the most probable radius r_0 .

recommended
 The best values for the width of the interval in size measurements of natural fog and cloud particles are $\Delta p = 0.2 - 0.25$, which still do not cause any noticeable deformation of the distribution curve, and at the same time assure the maximum statistical concentration

in each of its intervals taken separately.

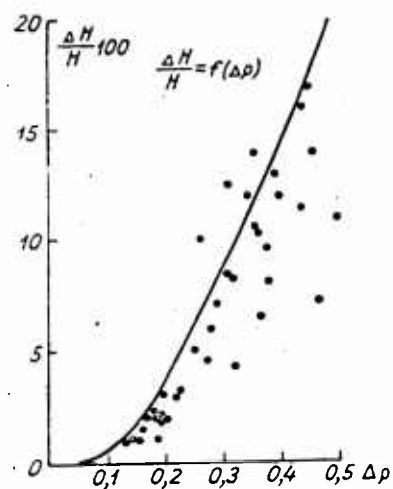


Fig. 4. Effect of the interval width.

with the results produced earlier by Prof. A.K. Mitropol'skiy by a different method.

The problem of the interval width is quite evidently connected with the question relative to the number of intervals in an experimental distribution. The necessary number of intervals at $\Delta p \approx 0.2 - 0.25 r_0$ appears on the average to be equal to 12-16 for experimental distributions in which the maximum variate value does ^{NOT} exceed _A 3-4 r_0 . Our estimates on the number of required intervals for all practical purposes coincide

Table 2.

Δp	0,1	0,2	0,3	0,4	0,5	0,6	0,7	0,8	0,9
$100 \frac{\Delta H}{H}$	0,6	3,8	8,5	14,1	20,6	27,2	33,9	40,0	45,5
Δp	1,0	1,5	2	4	8	16	32	64	∞
$100 \frac{\Delta H}{H}$	50,4	66,7	75,0	87,5	93,8	97,7	98,5	99,2	100

4. Influence of the Finiteness of a Random-Sample Volume.

The effect of the volume finiteness of a random sample in particle-size measurements in fog and clouds as polydispersed systems may be manifested in such a possible distortion of measurement results that this distortion could be considered as an accidental error whose magnitude must be determined with recourse to methods of probability theory and mathematical statistics.

Let n_i , as before, stand for the frequencies characterising the ^{number} of particles comprized in a finite number k of intervals with the total number of particles $N_k = \sum n_i$.

We shall consider one such arbitrarily selected interval.

It is obvious that the proportion of particles p of size ρ_i is unknown to us. Therefore, in utilizing the experimental data, we are compelled to regard the magnitude of relative frequency $\frac{n_i}{\sum n_i} = p'$ as an approximate value of the proportion of particles $p = n(\rho) \Delta \rho$ which is unknown to us, i.e. to assume in compliance with the law of large numbers that

$$p \approx p'$$

To estimate this approximate value it is necessary to select beforehand the value of reliability α so close to unity as to be able to discount the event with probability $1 - \alpha$ as practically impossible, and to determine such deviations of the unknown proportion of particles from the observed relative frequency $p' = \frac{n_i}{N_k}$ which may be expected with probability α in the case of a volume N_k random sample taken from an infinite general population.

It is known from the probability theory that the magnitude of these deviations may be determined from formula

$$\Delta p = x \sigma_p = x \sqrt{\frac{(1-p')p'}{N_k}}, \quad (31)$$

where σ_p is the standard proportion p ; $\alpha = \Phi(x)$ is the probability that the unknown proportion falls between the limits

$$p' - x \sigma_p < p < p' + x \sigma_p. \quad (31^a)$$

The numerical values of parameter x , ^{which} depends ~~on~~ on the selected reliability, are determinable from the ~~table~~ ^{table of the values of function}

$$a = \Phi(x) = \frac{2}{\sqrt{\pi}} \int_0^x e^{-\frac{t^2}{2}} dt, \quad (31^b)$$

which are usually provided in the reference section of textbooks in the theory of probability.

Expression (31) is hardly suitable for practical application since the errors appears to depend not only ^{on} sample volume N_k , but also on the magnitude of the relative frequency $\frac{n_1}{N_k}$.

Formula (31) yields an expression for relative error D_1 more convenient for practical utilization

$$D_1 = \frac{\Delta p}{p'} = x \sqrt{\frac{1-p'}{N_k p'}}. \quad (31^c)$$

In substituting $p' = \frac{n_1}{N_k}$ into the above expression, we obtain

$$D_1 = \frac{x}{\sqrt{n_1}} \sqrt{1-p'}. \quad (32)$$

From (32) it follows that for the curve sections of an experimental or ~~random~~ sampling distribution, where $p' = \frac{n_1}{N_k}$ is at its maximum and comparable to unity (this is possible only for excessively large intervals), the relative error value in measurement of n_1 depends both on n_1 itself, and on relative frequency $p' = \frac{n_1}{N_k}$, i.e. in the final count also on the number of particles N_k on the measurement of which the investigated experimental distribution is actually based.

In the remaining points, or more precisely in the experimental curve intervals where $p' \ll 1$ or $n_1 \ll N_k$ (and in the case of small intervals and a moderate peakedness also over the entire length of the experimental curve), the radicand $1-p'$ hardly differs from unity, and the square root from this quantity is the more so nearer to unity.

Thus, for an experimental distribution with arbitrary ^{peakedness} ~~shape of a single-peak~~ and ~~curve~~ ^{curve}, ~~for~~ with intervals $\Delta r = \frac{\Delta r}{r_0}$ so small that the condition

$$n_1 \ll N_k, \quad (33)$$

is secured everywhere, including the maximum itself, formula (32) may be rewritten in the following final form

$$D_i = \frac{x}{\sqrt{n_i}}; \quad (34)$$

On the basis of (16) condition (33) for the case $n_1 = n_m$ may be rewritten in the form of inequality

$$H\Delta\rho \ll 1,$$

which holds for arbitrary unimodal distributions. For a distribution with unit peakedness formula (33) assumes the aspect of

$$\Delta\rho \ll 1. \quad (35)$$

From formula (34) it follows that the relative error in determining n_1 for an arbitrary distribution with $n_1 \ll N_k$ is not the same for different experimental curve intervals, as this ^{indeed} was to be expected. At a given reliability α error D_1 becomes a function only of n_1 -- the number of particles contained in the given interval in which we are interested -- and is independent of N_k -- the number of particles ^{on} the measurement of which the investigated experimental distribution was actually based. Thus, we come to the conclusion that the relative error in determining n_1 , if the intervals are sufficiently small, does not essentially depend on the distribution law, nor on the volume of random sample. Consequently, formula (34) is applicable to any given experimental distribution, providing condition (33) is satisfied

In analyzing the errors in an interval, the numbers n_i -- if they denote the measure of particle concentration in which are the intervals, small in comparison with the most probable radius -- may, in approximation, be considered as independent, and the polydisperse fog regarded as consisting of a finite number of independent monodisperse components. In passing, we shall note that formula (34) gives higher relative error D_1 values if condition (35) ^{is} violated. In this case the excess value is greater for the maximum zone and smaller for the remaining intervals of the experimental distribution.

It, therefore, becomes apparent that the errors calculated on the basis of formula (34) -- if the intervals $\Delta\rho \ll 1$ are sufficiently small --

are applicable to any experimental distribution and to any of its intervals with an accuracy sufficient for all practical purposes, if the peakedness of the investigated experimental distribution differs little from unit [redacted] peakedness.

The relative error in determining the $\frac{\text{particle concentration in an}}{\text{interval [redacted]}}$, whose magnitude is numerically determinable by expression (34), is a function of frequency n_1 . Hence, it is not identical for the different intervals or regions of one and the same experimental curve.

In conclusion we shall dwell briefly on the matter of reliability. From a statistical point of view there necessarily must be a correspondence between any error and the reliability with which it is estimated. The very essence of the reliability concept indicates that it should be so close to unity in the solution of practical problems that the events with $1-\alpha$ probability could be considered as practically unfeasible. V.I. Romanovskiy (14) remarks that depending on the practical requirements α is being assumed equal to 0.95, 0.99, or 0.999. For our calculations we have used the value of $\alpha = 0.95$.

In all experimental studies known to us which deal with mathematical statistics in relation to the structure of natural fog, clouds, and rain (32), (34), (29), (10), as well as those devoted to research in disperse system concentrations (3), the ARITHMETIC MEAN error is usually discussed in estimating random errors. Important is the fact that reliability α (a definition of this concept, regrettably, is lacking in most works) in this case turns out to be congruent with its complement with respect to unity. Thus, for a deviation distribution obeying the normal law, reliability α , which characterizes the arithmetic mean error, appears to be equal to

$$\alpha = 0.68, \text{ and } 1-\alpha = 0.32.$$

This means that the probability of measurement with an error greater than arithmetic mean error, turns out to be considerable enough and [redacted]

comparable to the reliability itself. In this case, on the average, out of three measurements two may fit in, while the third may exhibit a deviation exceeding the arithmetic mean error. In our case the reliability is so close to unity that $1-\alpha = 0.05$. To utilize the arithmetic mean error without due consideration of the reliability which characterizes it, as this was ^{done} by Köhler (32), is obviously a mistake. Köhler and Niderdorfer, without paying any attention to the long since known concept of reliability, treated the arithmetic mean error in analyzing the amplitudes of a multipeak curve as if this error had a unit reliability. The observation results and the conclusions drawn from them by Köhler are, therefore, trustworthy only to the extent to which the events with probability $1-\alpha = 0.32$ may be attributed practical unfeasibility.

The utilization by Köhler of arithmetic mean errors characterized by small reliability α value actually constitutes the basic reason for the mistake he made in treating the experimental data. This ^{fallacy} thus caused him to formulate the physically untenable hypotheses and is sometimes mistakenly referred to as Köhler's multiplicity law.

A similar error was in its time made by Defant (26), and later by Niderdorfer (34), with regard to the size distribution of rain ^{drops}.

5. Sufficiency Test of a Random-Sample Volume.

In the preceding sections we have found a method of estimating the accuracy of an arbitrary experimental distribution curve in any of its intervals, if the interval is sufficiently small.

The described method may prove to be useful only in analyses of the statistical ^{filling} for the already plotted experimental curves. In those cases when the investigator approaches the problem of experimental curve construction, it is desirable to obtain the estimates for such total number of particles N_k in measuring which the required statistical ^{filling} could be assured at the maximum.

Until now the total number of particles $N_k = \sum n_i$ in measurements of

fog and cloud particle sizes is known to have been absolutely random. Its value varied over a wide range with totally unsubstantiated limits.

Houghton /31/ supposed that a "good" single-peak experimental curve in measuring the particle sizes present in natural fogs and clouds may be produced practically always when the number of particles measured to yield the curve is no less than 500-1000 with ^{the width/}of the interval corresponding to the diameter of 5 microns. Apart from this statement -- the insufficiency of which will become apparent in further discussion -- we could find no other information given by Houghton to this effect not only in terms of quantitative, but also in terms of qualitative characteristics. Yet, the need for a substantiated estimate of the required sample volume is evident. No appreciable advantages from the standpoint of accuracy can be derived in the case of larger and subsequently growing sample volumes, whereas the laboriousness of measurements increases unproductively. We shall define the sample volume sufficiency test as a quantitative ratio permitting to determine that total number of particles N_k of the investigated set which is sufficient for the experimental distribution curve to be characterized at the maximum by the relative error (due to the finiteness of the sample volume) whose magnitude does not exceed the preassigned value of D_m . Here we shall disregard the error due to the finiteness of the interval width (considered in Section 2) owing to its negligible value. This is admissible with respect to distribution (29) when $\Delta p \ll 0.2$ to 0.25 . To construct the test -- the essence of which transpires from the above definition -- we shall make use of the height of curve (16) in rewriting the equation in the form providing a solution with respect to n_m :

$$n_m = \bar{H} N_k \Delta p.$$

In substituting this expression for n_m in (34), and solving it with respect to N_k , we obtain

$$N_k = \frac{x^2}{H D_m^2 \Delta p}, \quad (35^a)$$

whence, upon transition to the dimensional aspect, it follows that

$$N_k = \frac{x^2 r_0}{\bar{H} D_m^2 \Delta r} \quad (36)$$

Formula (36), then, constitutes the criterion for sample volume sufficiency suited for any unimodal distribution. In order to estimate the required number of particles N_k it is necessary to preselect the value of measurement reliability α sufficiently close to unity, and to assign beforehand the desired relative error value at the maximum D_m .

The magnitude of this error should be negligible as compared to unity. Moreover, it is important to know the tentative value of the most probable radius r_0 to assure the most effective selection (see Table 2) of the interval width $\Delta r = \Delta p r_0$. The peakedness coefficient in formula (36) may be taken as equal to its minimum value as encountered in practice.

Formula (36) for $\bar{H} = 0.541$, corresponding to lognormal distributions with the most obtuse peak ($m = 2$, $n = 1$), with reliability $\alpha = 0.95$ ($x = 1.96$), may be rewritten as follows:

$$N_k = \frac{7r_0}{D_m^2 \Delta r} \quad (37)$$

The application of formula (37) for purposes of evaluation may assure a substantiated -- and, consequently, also an effective -- selection of the sample volume for measurements of particle sizes in natural fog and clouds. Further on in the text, in a corresponding section, the basis of the sufficiency test justification will be evaluated by way of comparison with the experimental data from formula (34) constituting the foundation of this test.

In this manner it will be seen that in contradistinction to Houghton's ideas, the required sample volume in our test turns out to be dependent through parameter x on the measurement reliability α , on the relative error at the maximum D_m , on the shape of the curve in terms of the peakedness coefficient, and, finally, on the interval-width to the most-probable-radius-value r_0 ratio. Houghton's considerations referred

to by us in the beginning of this section cannot serve as a sufficiently criterion. Rather, this ^{is} a correct, but sufficiently gross rule derived directly from ample empirical data, in which the dependence on the width of the interval and the magnitude of the most probable size remained unreflected.

6. Statistical Filling and Multimodality.

Published data on size measurements of particles in fog and clouds abound in experimental distributions the multimodality of which is sometimes attributed a special meaning ensuing from the widely known hypothetical constructions proposed by Köhler /32/, /33/ relative to the multiple relationship of cloud and fog particle masses.

Let us consider the problem concerning the authenticity of the multimodality of experimental distributions viewed from the positions of statistical probability, as this question was originally put forth by us /5/ in 1950.

The complexity of the problem is aggravated by the fact that multimodal distributions -- as noted by V.I. Romanovsky /13/;-- as a rule, are not studied in mathematical statistics.

In the preceding section we have derived an expression for the relative error in estimating the number of particles filling an individual interval. This error comes as a result of the boundedness of the sample volume. This fact makes it possible to provide the experimental curve with two supplementary curves. One of them is then is the envelope of the maximum possible deviations of the experimental curve from the general population curve; the other is the envelope of the minimum possible deviations (fig.5). The distance between the above envelopes along the vertical in any interval is evidently

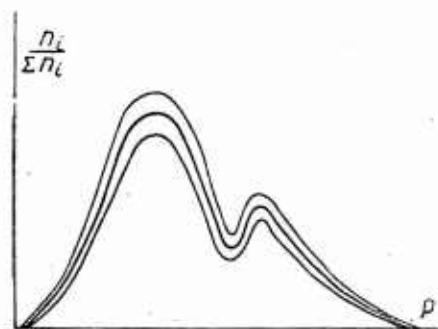


Fig.5. The envelopes of errors.

equal to the approximate double value of the absolute error, i.e.

$$2\Delta n_i \cong 2x\sqrt{n_i}. \quad (37^a)$$

The numerical value of the area enclosed between the error envelopes for a given distribution essentially depend on the sample volume, the measurement reliability, and the width of the interval, as this follows directly from (34). Reliability α sufficiently close to unity, as this is usually assumed when dealing with practical problems /14/, represents in the case under consideration the probability with which one may expect the appearance of an arbitrary curve contour in the zone bounded by the error envelopes. Hence, this zone may be considered as a locus where each point may belong to any arbitrarily selected distribution curve provided the normalization condition for it is observed. Each normalized distribution curve traced through this zone may be a population curve. The probability for the contour of a normalized distribution curve to pass beyond the error envelopes for each individual interval, apparently, is equal to $1 - \alpha$. The probability for the contour to emerge beyond the lower envelope is smaller even the more so. In accordance with A.K. Mitropol'sky's suggestions /12/ we shall call the zone enclosed between the error envelopes as the zone of fluctuations.

The portion of the curve area bounded by the lower error envelope and the X-axis is an authentic part of the experimental curve area, since the penetration of the contour of any experimental curve from the fluctuation zone into this region is so improbable that it can be considered as practically impossible.

A very useful characteristic of the authenticity zone is the fact that with infinitely growing sample volume, and infinitesimal intervals, it has the whole area of the population curve as its limit. The zone between the error envelopes (fluctuation zone) ultimately vanishes. This would not have been possible had there been no limit for each authentic part of any individual interval, and had the relative errors not been tending to zero.

So far we were dealing mainly with experimental curves plotted on the basis of measurements involving a finite and constant number of particles.

There arise a number of questions in practical statistical measurements the solution of which is possible only with due consideration of the variability of the sample volume. For example: What is the minimum number of particles required to assure that a curve plotted as a result of their measurement could be considered as an experimental distribution? Evidently, one particle is clearly insufficient for this purpose. An accounting of the sample volume variability is equivalent to a test in which the volume of a sample taken from a fixed set of particles grows as a result of sequential incorporation into it of individual particles. In such an experiment we shall be interested mainly in the changes manifested by the experimental curve as a result of statistical filling which is understood to mean a process connected only with an increase in the sample volume.

In passing now on to an arbitrary and separately taken interval and assuming the maximum value of the relative frequency density for it to be equal to the probability density $n(\varphi)$ of the general population, we shall obtain

$$n(\varphi)(1 - D_1) \quad (38)$$

as the mean value for the authentic portion of the interval particle concentration, and correspondingly $2n(\varphi)D_1$ for the components of the fluctuation zone.

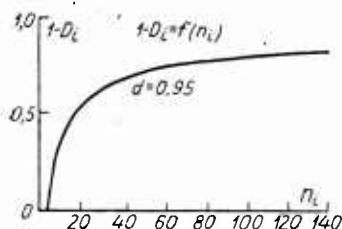


Fig. 6 Statistical interval. Hence, this difference may be considered as a measure of the statistical filling of the curve in the investi-

Evidently, the difference $1 - D_1$ in (38) characterizes the authentic part of probability density. In the case of an experimental distribution it characterizes the authentic part of the relative frequency density $\frac{n_1}{\Delta p N_k}$ for a given interval. Hence, this difference may be considered as a measure of the statistical filling of the curve in the investi-

gated interval. Figure 6 shows a graph of function

$$1 - D_i = f(n_i) = 1 - \frac{x}{V n_i}, \quad (35a)$$

from which it transpires that -- depending on the relationship between n_m and D_m there are for a given reliability value three basic stages of statistical filling or experimental curve shaping. We shall now pass on to a discussion of these stages.

The Initial (I) Shaping Stage.

The most densely filled interval contains $n_m < x^2$ number of particles and has no authentic portion in its filling, i.e. cases are possible when $\Delta n_m > n_m$. For all the remaining intervals the inequalities will be even more sharply expressed. The experimental curve in the first stage of shaping is characterized by absolute indefiniteness due to the absence of a positive authenticity zone portion. Such a curve, as a rule, has nothing in common with the ~~random~~ distribution of the universe from which the sample was drawn. This may be manifested in the fact that the universe distribution mode would fail to coincide with the the most densely filled interval. The number of peaks of such a curve in isolated cases may be comparable with the sample volume. It may not resemble the initial distribution by form. Addition of two-three particles may substantially change the shape of such a curve, the number of maxima, and the position of the most densely filled interval.

A sample with a volume sufficient for an experimental curve in the first shaping stage must be considered as totally unrepresentative from statistical point of view, provided, of course, that there had been no subdivision into excessively small intervals.

The Main (II) Shaping Stage.

The most densely filled interval contains a number of particles within the limits

$$x^2 < n_m < \frac{x^2}{D_m^2}$$

where $D_m \ll 1$. Here the case $n_m \approx x^2$ corresponds to the beginning of the appearance of the authentic part of the interval filling, and $n_m \approx \frac{x^2}{D_m^2}$ signifies the filling with error D_m at the maximum, when the authentic portion of the interval filling grows to $(1-D_m)n_m$. By the end of the second shaping stage the experimental curves in their main central part have a shape corresponding [redacted] to the population distribution. The most densely filled interval, if it is not too small, comprises the mode of the initial distribution. The multimodality registered in the central part of the experimental curve at the beginning of the second shaping stage shifts by the end of the stage into the region of the curve tails. Further addition of no matter how large a number of particles does not substantially alter the empiric curve shape at the end of the second stage.

The experimental curve constructed up to the end of the second shaping stage graphically represents the sample which is statistically representative, provided the error D_m with which the peak was determined satisfies the requirements of a given problem.

The Ultimate (III) Shaping Stage.

The curve maximum is filled to the extent that

$$\frac{x^2}{D_m^2} < n_m < \infty. \quad (A)$$

Moreover, the inequality $D_m \ll 1$ continues to grow and ultimately $D_m \rightarrow 0$. At this shaping stage the experimental curve, without exhibiting any appreciable changes, attains the state of perfect identity with the universe distribution. The numerical value of any experimental curve parameter approaches asymptotically to its maximum value. With regard to the curve altitude this fact may be [redacted] in Fig.3.

Unlike the first two stages of experimental distribution curve shaping, the last stage is characterized by the fact that the size and the shape of the experimental distribution curve authenticity zone turn out to be practically independent from the volume of the random sample. In the light of the above ideas, only such experimental curves, [redacted]

as have been plotted up to the end of the second and the beginning of the third shaping stages (i.e. ^{as} λ are statistically filled), appear to be suitable for ~~an~~ an analysis of possible multimodality, its character, and causes of its origin.

Consideration of the character of statistical filling makes it possible to develop a reality test for the multimodality of empirical distributions.

Authentic or real multimodality of an arbitrary experimental distribution is understood to mean ~~the~~ a multimodality only such as acquires a perfectly definite character in terms of number, shape, and ~~the~~ relative position of the peaks in the process of further growth of the random sample volume.

If, however, as a result of observations a multipeak experimental curve is produced which with further growth of random sample volume turns into a single-peak curve only in consequence of statistical filling, then the multimodality of an experimental distribution is not authentic and we shall consider it as accidental multimodality resulting from the boundedness of the sample volume, or -- which is the same -- from insufficient statistical filling of the experimental distribution intervals which interest us.

Thus, the best method for the solution of the question relative to the authenticity of ~~the~~ the multimodality of experimental distributions is to increase the volume of the random sample to assure the required statistical filling.

When random sample volume cannot be increased, the character of the observed multimodality may be approximately estimated in the following manner: the contour of the investigated empirical curve is accompanied by the envelopes of errors calculated from formula (34). If it proves to be impossible ^{to} draw a single one-peak curve ~~through the zone~~ enclosed between the two envelopes without the contour of the curve

penetrating outside the zone (see Fig.5), then the multimodality of such an experimental distribution can be considered as practically authentic. One might proceed also in the inverse order: by superposing a normalized, averaged single-peak curve with error envelopes on the investigated experimental distribution. ^A multimodality the amplitudes of which do not noticeably pass beyond the error envelopes should be considered as accidental. One should bear in mind here, that the

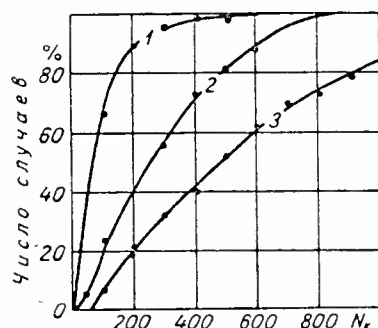


Fig.7. Statistical filling of experimental distributions (319 curves).

1 - after Diem, 2 - after Zaytsev, 3 - after Borovikov.

very concept of reliability presupposes the possibility of a transgression of ^{accidental} multimodality amplitudes in 1- α cases, if the number of the investigated experimental curves is sufficiently large.

The necessary corollary ^{to} an analysis experimental distribution multimodality consists in that not any multimodality is authentic or real. Consequently, ~~the~~ physical investigation of ~~the causes for~~ the multimodality of experimental curves must be pre-

ceded by its verification from the statistical point of view. The method of the envelopes is perfectly convenient for this purpose. On the basis of the above ideas it became possible to review the extensive material on experimental distributions published in the works by Hagemann /30/, Chestnaya /22/, Zaytsev /7/, Diem /27/, /28/, and Borovikov /1/. These papers distinguish themselves advantageously from other works by the considerable number of observed cases, ^a detailed description and sufficiently comprehensive information on the investigated distributions. The papers of other authors are not always as interesting. Findeisen /29/, for example, has produced distributions many of which have no maximum. All his distributions are characterized by a considerable shift of the curve to the left from the values obtained by other investigators. This

is, apparently, due to the excessive heating of the drops in the measuring volume of his apparatus. The results of many years of Houghton's /31/ research [redacted] are reduced to three "typical" curves and the direct observation data are not published. Bricard /25/ also avoided to publish his data on distribution curves. All [redacted] experimental curves considered by us were produced by the commonly known method of taking photomicrographs of drops collected on a glass slide coated by a thin layer of mineral oil. Information on this method and its variants [redacted] was repeatedly published in [redacted] the [redacted] papers by Tarayan /18/, Katchenkov /8/, Fuks /20/, Hagemann /30/, Selezneva /15/, Kucherov /10/, Chestnaya /22/ and other authors. In a more comprehensive form these data are presented by Zaytsev /6/ and Borovikov /1/. From the statistical viewpoint not all the experimental distributions referred to above are equivalent. The sample volume in each of them is the standard which, in the main, determines the quality of the experimental material. Represented in Fig. 7 are the integral distribution curves produced by Diem /27/, /28/, Zaitsev /7/, and Borovikov /1/. In Table 3 one will find the comparative data showing the minimum, average, and maximum sample volumes, as well as the number of experimental curves classified according to the ^{shaping} [redacted] stages.

A comparison of the curves from Fig. 7 and the data from Table 3 shows that the best [redacted] from the standpoint of statistical filling are Borovikov's experimental distributions. The worst are the data given in Diem's two papers. The results of Hagemann's /30/ and Chestnaya's /22/ observations are hardly distinguishable from the distributions produced by Zaytsev /7/ which occupy an intermediate position. The principal characteristic of Diem's distributions is that the ^{shaping} [redacted] of most of his curves was stopped at the first stage. The majority of his curves were not brought up to the required level of statistical filling. A common defect of all the published distributions consists

in the fact that ^{the} sample volume of experimental curves was taken at random. It goes without saying that from the experimental point of view it is easier to catch many small drops and much more difficult to collect a large number of large drops. Experimental distributions with small sample volumes turned out to be constructed, as a rule, for the cases of large-drop clouds, whereas large sample volumes were used in the main for the cases of fine-drop clouds. Yet, it follows from the sufficiency test ~~xxx~~ for the case when the interval width is constant that one should take the experimentally more difficult path in order to produce statistically comparable experimental data.

Table 3.

Author	Sample volume			Number of curves			
	mini- mum	ave- rage	maxi- mum	$N_k < 50$	$N_k = 50$ - 500	$N_k > 500$	Total
Borovikov /1/							
Zaytsev /7/	63	500	2455	—	44	44	88
Diem /27/	8	250	1388	5	85	20	110
/28/	10	60	640	40	92	2	134

We shall now pass to the problem of the multimodality of experimental curves and its connection with the well known relationship of multiple masses which was originally registered by Defant /26/ with respect to rain drops, and later extended by Köhler over the particles of natural fogs and clouds.

The method of error envelopes is most convenient for the investigation of the amplitudes of multimodal experimental distributions. The fluctuation zone here should be considered as the region of possible accidental multimodality.

Analysis of the published experimental distributions ^{with} high reliability ~~α~~ shows that all of them have a multimodality of accidental character. The number of cases involving the passage of experimental curves in

individual intervals beyond the error envelopes, expressed in percentage values, is noticeably lower than the admissible 5% ($\alpha = 95$).

In analyzing the possible errors of the photomicrography method, A.M. Borovikov /1/ comes to the conclusion: "In our opinion the total error in measuring the number of drops does not exceed 10%, and then this error in the overwhelming majority of cases affects the fine-drop measurements" (page 19). This conclusion may be assumed as correct only for the intervals statistically so filled that error D_1 in them is negligible in comparison with other statistical errors. For many experimental distributions analyzed by us error D_m exceeds considerably all other errors put together.

A structural analysis of multimodality in experimental distributions to determine its correspondence to the relationship of multiplicity of masses shows that this relationship does not hold for the entire length of any experimental curve. This fact was already registered in Ye.S. Selezneva's /16/ and I.I. Chestnaya's /22/ works. Of interest is the question regarding the conditions which should be satisfied by a statistically unfilled experimental distribution to cause its multimodality to satisfy the multiplicity ratio. For this purpose we shall examine the maxima r_1 and r_2 of an arbitrary multipeak experimental curve. These maxima satisfy the multiplicity relation in the case of the obvious ratio

$$\frac{r_2}{r_1} = \sqrt[3]{2}. \quad (39)$$

The distance between maxima r_1 and r_2 expressed through one of them may be found from (39) as

$$r_2 - r_1 = (\sqrt[3]{2} - 1)r_1. \quad (39a)$$

The same distance may also be expressed in terms of the interval width Δr of a given experimental distribution in the form of

$$r_2 - r_1 = (l + 1)\Delta r, \quad (40)$$

where l is the number of intermediate intervals situated between maxima r_1 and r_2 .

It follows from (39) and (40) that maxima r_1 and $r_2 = \sqrt[3]{2r_1}$ ^{strictly/}satisfy the mass multiplicity ratio if condition

$$r_1 = \frac{(l+1)\Delta r}{\sqrt[3]{2}-1} \quad (41)$$

is observed.

Observations indicate that the sequence with which the maxima alternate is fortuitous. Furthermore, most frequent are the cases when the maxima alternate after one interval, which corresponds to the case $l = 1$. Recorded below by way of an example is a table of the recurrence of l . The data for this table are taken from the experimental material produced by I.I. Chestnaya /22/

T a b l e 4.

l	1	2	3	4	5	6	7	8	9	10 and more	Total
Number of cases	176	80	39	20	13	3	5	2	3	5	346

For Chestnaya's distributions constructed with intervals of 1.3 microns (in ^{terms of} diameter) in accordance with (41) one should expect that the mass multiplicity relation may best be satisfied at $l = 1$ in the size group 10-12.6 microns, and for $l = 2$ in the size group 15-19 microns, respectively. [REDACTED] Out of 87 experimental curves of Chestnaya there was only one for which the multiplicity relation was met over a large segment of the curve. We shall cite this example in designating the position of the six peaks of the curve by figures in parentheses to indicate the number of intermediate intervals between the maxima: 7.8(1), 10.4(1), 13.0(1), 15.6(2), 19.5(2), 23.4 microns.

This example graphically demonstrates the mechanism of producing experimental distributions satisfying the multiplicity relationship. It can be shown without too much of an effort that for a limited sample from any set of real particles (including, of course, a single-peak one)

the compliance with the mass multiplicity relation may be demonstrated on individual experimental curves in any preselected region of the experimental curve and for any maxima known beforehand. For this purpose -- apart from the statistical incompleteness without which it is possible that there might be no accidental multimodality -- it is only necessary to select the interval width in conformity with condition (41).

It is well known that one of the elementary requirements in mathematical statistics is that the samples should be drawn randomly. For an experimental confirmation of the mass multiplicity relation it turns out to be necessary, in violation of this rule, to resort to a selective separation of a certain portion of the experimental data, and then precisely that part of it which is useful for the substantiation of ^{Köhler's} hypothetical views. This is the second serious error of statistical character made by Köhler in his analysis of the structural characteristics of the multimodality of experimental distributions.

Let it be mentioned in passing that the method used by Köhler ^{also} offers an equal opportunity to "substantiate" a counter hypothesis concerning the predominant non-coalescence of equal-size drops. To achieve this goal it suffices to select those cases from the observation results in which the maxima of a statistically unfilled distribution curve are followed by minima appearing at definite distances.

Thus, as we can see, the "Köhler law", ^{as the allegedly experimentally} "observed" mass multiple ~~relation~~ relation is sometimes referred to) has no direct bearing on the microphysics of clouds and fog and is not a physical law. As a matter of fact, the phenomenon registered by Köhler is the inevitable result of the manifested boundedness of the sample volume.

7. The Mean Sizes in Polydisperse Fog.


In distribution research in natural fog and clouds it is customary to make use of the the concept of the, so-called, mean sizes. The following designations may be found in literature: the most probable,

the predominant, the arithmetic mean, the ^{mean}/quadratic, the mean cubic, the mean size after Houghton, the average size. Recently N.S. Shishkin (23) has utilized the concept of the ^{radius of the drops} [redacted] responsible for the greatest contribution to the liquid-water content. By analogy one might as well speak of the radius of the drops responsible for the greatest contribution to the surface area. As mentioned before, different methods of experimental distribution curve construction are adopted in the Soviet Union and Europe, on the one hand, and in the USA, on the other hand. As a result of this discrepancy in methods there is no uniformly accepted system of mean size concepts and designations, and this sometime leads to obvious errors. Ye.S. Selezneva (16) has pointed out in her paper to one of such misconceptions of M. Diem who believed that the American fogs consist of larger drops than the European. One could mention another absurdity of this kind encountered in J. Bricard's work (25), where the arithmetic mean size was referred to as simply an "average" and was used for the calculation of liquid-water content on the basis of a certain number of observed particles in a unit volume. It is evident that in this case it was necessary to use the mean cubic size. The ^{inaccuracy} [redacted] in liquid-water content determination arising from this type of error depends on the nature of the distribution and in individual cases may be comensurate with the evaluated liquid water. Moreover, it should be borne in mind that the concept "mean size" without a reference to the meaning of the mean is hollow and, consequently, erroneous. Owing to the above mentioned difference in the methods of experimental curve construction one and the same mean size is sometimes designated in a different way, while different sizes are often identically designated. Thus, for example, Shishkin /23/ refers to the mode of volume distribution as the radius of the drops responsible for the greatest contribution to liquid-water contents. In Houghton's paper this is called the predominant size. The predominant size in Houghton's

interpretation and the predominant size in ^{the} works by Soviet investigators /1,7,16/ are not one and the same thing because of the different method of empirical curve construction. Houghton (31) uses only one "average size" which he has calculated by formula

$$\bar{r} = \frac{\sum n_i r_i^3}{\sum n_i r_i^2} \quad (A)$$

without distinguishing it from his predominant size, in assuming that they are coincident. In the section devoted to the method of coronal rings, we read: "In usual application it yields only an average or predominant particle size" (page 5). The only "average size" of Houghton does not coincide with the only "average size" of Bricard (25), who has computed it as the arithmetic mean size, and utilized it as the mean cubic size. Finally, one also finds such studies /9/, /16/ in which the mean cubic size is identified as the mode of volume distribution, with a reference to which we have begun this discussion.

 The existence of a monodisperse fog such as would in all cases be equivalent to the investigated polydisperse fog is fundamentally impossible. In view of this fact we are compelled instead of a polydisperse fog to construct for each separate case a model of such a monodisperse fog that would be equivalent to polydisperse fog only with respect to a given property called the determining property in statistics.

The calculation operation for one or another mean size does not determine only the particle size of a certain equivalent monodisperse fog, but simultaneously also establishes a corresponding equivalence condition with respect to the given determining property.

To clarify the question of the correspondence of the exposed ideas on the mean particle sizes of a polydisperse fog to the basic positions of mathematical statistics in this matter we shall turn to a pertinent passage in V.I. Romanovsky's book (13): "The most general and precise definition of the concept of the mean was formulated almost

simultaneously (in 1929) by the Italian scientist Cazini and the Soviet scientist Boyarskiy. We shall now quote this definition which will be called the Boyarskiy-Cazini definition.

Supposing we have a certain statistical collective S with volume n which is characterized by values

$$x_1, x_2, \dots, x_n \quad (28.1)$$

of a quantitative variable x . As the determining property of collective S we shall designate such its property related to values (28.1) which must remain invariable at all possible variations of values (28.1).

Then the variable mean \bar{x} with respect to the considered determining property of collective S will be called that value of variable x , equal for all the collective members, which may be attributed to them without changing the determining property of the collective". (page 95).

From the great abundance of various means which are known in mathematical statistics we are interested only in those which belong to the characteristic class of means called regular. (According to Romanovskiy, included among these means are such which are monotone, associative, and single-valued, while the determining property is given in the form of a continuous and symmetric function).

About such a mean and its correct statistical interpretation Romanovskiy /13/ writes: " This quantity is obtained when under the condition of invariability of the determining property, instead of the given collective, and abstract levelled collective is constructed having one and the same criterion \bar{x} for all its members. This quantity in the sense of preserving the determining property is thus equivalent to the totality of x_i values in the investigated collective and, therefore, actually represents one of the means of describing the statistical collective which characterizes the collective with respect to the determining property as completely as the totality of x_i values of variable x " (page 101).

The objective of this paragraph is to venture to reconsider once again the concepts of the basic mean [redacted] particle sizes of polydisperse fog together with their designations in accordance with the ideas outlined above.

The Most Probable Radius.

As stated earlier we have adopted the most probable radius as the initial, the unit radius. It becomes clear from the designation itself that this size corresponds to the radius of drops such as are being most frequently encountered in size distributions.

For distribution (7) given in analytical form the most probable radius $r = r_0$, or $\rho = 1$, corresponds to the maximum of probability density. Therefore, its magnitude may be determined by solving equation

$$\frac{d}{d\rho} n(\rho) = 0. \quad (42)$$

with respect to r .

In the case of an emperic distribution based on size measurements of a finite number of particles, their sizes are usually plotted on the X-axis. On the Y-axis one plots the relative frequency $\frac{n_i}{\sum n_i}$ whose density, if the number of particles $N_k = \sum n_i$ and small intervals $\Delta\rho$ is sufficient, will be equal to

$$\frac{n_i}{\Delta\rho \sum n_i} \approx n(\rho), \quad (43)$$

where $n(\rho)$ is the function of the [redacted] probability density of distribution (7) which in this case is assumed to have a range satisfying the experiment.

From the approximate character of equation (43), which is an expression of the law of large numbers, it follows that [redacted] ^{with} $n(\rho)$ unknown to us the relative frequency density maximum appears to coincide with probability density only for an infinite sample volume and infinitesimal interval width. Therefore, the maximum of any experimental curve, and consequently, also the most probable radius for any experimental distribution is always determined approximately, and the more accurately, the

greater the sampling scale and the smaller ~~the~~ intervals. The remaining mean sizes which will be considered later will be measured in fractions of the most probable radius.

Apart for size distributions, other distributions are also possible, as noted in section 1. Each of these distributions has its mode distinguishable from the most probable size. The mode of surface-area distributions ρ_s , expressed in linear measures, is the predominant size in terms of surface area, whereas the mode of volume distributions ρ_v represents a predominant size in terms of volume, and is also expressed linearly. In future discussion we shall refer to them as such.

Houghton /31/ in utilizing a volume distribution~~s~~ erroneously referred to the mode ~~as~~ this distribution as the "predominant" size. Lacking in this designation is the ~~an~~ indication of the criterion in terms of which the predominance was registered. The size distribution mode or the most probable size sometimes /1/, /7/, /16/ ~~are~~ referred to as the predominant size. Statistically this is correct, but if one takes into account the presence of the predominant size in Houghton's investigation, then it becomes apparent that the use of this term is undesirable and should be discontinued mainly to avoid confusion similar to that described above.

Linear Equivalence Radius, or Arithmetic Mean Radius.

Let us select linear particle-sizes for an investigated set to serve as the determining property. For this purpose it~~s~~ suffices to equate the total length formed by N_k polydisperse fog drops /7/ to the same number of particles of a monodisperse fog. The condition of linear equivalence may be expressed as

$$2N_k \int_0^{\infty} n(\rho) \rho d\rho = 2N_k \bar{\rho}_1, \quad (44)$$

where $\bar{\rho}_1$ is the particle radius in monodisperse fog~~/~~ equivalent to ~~a~~ given polydisperse system with respect to linear sizes. From the

~~EXACT~~ expression

$$\bar{\rho}_1 = \frac{\bar{r}_1}{r_0} = \int_0^{\infty} n(\rho) \rho d\rho, \quad (45)$$

ensuing from (44) and valid only for distributions given in a differential form, it is easy to pass over to a form suitable for experimental distribution investigations. For this purpose in formula (45) the probability density should be replaced by its approximate value from (43), viz. $\frac{n_i}{\sum n_i \Delta \rho}$ which is the relative frequency density, and in accordance with (6) to assume ρ and $d\rho$ equal to

$$\rho \approx \frac{r_i}{r_0}; \quad d\rho \approx \Delta\rho = \frac{\Delta r}{r_0}. \quad (45^a)$$

In replacing the integral sign by the summation sign, we have

$$\bar{r}_1 = r_0 \int_0^\infty n(\rho) \rho d\rho \approx \frac{\sum n_i r_i}{\sum n_i}. \quad (45^b)$$

i.e.

$$\bar{r}_1 \approx \frac{\sum n_i r_i}{\sum n_i}. \quad (46)$$

Leaving aside the question of the accuracy of ~~the~~ approximate relationship (46) as a matter transcending the ~~scope~~ of this discussion, we shall only state that ~~with~~ $\sum n_i$ tending to infinity and vanishing Δr , the approximate expression has as its stochastic limit the exact expression (45), of course, if the finite-volume random sample is drawn from distribution (7). The arithmetic mean size estimated on the basis of formula (46) is determined with an error, the greater, the smaller the volume of the random sample.

The arithmetic mean radius $\bar{r}_1 = \frac{\bar{r}_1}{r_0}$ is the radius of the drops of a monodisperse fog such as for the same number of particles possesses a sum of linear sizes identical to that of a polydisperse fog. In operating with the concept of arithmetic mean radius, we, by virtue of this very fact, are actually dealing with a monodisperse fog equivalent to the investigated polydisperse fog in terms of linear sizes. The basic usefulness of mean size \bar{r}_1 consists in the fact that it (after a simple calculation) approximates most closely the distribution mode which for skewed experimental distributions is usually not calculated. The designation "mean size" in application to \bar{r}_1 used in a number of papers /1/, /25/, and so on, is undesirable in view of the indefiniteness of this term of reference.

Surface Equivalence Radius, or Mean Quadratic Radius.

If the total surface (section) of polydisperse fog particles be considered as the determining property, then in a similar way it ~~may~~ be possible to obtain an expression for the mean quadratic radius:

$$\bar{\rho}_2 = \frac{\bar{r}_2}{r_0} = \sqrt{\int_0^{\infty} n(\rho) \rho^2 d\rho}. \quad (47)$$

Applicable for experimental distributions is a formula expressed in sums (in view of their obviousness we leave out the conversion operations):

$$\bar{r}_2 \cong \sqrt{\frac{\sum n_i r_i^2}{\sum n_i}}. \quad (48)$$

The mean size \bar{r}_2 is the radius of particles of a monodisperse fog equivalent to a given polydisperse fog in terms of surface area (section). In operating with the concept of mean square radius, we, by virtue of this very fact, are actually dealing with a monodisperse fog such as, ~~in case of the invariability of the particle number,~~ possesses a total surface area (section) identical to that of a polydisperse fog. This size was used so far in the analyses of optical problems /9/, /10/, but may, in principle, be applied in future to investigations of any phenomena the mechanism of which depends on the surface area (section) of polydisperse fog particles.

Volume Equivalence Radius, or Mean Cubic Radius.

Corresponding to the total volume of polydispersed fog particles, which is considered as the determining property, is the mean cubic size numerically equivalent to

$$\bar{\rho}_3 = \frac{\bar{r}_3}{r_0} = \sqrt[3]{\int_0^{\infty} n(\rho) \rho^3 d\rho}, \quad (49)$$

where \bar{r}_3 is the dimensional value of this mean size.

For experimental distributions use is made of the obvious approximate expression in sums

$$\bar{r}_3 \cong \sqrt[3]{\frac{\sum n_i r_i^3}{\sum n_i}}. \quad (50)$$

In operating with the concept of mean cubic size, we thereby reduce the problem to an analysis of a monodisperse fog such as, in case of the same number of particles, as is present in a polydisperse fog, has a

volume identical to that of the latter. This size is used for the solution of problems connected with the study of fog water, since the latter coincides/pretty accurately with the volume of particles. The size \bar{r}_3 has found the widest and consistent application in the calculations of natural fog water carried out by N.V. Kucherov /10/ and B.V. Kiryukhin /9/.

The Specific-Surface Equivalence Radius.

As for any disperse system, the dispersity of fog may be evaluated through specific surface σ which is usually assumed equal to the surface of a matter dispersed in the volume of one cubic centimeter.

For monodisperse fog, the particle radius of which is equal to \bar{r}_c , the specific surface σ_M will be equal to the surface of the drops which after coalescence occupy a volume of 1 cm^3 , and may be numerically determined from the following relationship

$$\sigma_M = \frac{N' 4\pi \bar{r}_c^2}{N' \frac{4}{3} \pi \bar{r}_c^3} = \frac{3}{\bar{r}_c}, \quad (51)$$

where N' is the number of monodisperse fog drops with radius \bar{r}_c which form a 1-cm^3 volume after coalescence.

In the case of polydisperse fog, its specific surface σ_n will be determined in accordance with the definition from expression

$$\sigma_n = \frac{4\pi N' \int_0^\infty n(\rho) \rho^2 d\rho}{\frac{4}{3} \pi N' \int_0^\infty n(\rho) \rho^3 d\rho} = \frac{3 \int_0^\infty n(\rho) \rho^2 d\rho}{\int_0^\infty n(\rho) \rho^3 d\rho}. \quad (52)$$

The two mentioned fogs will be equivalent in terms of specific surface if one assumes

$$\sigma_M = \sigma_n. \quad (52^a)$$

$$\bar{\rho}_s = \frac{\int_0^{\infty} n(\rho) \rho^3 d\rho}{\int_0^{\infty} n(\rho) \rho^2 d\rho} \quad (53)$$

In equating (51) and (52) and solving the thus produced equivalence equation with respect to $\bar{\rho}_s$, we obtain

In making use of (48) and (49), it is easy to produce

$$\bar{\rho}_s = \frac{\bar{\rho}_3^3}{\bar{\rho}_2^2} = \frac{\bar{r}_3^3}{\bar{r}_2^2 r_0} \quad (54)$$

or

$$\bar{r}_s = \frac{\bar{r}_3^3}{\bar{r}_2^2} \quad (55)$$

From expressions (51) and (52) it follows that the magnitude of the specific surface of monodisperse fog is determined only by the drop radius, while the magnitude of the specific surface of polydisperse fog depends both on particle radius as well as on the form of the distribution function.

The magnitude of the specific-surface equivalence radius for empirical distributions is determined by the self-evident approximate formula

$$\bar{r}_s \approx \frac{\sum n_i r_i^3}{\sum n_i r_i^2} \quad (56)$$

In calculating the size $\bar{\rho}_s$ or \bar{r}_s by formulas (53), (54), and (55) if the distribution is given in analytical form, and from (55) and (56) for experimental distributions, we thereby find the size of particles contained in ^a monodisperse fog ~~having~~ a specific surface identical to that of the investigated polydisperse fog. In all cases when the mechanism of the investigated fog phenomenon is determined by the magnitude of specific surface, we can -- in applying the concept

of the specific-surface equivalence radius [REDACTED]--- instead of a polydisperse fog utilize a model of monodisperse fog equivalent only in this respect. Instead of the specific surface we may be interested in the sum of cross-sections per 1 cm^3 of fog liquid water (specific section). In this case, too, the equivalent monodisperse fog will be that, the particle size of which is determinable from formulae (53)-(56). This fact (we shall omit here the derivation of the pertinent formula) makes it possible to considerably widen the scope of application of the specific-surface equivalence radius. We see that the mean size \bar{r}_g corresponds to specific surface g selected as the determining property. As on previous occasions this is the radius of particles present in a monodisperse fog having the same specific surface as the investigated polydisperse fog.

Houghton /31/ was first to use the numerical value of size \bar{r}_g . He has also discovered the experimental numerical closeness between this size and the volume distribution mode. With reference to the volume distribution curve plot he writes /31/:".... the average diameter is approximately equal to the abscissa corresponding to the maximum of the drop-size distribution curve" (page 71).

We shall see later in the text that the numerical closeness between size \bar{r}_g and volume distribution mode r_v could have, indeed, been observed in certain particular cases, but it is not a general statistical rule.

Houghton was unable at that time to reveal the meaning of this mean size and to substantiate the legitimacy of its application to volume distributions. This fact, then, became subsequently the direct cause of the confusion [REDACTED] involved in the problem of mean sizes.

As it follows from our analysis, the size \bar{r}_g with its inherent simple and obvious physical meaning constitutes the mean of size distri-

butions and does not in an obvious way become a part of the system of volume distribution means.

The designation "average" size used by Houghton (and subsequently by other authors), inaccurate as it is, has not only failed in helping to clarify the meaning of this mean, but, on the contrary, has lead in a number of cases /27/, /2/, /25/, to the formation of erroneous ideas about the mean particle sizes of natural fog and clouds.

We have examined in detail the mean sizes r_0 , \bar{r}_1 , \bar{r}_2 , \bar{r}_3 , and r_e which are [REDACTED] quite sufficient for the solution of basic problems arising in the process of statistical investigation of natural clouds and fog as polydisperse systems analyzed in the form of size distributions. Apart from the considered mean sizes, use is made in some studies of the volume distribution mode (see Section 1) expressed in linear measures. This is the size already familiar to us: r_v - the predominant radius in terms of volume. The most probable volume v_0 of distribution (12) corresponding to the maximum of this distribution may be found as the only root of equation

$$\frac{d}{dv} n(v) = 0. \quad (56^a)$$

Then with the aid of v_0 the predominant volume radius may be found from the obvious formula

$$r_v = \sqrt[3]{\frac{3v_0}{4\pi}} \quad (56^b)$$

but it does not coincide with any of the mean sizes in a general case. The predominant volume radius is of no interest for purposes of practical utilization since it is not a mean of size distribution. The predominant surface size r_s is not directly discussed in literature, and will, therefore, not be discussed here.

[REDACTED]
In conclusion we shall pass to the question concerning the relationship of the

distribution means of particle sizes in natural fog and clouds.

8. The Relationship of Mean Sizes.

We have already shown in Section 6 that the distributions of parent population particles in clouds and fogs must necessarily be considered as single-peak distributions with a continuous variate. The form of the law, however, remains unknown.

There arises a ^{problem} ~~question~~ - to define a law of distribution of the parent population, i.e. to find an analytical curve which could in the best possible way fit an empiric distribution or a group of them if all of them are obtained from clouds structurally similar in form. It is ^{smoothing} ~~known~~ from mathematical statistics that a curve capable of ~~fitting~~ an experimental distribution in the best possible way/ ~~is a curve whose~~

theoretical and empirical moments coincide. The theoretic moments in our case are the mean sizes $\bar{p}_1, \bar{p}_2, \bar{p}_3$, and \bar{p}_σ . The same sizes resulting from approximate relationships (46), (48), (50), and (56) may be considered as empirical moments. In solving the problem of finding such a curve it is necessary to have a sufficiently general class of single-hump curves satisfying conditions (2) and ~~depending on the least~~ possible number of parameters. In the capacity of such a class use was made of class (19) previously utilized in Section 2, and exhibiting a generality sufficient for our purposes.

We shall find the mean sizes for this class as functions of parameters m and n .

It is evident that

$$dV = \frac{4}{3} \pi \rho^3 dN = \frac{4}{3} \pi C N \rho^{m+3} e^{-\frac{m}{n} \rho^n} d\rho, \quad (56c)$$

where V - volume of distribution particles numerically equal to

$$V = \frac{4}{3} \pi C N \int_0^\infty \rho^{m+3} e^{-\frac{m}{n} \rho^n} d\rho. \quad (57)$$

In replacing the variables by formula

$$\frac{m}{n} \rho^n = z^n, \quad (57^a)$$

we obtain for (57)

$$\begin{aligned} \frac{4}{3} \pi C N \int_0^\infty \rho^{m+3} e^{-\frac{m}{n} \rho^n} d\rho &= \frac{4}{3} \pi C N \left(\frac{n}{m}\right)^{\frac{m+4}{n}} \int_0^\infty z^{m+3} e^{-z^n} dz = \\ &= \frac{4}{3} \pi C N \left(\frac{n}{m}\right)^{\frac{m+4}{n}} \frac{\Gamma\left(\frac{m+4}{n}\right)}{n}. \end{aligned} \quad (57^b)$$

In substituting the expression C from (19) in the above equation, we produce

$$V = \frac{4}{3} \pi N \left(\frac{n}{m}\right)^{\frac{3}{n}} \frac{\Gamma\left(\frac{m+4}{n}\right)}{\Gamma\left(\frac{m+1}{n}\right)}. \quad (58)$$

On the other hand it is evident that

$$V = \frac{4}{3} \pi N \bar{\rho}_3^3. \quad (58^a)$$

In equating the above equation and (58), we shall obtain the equivalence condition in solving which with respect to $\bar{\rho}_3$ we shall find the expression for the mean cubic size of class (18) curves in a general form

$$\bar{\rho}_3 = \left(\frac{n}{m}\right)^{\frac{1}{n}} \sqrt[3]{\frac{\Gamma\left(\frac{m+4}{n}\right)}{\Gamma\left(\frac{m+1}{n}\right)}}. \quad (59)$$

Similarly in considering surface and size distributions it is possible to obtain an expression for the arithmetic mean and mean quadratic sizes. On the basis of (54), when $\bar{\rho}_3$ and $\bar{\rho}_2$ are known, it is easy to determine the specific-surface equivalence radius $\bar{\rho}_s$.

In omitting the intermediate calculations, we shall write the generalized expressions:

for the arithmetic mean size

$$\bar{\rho}_1 = \left(\frac{n}{m}\right)^{\frac{1}{n}} \frac{\Gamma\left(\frac{m+2}{n}\right)}{\Gamma\left(\frac{m+1}{n}\right)}, \quad (60)$$

for the mean quadratic

$$\bar{\rho}_2 = \left(\frac{n}{m}\right)^{\frac{1}{n}} \sqrt{\frac{\Gamma\left(\frac{m+3}{n}\right)}{\Gamma\left(\frac{m+1}{n}\right)}} \quad (61)$$

and for the specific-surface equivalence radius

$$\bar{\rho}_s = \left(\frac{n}{m}\right)^{\frac{1}{n}} \frac{\Gamma\left(\frac{m+4}{n}\right)}{\Gamma\left(\frac{m+3}{n}\right)}. \quad (62)$$

The mode of volume distribution ρ_v , expressed in fractions of the most probable radius for class (19) curves may be determined in an elementary way and turns out to be equal to

$$\rho_v = \sqrt[n]{\frac{m+3}{m}} \quad (63)$$

A numerical coincidence of sizes $\bar{\rho}_0$ and $\bar{\rho}_v$, observed by Houghton for his experimental curves, which, possibly, has served as a basis for treating these sizes as identical, occurs for class (19) curves at $n = 1$. Houghton's conclusion anent the numerical coincidence of sizes $\bar{\rho}_0$ and $\bar{\rho}_v$ is not contradicted by the experimental data produced by N.V. Kucherov /10/, I.I. Chestnaya /22/, and V.A. Zaytsev /7/. We shall, therefore, seek the best fitting curve among the $n=1$ family of class (19). For this purpose we shall identify certain properties of the family of curves we are interested in. We shall find the expressions for the mean sizes of the family of curves $n=1$ of class (19).

In taking advantage of the well known formula $\Gamma(x+1) = x!$, from which it follows that

$$\frac{\Gamma(x+1)}{\Gamma(x)} = x, \quad (63^a)$$

we shall obtain instead of (60), (59), (61), and (62) the following precise and simple expressions

$$\bar{\rho}_1 = \frac{m+1}{m}, \quad (64)$$

$$\bar{\rho}_2 = \frac{\sqrt{(m+2)(m+1)}}{m}, \quad (65)$$

$$\bar{\rho}_3 = \frac{\sqrt[3]{(m+3)(m+2)(m+1)}}{m}, \quad (66)$$

$$\rho_3 = \frac{m+3}{m}. \quad (67)$$

We shall introduce an auxiliary parameter $\epsilon = \frac{1}{2m}$ and assume

$$(m+2)(m+1) \cong \left(m + \frac{3}{2}\right)^2 \quad (68^a)$$

and

$$(m+3)(m+2)(m+1) \cong (m+2)^3. \quad (67^b)$$

Then instead of (64), (65), (66), and (67) we shall obtain even simpler expressions for the mean sizes:

$$\bar{\rho}_1 = 1 + 2\varepsilon, \quad \bar{r}_1 = r_0(1 + 2\varepsilon), \quad (68)$$

$$\bar{\rho}_2 = 1 + 3\varepsilon, \quad \bar{r}_2 \cong r_0(1 + 3\varepsilon), \quad (69)$$

$$\bar{\rho}_3 = 1 + 4\varepsilon, \quad \bar{r}_3 \cong r_0(1 + 4\varepsilon), \quad (70)$$

$$\bar{\rho}_s = 1 + 6\varepsilon, \quad \bar{r}_s = r_0(1 + 6\varepsilon). \quad (71)$$

Here (68) and (71) are ~~exact~~ expressions. In spite of the fact that (69) and (70) are approximate, the resulting error for $m = 2$ does not exceed 2%. For example, for curve $\rho^2 e^{-2\rho}$ used by A.Kh. Khrgiyan and I.P. Mazin [21], the latter formulae give $\bar{\rho}_1 = 1.50$, $\bar{\rho}_2 = 1.75$, $\bar{\rho}_3 = 1.50$, $\bar{\rho}_s = 2.50$, while the exact values are but slightly differing and are equal to $\bar{\rho}_1 = 1.50$, $\bar{\rho}_2 = 1.73$, $\bar{\rho}_3 = 1.96$, $\bar{\rho}_s = 2.50$.

At higher m values the error becomes negligibly small.

An important property of the $n = 1$ family of class (19) curves follows from (68), (69), (70), and (71). In passing from one mean size to another they change by a definite value multiple ~~of~~ the integer $\varepsilon = \frac{1}{2m}$. Moreover, the arithmetic mean size for the $n=1$ family is always larger than the most probable size by $2\varepsilon r_0$, and the specific-surface mean - by $6\varepsilon r_0$. This enables the investigator, if the mean sizes are known, to produce a definite answer to the question of whether a given experimental distribution may be considered as satisfying the $n=1$ family of class (19).

It is well known that the most probable size for arbitrary experimental distributions cannot be calculated. We shall attempt to produce an analytical expression of r_0 for the $n=1$ family for the case of any m 's. It follows from (68), (70), and (79) that:

$$\bar{\rho}_s - \bar{\rho}_1 = 4\varepsilon, \quad (71^a)$$

$$\bar{\rho}_s - \bar{\rho}_3 \cong 2\varepsilon, \quad (71^b)$$

$$\bar{\rho}_3 - \bar{\rho}_1 \cong 2\varepsilon, \quad (71^c)$$

whence,

$$6\varepsilon \cong \bar{\rho}_s - \bar{\rho}_1 + \frac{1}{2}(\bar{\rho}_s - \bar{\rho}_3) + \frac{1}{2}(\bar{\rho}_3 - \bar{\rho}_1) \cong \frac{3}{2}(\bar{\rho}_s - \bar{\rho}_1), \quad (71^d)$$

and if one considers (64) and (67), then instead of an approximate

expression it becomes possible to write an exact expression in the form of

$$\frac{3}{2}(\bar{\rho}_2 - \bar{\rho}_1) = 6\epsilon. \quad (71^e)$$

Hence, for the most probable unit size value one may write

$$\bar{\rho}_2 - 6\epsilon = \bar{\rho}_2 - \frac{3}{2}(\bar{\rho}_2 - \bar{\rho}_1) = \frac{3\bar{\rho}_1 - \bar{\rho}_2}{2} = 1. \quad (71^f)$$

In passing on to dimensional presentation, we produce an expression for the most probable size

$$r_0 = \frac{3\bar{r}_1 - \bar{r}_2}{2}. \quad (72)$$

Formula (72) is exact from the analytical point of view. Stochastically its accuracy is not inferior to that of the well known formulae (46), (48), (50), and (55).

In making use of formula (72), and utilizing the known values of \bar{r}_1 and \bar{r}_2 , the most probable size may be determined more precisely than from a distribution curve.

Incorporated in Table 5 are the calculated values of the mean sizes for different m 's

T a b l e 5

ρ	m									
	1	2	3	4	5	6	7	8	9	10
$\bar{\rho}_1$	2,00	1,50	1,33	1,25	1,20	1,17	1,14	1,12	1,11	1,10
$\bar{\rho}_2$	2,22	1,73	1,49	1,37	1,30	1,25	1,21	1,18	1,17	1,15
$\bar{\rho}_3$	2,88	1,96	1,64	1,49	1,39	1,33	1,28	1,24	1,22	1,20
$\bar{\rho}_4$	4,00	2,50	2,00	1,75	1,60	1,50	1,43	1,38	1,33	1,30

In order to find the equation of a curve satisfying the experimental distribution, it is necessary, in using formula (72), to determine the empirical moments $\frac{\bar{\rho}_2}{\bar{\rho}_0}$, $\frac{\bar{\rho}_3}{\bar{\rho}_0}$, and $\frac{\bar{\rho}_4}{\bar{\rho}_0}$, and to make sure that they are compatible with (64) - (67) with respect to their differences. If the increments of the moments satisfy (64) - (67) then it can be said that the experimental distribution is described by the family of curves $n = 1$.

Thereupon one looks for such an integer m in Table 5 for which the mean size ratio \bar{p}_1 complies best of all with the experiment.

If there are no doubts that the experimental distribution belongs to the $n = 1$ family, a simpler method of parameter m determination may be used and, consequently, also of determining the analytical expression of the curve for the experimental distribution. The essence of this method consists in the following. In utilizing (64) and (67) a ratio of moments or mean sizes is composed

$$\frac{\bar{p}_2}{\bar{p}_1} = \frac{\bar{r}_2}{\bar{r}_1} = \frac{m+3}{m+1}, \quad (72a)$$

the numerical values \bar{p}_2/\bar{p}_1 of which for different m 's are given in Table 6.

T a b l e 6.

m	1	2	3	4	5	6	7	8	9	10
$\frac{m+3}{m+1}$	2,00	1,67	1,50	1,40	1,33	1,29	1,25	1,22	1,20	1,18

In composing the ratio of sizes $\frac{\bar{r}_2}{\bar{r}_1}$ for the analyzed experimental distribution, which is numerically equal to $\frac{\bar{p}_2}{\bar{p}_1}$, and making use of Table 6, it is easy to find an integer m , and, consequently, the corresponding equation.

Both above methods are variants of the method of moments. The first method is described by us for the sake of consistency and ~~completeness~~ of the discussion, the second for purposes of practical application. Both methods are practically equivalent from the point of view of accuracy and yield identical results. This is attributable to the fact that \bar{p}_2 is a moment of a higher order than \bar{p}_1 and \bar{p}_3 and, in addition to that, in accordance with (54) it constitutes an explicit function of \bar{p}_3 and \bar{p}_1 and, therefore, also of both \bar{r}_3 and \bar{r}_1 which are not explicitly utilized in the second method.

After the selection of an integer m from Table 6 the particle-size distribution function for family $n=1$ of class (19) may be written in the form

$$n(\rho) = \rho^m e^{-m\rho}$$

(73)

or in the corresponding dimensional form, a transition to which does not present any particular difficulty.

The questions of the accuracy in determining $\bar{p}_0, \bar{p}_1, \bar{p}_2$, and $n(p)$ from the stochastic standpoint are not considered in this paper since this transcends the scope of the investigation. The more so, because in the form of the goodness-of-fit test of the empiric and theoretical distributions they are comprehensively discussed in textbooks on mathematical statistics.

All the published distribution functions for fog and cloud particles /23, 21, 24, 11, etc./ are particular cases of the class of curves (19) and its family (73) proposed by us /5/.

In K.S. Shifrin's and N.P. Bogdanovskaya's paper /24/ a four-parameter class of curves ~~is~~ utilized, from which a curve of best possible fit may be selected. An increase in the number of parameters in this case is related to the fact that the coefficient at the particle size in the exponent (in our designations - $\frac{m}{n}$) and the normalizing ~~constant of~~ the distribution are assumed to be its independent parameters.

Actually, as we were able to show, both these quantities are functions of two independent distribution parameters and do not possess the property of independence. Hence, an increase of the number of parameters cannot be considered ^{as} substantiated in this case.

In the method proposed by L.M. Levin /11/ the mean sizes or the corresponding moments of the experimental distribution are not calculated. This simplifies the selection of a curve from a one-parameter family. However, Levin does not offer a method permitting to determine whether the investigated experimental distribution actually belongs to a single-parameter family of curves. In view of this fact, and also because the geometric constructions introduce an indefinite arbitrariness in the matter of ~~curve~~ curve parameter selection, the potentialities of Levin's method are restricted ~~in terms of accuracy.~~

In conclusion we shall find the relationship which makes it possible on the basis of mean sizes to determine by analytical method the value of parameter m and, consequently, also to find the equation of the curve smoothing the experimental distribution.

In utilizing (68) and (71), we note that

$$\bar{\rho}_2 - 1 + \bar{\rho}_2 - \bar{\rho}_1 = 10\epsilon. \quad (73^a)$$

In order to produce the final expression this equation must be solved with respect to ϵ , which should be replaced by m in accordance with formula $\epsilon = \frac{1}{2m}$, whereupon in dimensional form we obtain

$$m = \frac{2\bar{r}_1}{\bar{r}_2 - \bar{r}_1} - 1. \quad (74)$$

Formula (74), when the mean sizes of the experimental distribution \bar{r}_2 and \bar{r}_1 are known, permits the curve parameter m to be calculated analytically up to ITS FRACTIONAL VALUES IN A SIMPLE AND EXACT MANNER. In this case there is no need to resort to graphic constructions, as this is required in Levin's method /11/.

9. A Few Experimental Data.

All the deductions and corollaries ensuing from the consideration of the problem of natural fog and cloud particle size determination by sampling method which were recorded so far need, of course, to be compared with experimental data, just as the results of any theoretical research. In part this was already done in the process of discussion. For example, in Section 2 with regard the height-of-curve evaluation, in Section 3 in connection with the problem of the finiteness of the interval width, and in Section 6 in analyzing the "law of multiple masses". A comparison of the contents of other sections with experimental data does not appear possible owing to the unavailability of published experimental materials suitable for this purpose. The experimental data discussed in this section are, therefore, designed to fill in this gap.

The experimental part of the study includes:

- a) verification of the applicability of formula (34) to experimental

distributions of fog and cloud particles;

b) investigation of the statistical filling of ^{the} experimental curve;

c) practical application of the method of moments in the analysis of experimental distributions.

The first two problems were solved by means of the ~~serial sampling~~ ~~method~~ ~~well known in statistics~~. This method, which so far was not applied in microphysical investigation of fog and clouds, essentially consists in the following. A random sample of large volume consisting of a group or series of small samples, also randomly taken, is drawn from a homogeneous set of particles. To elucidate the question of the curve of best possible fit, several experimental distributions were produced. The mean sizes of these distributions made it possible for the first time to utilize the method of moments.

All particle size measurements were carried out by the commonly known /1/ method of photomicrography of particles suspended in a thin layer of oil. The filming was made through GOMAZ microscope on a standard positive cinematographic film (80° KhD) with the aid of a "Sport" mirror camera. Total magnification (magnification of filming and projection) was equal to 1000. Fog moisture was measured by means of an aspiration psychrometer by the method proposed by O.V. Levitskiy /17/, and was found to be equal to 100% in all cases.

The experimental data are recorded in five appendices in the form of 7 distributions. They were produced on the basis of 63,547 particle measurements. Incorporated in appendices 1, 2, and 3 are the data on size distributions of particles of advection fogs observed ~~an~~ late fall of 1946 over LAKE LABOGA in the region of Priozersk. The observations were carried out ^{from} ~~a~~ sand bar protruding far into the open lake.

The data illustrating the conditions under which these fog observations were carried out are furnished in Table 7.

Table 7.

Appendices.	Air temperature in degrees		Surface water temperature in degrees	Wind		Visibility range, m.
	at 2-m altitude.	at water level		velocity m/sec.	direction	
2	3,6	3,9	5,4	8-10	W	500
3	1,0	3,0	5,0	2-3	SWW	500
1	-1,2	-0,2	4,2	3-4	SW	200

In other appendices (4 and 5) are represented four distributions obtained for radiation fog particles observed at the outskirts of Leningrad (Novaya Derevnaya) in summer and fall, 1948. The radiation fogs were observed in night-time at the fringe of a large field without any trees or buildings. As a rule, there was no wind.

The mean sizes \bar{r}_1 , \bar{r}_2 , \bar{r}_3 and \bar{r}_6 were calculated for all the plotted experimental distributions.

[REDACTED] Filming of 30,000 particles simultaneously drawn from natural advection-origin fog was made for experimental clarification of the questions connected with the application of formula (34). This fog was observed for several hours without noticeable variation of visibility (300 - 500 m) and size of particles, on November 3, 1946. Sampling for oil tests was made on a sand bar extending far into the open lake, and the pictures were taken right away on the spot.

The particle size data were represented in the form of 100 separate experimental curves, each curve covering a sample volume of 300 particles. Complete information relative to these curves, as well as the general distribution, will be found in Appendix 1. On the basis of these data deviation distributions were obtained for each i -th interval. For the sake of brevity deviation will be referred to as the difference

$$/n_{ij} - \bar{n}_i/,$$

wherein \bar{n}_i is the mean or most probable [REDACTED] frequency value of the i -th interval, and j - the ordinal number of the curve in the series.

The experimental values of relative error D_1 with reliability α were determined from the deviation distributions. An error with reliability α

(determined experimentally) was considered to be that deviation which was exceeded for the investigated interval in 100 α -cases. Relative errors D_1 with two reliability values: $\alpha_1 = 0.68$, and $\alpha_2 = 0.96$ were experimentally obtained in this manner. To avoid the effect of supplementary errors arising from measurement of excessively fine drops, only the intervals situated to the right of the experimental curve maximum were subjected to investigation. The graph in Fig. 8 shows the experimentally evaluated errors D_1 accompanied by the [redacted] corresponding curves of relative errors calculated from formula (34). A comparison of the experimental data with the theoretical curve shows that formula (34) satisfies the conditions of the experiment over a wide range of frequencies. For the small frequencies (fractions of ten) the real errors were found noticeably to be [redacted] exceeding the calculated values. An explanation for this experimentally observed phenomenon is provided by V.I. Romanovskiy /14/. He has shown theoretically that in case of a small number of measurements the estimates of errors, in accordance with the classical statistical theories, lead to results characterized by [redacted] higher precision. In referring the reader interested in greater details to the above source, we shall [redacted], for purposes of comparison, reproduce here a theoretical curve plotted in accordance with Romanovskiy's [redacted] ideas, and our own experimental data which confirm these views (Fig. 9).

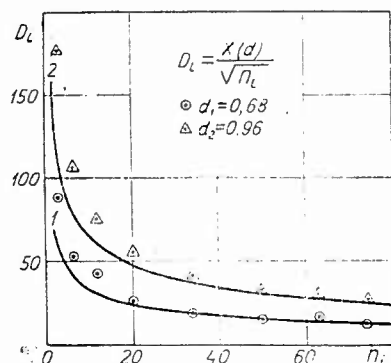


Fig. 8. Statistical errors of experimental distributions in relation to the concentration of particles in the interval and the reliability parameter.

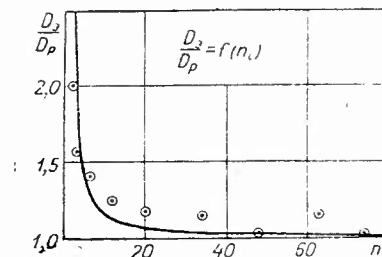


Fig. 9 Statistical errors for the case of small frequency ratios.

We can thus see that formula (34) is entirely suitable for a practi-

cal estimate of errors in those intervals of experimental distributions whose frequencies are not too small. For frequencies of the order of fractions of ten formula (34) yields appreciably underrated results.

Let us turn now to experimental distributions in which it is possible to trace the process of statistical filling. As a typical example we shall examine the distribution obtained for the particles of a radiation fog observed in the night of August 12, 1948 at the outskirts of Leningrad in the region of Novaya Derevnja (Appendix 4). This distribution with the sample

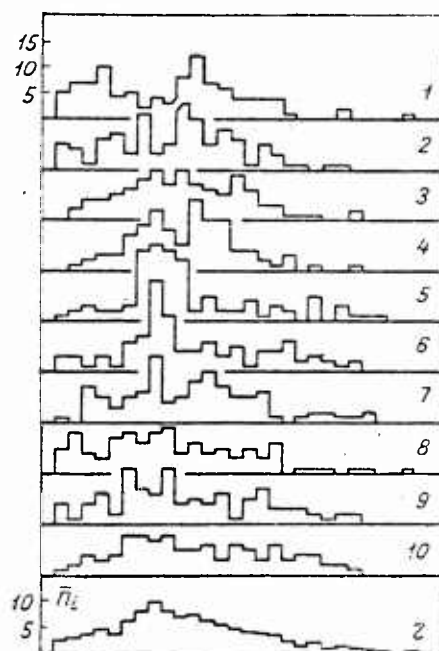


Fig.10. Experimental distribution (1000 particles) and its 10 components.

component curves, each with 100 particles, are shown in Fig.10.

The general distribution, as it may be seen from Fig.10, has a single peak, whereas the individual component distributions, almost all, have several peaks. Essential, however, is the fact that each of these 10 curves does not resemble the initial distribution of which each of them is a random sample. Concentrated about the maximum of the full curve are about 100 particles. The maxima of the individual curves of the series, each, on the average, contain about 10 particles. The calculated relative error in the maximum determination in the case of statistical filling diminishes from 64% for 10 particles to 20% for 100 particles per interval. The degree of statistical concentration in each of the 10 curves may be considered as the beginning of the main shaping stage (II stage).

Experimental curves in the initial shaping stage (I stage) may be obtained and similarly analyzed, if one of the 10 curves with a sample volume comprizing 100 particles be visualized as consisting, in turn, of

a series of experimental curves with a still smaller sample volume. We shall refrain from doing so because there is no need for this. Among the published experimental distributions there is a considerable number of curves the formation of which was discontinued at the initial shaping form. Out of a total of 134 experimental curves produced by M. Diem /27/ /28/, 40 are plotted on the basis of measurement of 50 particles and less, as this may be seen from Table 3.

The position of the interval with the greatest concentration of particles varies in the process of statistical filling.

The interval containing the mode of the distribution becomes finally evident by the end of the main shaping stage. The maxima of accidental multimodality in the process of filling of the experimental curve (after the basic maximum has been finally formed) shift into the region of intervals with lesser statistical concentration. This may be observed on all experimental curves with a sufficient sample volume. The subsequent displacement of accidental maxima into the region of the curve tails may be observed ⁱⁿ the distribution of 30,000 particles, which was already discussed, and also in the cases of two curves with a larger sample volume (Appendices 2 and 3).

Thus, the results obtained in the study of the process of experimental curve formation by method of serial samples (the results were partly represented in Fig.10) fully confirm the character of statistical filling discussed in Section 6.

In conclusion we shall attempt to apply the method of moments to clarify the question concerning the shape of the curve of the best fit for distributions in fog.

Incorporated in Table 8 are the ratios of the mean sizes obtained by us ^{experimentally} for advection and radiation fogs (Appendices 1-5), and also the values of parameter m , calculated for our distributions from formula (74).

T a b l e 8.

Moment or mean size.	F o g						
	advection (1946)			radiation (1948)			
$\bar{\rho}_1$	1,35	1,35	1,24	1,23	1,17	1,12	1,10
$\bar{\rho}_2$	1,55	1,51	1,35	1,34	1,27	1,19	1,15
$\bar{\rho}_3$	1,76	1,68	1,40	1,45	1,34	1,25	1,17
$\bar{\rho}_\sigma$	2,23	2,06	1,73	1,69	1,50	1,37	1,30
$m_{calc.}(74)$	2,1	2,8	4,1	4,9	6,0	8,0	9,9
Appendix No.	3	2	1	4	5a	5b	5b

Comparison of Table 8 experimental data with the calculated data of Table 5 shows a good agreement of the mean size ratios.

The data of Table 8 reveal a substantial difference in the relationship between the mean sizes for radiation and advection fogs. Two curves are plotted in Fig. 11, one of which ($m = 6$) corresponds to the moderately skewed distributions (radiation fog); the other ($m = 3$) complies with the experimental distributions manifesting a considerable skewness (advection fog).

The experimental curves for fogs of advection nature are constructed in the form of volume distributions and have a mode displaced to the right with respect to $\frac{\bar{r}_s}{r_0} \approx 2$, while for radiation fogs this ratio is smaller averaging about 1.5. In utilizing these relationships, and bearing in mind the fact that Houghton /31/ plotted his volume distributions precisely for fogs of advection origin, we may estimate the most probable particle size of American fogs at 10 - 12.5 microns (in radius) instead of 40 - 50 microns as indicated by Houghton /31/ for the predominant diameter in terms of volume. Houghton's data, therefore, indirectly confirm the presence of a considerable skew in the size distributions observed by him in advection fogs.

The results of our evaluation agree with the results of a recalculation of the American curves undertaken by B.V. Kiryukhin /9/.

As to the structure of clouds, it is known that the most symmetrical distributions are observed for St, and the most skewed ones - for Ns.

The other cloud forms occupy an intermediate position.

V.A. Zaytsev /7/, for cauliflower clouds, and A.M. Borovikov /1/, for the remaining forms, have established the fact that the bases of clouds with noticeable vertical development are characterized by an

almost symmetrical distribution curve. For the central and top parts of clouds, however, a distribution manifesting a moderate or noticeable skew in the direction of large drops is to be registered. This phenomenon is so clearly displayed that it is possible

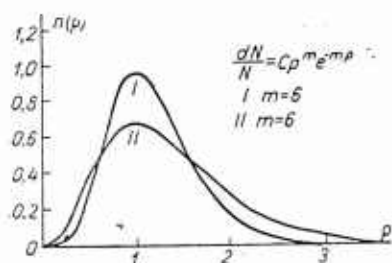


Fig.11. Particle distribution functions:

I - radiation fog; II - advection fog. (1, 1.08, 1.12, 1.15, 1.23) at the lower boundary of Ns than at the upper boundary of St (1, 1.16, 1.24, 1.32, 1.57). The parenthesized mean sizes result from the observations carried out by A.M. Borovikov. The sample volumes are: 1169 and 1029 drops for Ns and St, respectively.

With regard to the shape of the experimental distribution curves, we were unable to establish a difference between the clouds and fogs on the whole. Nevertheless, a conclusion suggests itself about the structural similarity between the lower boundary zone of clouds with a considerable vertical development and radiation fogs, on the one hand, and between the middle and upper sections of the same type of clouds and advection fogs, on the other hand.

The number of observed cases is, however, insufficient to consider the question of the mentioned structural differences as satisfactorily answered. It is hoped that further accumulation of empiric data and the application of the method of moments will enable future investigators to estimate the structural characteristics of fogs and clouds, not only qualitatively, but quantitatively as well, depending on the conditions of their formation.

C o n c l u s i o n s .

The experimental problem of size determination of natural fog and cloud particles by sampling method was discussed in this paper from the positions of statistical probability. The principal results and conclusions of this research consist in the following:

1. It has been established that the American method of experimental curve construction developed in Houghton's works, in contrast with the method adopted in the USSR and in Europe, is statistically inconsistent.

2. It has been shown that the evaluation of the experimental distribution peakedness as carried out by Houghton is wrong.

3. A new characteristic -- the height of ^{experimental} curve -- which was utilized in this paper in the solution of a number of concrete problems, has been introduced. As a result of a comparison with the experimental data it has been shown that a value approaching unity may be used as the most probable value of the altitude of an experimental curve.

4. A new class of single-peak curves, whose shape is a function of two parameters, was proposed. For this class of curves manifesting a peakedness close to unity a relationship was demonstrated between the height of the curve and its width.

5. The influence of the finiteness of the interval width was investigated, as a result of which an effective selection both of the interval widths and the number of intervals was found to be possible for natural fog and cloud experimental distributions.

6. The effect of the finiteness of the sample volume was investigated. It was shown thereby that the frequencies n_i , if the intervals are small enough, may be approximately considered as independent, and a polydisperse fog or cloud may be assumed as consisting of a finite number of monodisperse components. ↑

3. (The possibility of estimating the accuracy at a given point of

of an experimental curve with due consideration of measurement reliability was substantiated for the case when the width of the intervals is smaller than the most probable size.

7. An analysis of experimental distributions has shown that an incorrect statistical approach to the problem of particle size determination for natural fogs and clouds often leads to the publication of data which turn out to be inadequate in view of the extremely small number of measured drops.

8. In investigating the amplitudes of multimodal experimental distributions, ^{IT WAS SHOWN THAT} Köhler has wrongly utilized the errors with low reliability and has infringed upon the principle of the randomness of samples which caused him to formulate an erroneous hypothesis.

9. A sufficiency test was established permitting rational selections to be made of the sample volume for a newly plotted empirical curve, depending on the statistical error in the interval of the greatest particle concentration, the width of the interval, reliability of measurement, and the most probable size and height of curve.

10. Proposed was a method of experimental curve multimodality analysis with the view to establishing the character of the curve (method of the error envelopes), which is a further development of Prof. A.K. Mitropol'skiy's ideas.

11. The problem concerning the multimodality of experimental distributions in connection with the character of their statistical filling was investigated. The process of complete shaping of the experimental curve was examined and found to be consisting of three stages substantially differing by character of the sample's statistical representativeness.

12. It was demonstrated that the multimodal character of the overwhelming majority of experimental distributions involving the particles of natural fogs and clouds is not authentic. The reason for the experi-

mentally observed accidental multimodality is to be sought in the inadequacy of the sample volumes.

13. In accordance with the basic principles of mathematical statistics a new physically substantiated system of size distribution means has been developed.

14. The mean sizes were for the first time used in finding a curve which in the best possible manner smooths ^{an} investigated experimental distribution for the case of natural fogs (method of mean size ratios, or method of moments).

15. The method of mean size ratios was applied to establish the structural distinctions between distributions for fogs of ^{radiation} and advection origin. A comparison with vertically developed clouds has shown that radiation fogs are structurally similar to the lower boundary zone of clouds, whereas advection fogs are analogous to the central and upper portions of clouds.

16. Some results described in this paper were compared with the experimental data published in the studies of other authors. A comprehensive statistical survey, which comprizes the experimental part of this study, was carried out in order to check the principal results. The method of serial samples was selected as the working method and was found to have entirely proved its value. Comparison with experimental data has shown satisfactory agreement.

References.

1. Borovikov A.M. Transactions of TsAO, No.3, 1948
2. Gertner G. Prozrachnost' zamutnennoy atmosfery dlya infrakrasnykh voln (Transmittance of Atmospheric Turbidity for Infrared Waves). Gosenergoizdat, 1949.
3. Deryagin G., Vlasenko G. DAN SSSR, vol. XIII, No.2, 1948.
4. D'yachenko P.V. Meteorologiya i gidrologiya (Meteorology and Hydrology) No.10, 1951.
5. D'yachenko P.V. Opyt primeneniya metodov matematicheskoy statistiki v izucheniye struktury yestestvennykh tumanov (Experimental Application of Mathematical Statistics Methods To Structural Research of Natural Fogs. Author's Report, Leningrad State University (LGU), 1950.
6. Zaytsev V.A, Transactions of GGO, No.9 (71), 1948.
7. Zaytsev V.A. Transactions of GGO, No.13(75), 1948.
8. Katchenkov S.M. Transactions of the Leningrad Institute of Experimental Meteorology, No.1, 1937.
9. Kiryukhin B.V. Transactions of NIU GUGMS, series 1, No.28, 1946.
10. Kucherov N.V. Transactions of GGO, No.6(68), 1947.
11. Levin L.M. (On the Size Distribution Functions of Cloud Drops. The Optical Density of Clouds) O funktsiyakh raspredeleniya oblachnykh kapel' po razmeram. Opticheskaya plotnost' oblaka. Izv. AN SSSR, ser. geofiz., No.10, 1959.
12. Mitropol'skiy A.K. Tekhnika statisticheskogo ischisleniya (The Technique of Statistical Analysis). Gos. izd-vo s.-kh. i kolh-koop literatury (State Publishing House of Agricultural and Collective-Cooperative Farming Literature), Moscow-Leningrad, 1931.
13. Romanovskiy V.I. Matematicheskaya statistika (Mathematical Statistics) GONTI NKTP SSSR, Moscow-Leningrad, 1938.
14. Romanovskiy V.I. Osnovnyye zadachi teorii oshibok (THE Main Problems of the Theory of Errors), Gostekhzdat, 1947.
15. Selezneva Ye.S. Transactions of NIU GUGMS, series 1, No.7, 1945.
16. Selezneva Ye.S. Meteorologiya i gidrologiya, No.2, 1948.
17. Sternzat M.S. Transactions of NIU GUGMS, ser. 1, No.23, 1948.
18. Tarayan G.I. Transactions of the Leningrad Institute of Experimental Meteorology, No.1, 1937.
19. Tverskoy P.N. Vesnik LGU (Bulletin of the Leningrad State University), No.1, 1947.

20. Fuks N. Zhurnal eksperimental'noy i teoreticheskoy fiziki (Journal of Experimental and Theoretical Physics), v. 7, No.4, 1947.
21. Khrigan A.Kh., Mazin I.P. Transactions of TAO, No.7, 1952.
22. Chestnaya I.I. Transactions of GGO, No.7(69), 1948.
23. Shishkin N.S. Transactions of GGO, No.7(69), 1948.
24. Shifrin K.S., Bogdanova N.P. K teorii vliyaniya tumana na radiatsionnyy balans (To the Theory of Fog Effect on Radiative Equilibrium), Transactions of GGO, No.46(108), 1955.
25. Bricard J. La Meteorologie, 1943, Jul-Dec.
26. Defant A. Wein Sitz. Ber. Mat-nat. Kl. B., 114, 1905.
27. Diem M. Ann. d. Hydrographie u Marit. Meteorologie, H.V., 1942.
28. Diem M. Meteorologische Rundschau, H. 9/10, 1948.
29. Findeisen W. Gerl. Beitr. z. Geophysik. Bd 35, 1932.
30. Hagemann V. Gerl. Beitr. z. Geophysik, Bd. 46, 1936.
31. Houghton H, Radford W. Papers of Phys. Ocean. and Meteorology, MIT., v. VI, No.4, 1938.
32. Köhler H. Meddelanden fran statens Met.-Hydrograf. Anst., Bd.2, No 5, 1925
33. Köhler H. Met. Zeitschrift, Bd. LXVI, 1929.
34. Miderdorfer E. Met. Zeitschrift, Bd. 49, 1932.

Note: TAO - Central Aerological Observatory.

DAN SSSR - Reports of the USSR Academy of Sciences.

GGO - Main Geophysical Observatory

GUGMS - Main Administration of Hydrometeorological Service.

Izv. AN SSSR - Bulletin of the USSR Academy of Sciences,

GONTI NKTP SSSR - State General Scientific and Technical Publishing House of the People's Commissariat of Commerce and Industry of the USSR.

Pages 45-47.

Prilozheniye = Appendix
Seriynnye chastoty * Serial frequencies.

r_{12}	Serial frequency																
	1	2	3	4	5	6	7	8	9	10	11	12	13	14	15	16	17
1	—	—	—	—	—	—	—	—	—	—	—	—	—	—	—	—	—
2	28	28	30	28	22	24	33	17	45	25	58	36	26	35	26	42	32
3	56	47	64	58	55	59	54	59	60	51	55	61	74	54	79	62	82
4	69	70	72	71	76	62	64	77	66	79	79	87	78	87	75	79	74
5	51	50	46	52	49	53	45	63	58	59	48	42	58	51	52	50	42
6	37	48	35	35	41	37	35	29	32	40	27	32	28	42	28	34	33
7	23	29	23	21	32	26	36	29	21	27	18	17	19	16	17	10	16
8	17	7	14	15	7	20	18	9	12	4	7	10	6	9	6	5	9
9	7	14	7	9	8	7	10	9	2	7	4	6	5	3	6	5	6
10	6	2	3	7	5	4	1	6	1	4	2	5	3	1	6	7	1
11	2	4	3	2	2	5	3	2	—	1	1	2	1	1	4	2	2
12	4	1	1	—	2	—	—	—	2	2	1	2	2	1	1	1	1
13	—	—	1	1	—	3	1	—	—	1	—	—	—	—	2	1	—
14	—	—	—	1	1	—	—	—	—	—	—	—	—	—	1	—	2
15	—	—	—	—	—	—	—	—	—	—	—	—	—	—	—	—	—
16	—	—	1	—	—	—	—	—	1	—	—	—	—	—	—	—	—
17	—	—	—	—	—	—	—	—	—	—	—	—	—	—	—	—	—
18	—	—	—	—	—	—	—	—	—	—	—	—	—	—	—	—	—
19	—	—	—	—	—	—	—	—	—	—	—	—	—	—	—	—	—

r_{12}	Serial frequency																
	18	19	20	21	22	23	24	25	26	27	28	29	30	31	32	33	34
1	—	—	—	—	—	—	—	—	—	—	—	—	—	—	—	—	—
2	37	23	26	26	39	24	36	43	25	35	31	35	19	31	33	24	31
3	68	54	56	54	52	50	43	57	64	46	55	51	62	77	42	59	52
4	83	99	77	68	74	68	89	69	74	67	79	65	85	56	82	74	76
5	42	55	48	37	49	55	51	35	44	51	50	72	46	43	45	50	45
6	30	37	41	33	30	41	35	36	37	39	35	25	41	37	49	29	37
7	19	13	24	17	18	21	14	30	19	25	21	19	16	22	20	25	20
8	9	3	18	9	12	25	21	15	19	22	10	16	18	19	14	12	13
9	6	8	7	8	9	12	6	4	6	9	6	4	7	7	8	9	18
10	2	5	1	3	7	3	3	3	6	2	4	5	4	5	2	11	5
11	3	1	2	7	3	—	—	5	3	2	4	3	1	1	3	6	2
12	1	1	—	1	2	1	1	1	1	2	1	3	1	1	2	—	—
13	—	1	—	—	3	—	—	2	—	—	—	—	—	—	—	1	—
14	—	—	—	—	1	—	1	—	1	1	1	1	—	—	—	—	1
15	—	—	—	—	1	—	—	—	—	—	—	—	—	—	—	—	—
16	—	—	—	—	—	—	—	—	—	—	1	1	—	—	—	—	—
17	—	—	—	—	—	—	—	—	—	—	—	—	—	—	—	—	—
18	—	—	—	—	—	—	—	—	—	—	—	—	—	—	—	—	—
19	—	—	—	—	—	—	—	—	—	—	—	—	1	—	—	—	—

r_{ik}	Serial frequency																
	35	36	37	38	39	40	41	42	43	44	45	46	47	48	49	50	51
1	—	—	—	—	—	—	—	—	—	—	—	—	—	—	—	—	—
2	30	17	23	21	30	26	46	48	33	39	37	47	30	31	20	38	31
3	57	59	68	70	55	49	56	81	78	62	65	60	62	71	73	47	61
4	80	85	78	85	81	84	72	56	61	64	63	71	66	68	85	85	57
5	50	51	53	36	33	40	47	34	44	48	44	43	56	49	51	58	70
6	42	31	30	29	32	44	22	28	32	32	38	40	36	39	36	29	48
7	20	18	21	21	26	12	16	18	23	18	21	15	24	19	18	18	19
8	9	20	14	16	21	19	18	14	16	15	14	8	13	12	6	12	7
9	5	9	7	13	15	10	6	13	7	10	11	8	5	4	6	7	3
10	3	2	5	4	5	6	6	4	3	6	4	2	1	2	2	3	3
11	1	4	—	3	1	4	7	2	2	4	1	4	3	4	1	1	—
12	2	2	1	2	—	4	3	1	—	2	2	1	2	1	2	1	1
13	—	—	—	—	1	1	1	—	—	—	—	1	—	—	—	1	—
14	—	2	—	—	—	—	—	—	—	—	—	—	—	—	—	—	—
15	1	—	—	—	—	1	—	—	—	—	—	—	—	—	—	—	—
16	—	—	—	—	—	—	—	—	—	—	—	—	—	—	—	—	—
17	—	—	—	—	—	—	—	—	—	—	—	—	—	—	—	—	—
18	—	—	—	—	—	—	—	—	—	—	—	—	—	—	—	—	—
19	—	—	—	—	—	—	—	—	—	—	—	—	1	—	—	—	—

r_{ik}	Serial frequency																
	52	53	54	55	56	57	58	59	60	61	62	63	64	65	66	67	68
1	—	—	—	—	—	—	—	—	—	—	—	—	—	—	—	—	—
2	30	41	39	39	30	37	32	49	37	42	40	43	50	41	35	34	34
3	81	77	73	76	64	70	73	70	75	57	81	62	74	74	60	61	47
4	67	75	68	70	74	81	87	81	81	72	93	83	90	84	84	83	92
5	57	34	56	54	50	58	41	47	52	61	93	45	42	37	57	46	37
6	32	26	41	34	42	26	39	32	26	35	34	32	24	29	38	38	39
7	22	25	12	14	21	14	13	9	15	13	14	17	13	17	17	20	20
8	9	10	2	6	10	5	6	8	8	6	5	6	7	5	3	10	15
9	2	7	3	4	2	4	2	—	3	1	4	1	4	4	3	4	8
10	—	1	3	2	3	3	2	2	3	2	1	—	2	2	1	2	4
11	—	1	2	—	2	1	2	1	—	2	1	—	—	1	1	2	3
12	—	2	—	—	1	1	3	1	—	—	—	—	1	—	1	—	1
13	—	1	1	1	—	—	—	—	—	—	—	—	—	—	—	—	—
14	—	—	—	—	1	1	—	—	—	—	—	—	—	—	—	—	—
15	—	—	—	—	—	—	—	—	—	—	—	—	—	—	—	—	—
16	—	—	—	—	—	—	—	—	—	—	—	—	—	—	—	—	—
17	—	—	—	—	—	—	—	—	—	—	—	—	—	—	—	—	—
18	—	—	—	—	—	—	—	—	—	—	1	—	—	—	—	—	—
19	—	—	—	—	—	—	—	—	—	—	—	—	—	—	—	—	—

$r_i \mu$	Serial frequency																
	69	70	71	72	73	74	75	76	77	78	79	80	81	82	83	84	85
1	—	—	—	—	—	—	—	—	—	—	—	—	—	—	—	—	—
2	24	26	35	37	38	41	39	24	44	51	38	49	34	25	56	45	52
3	68	55	51	49	64	72	58	57	60	67	63	69	87	76	70	68	68
4	71	78	77	72	62	67	63	102	78	76	77	58	74	90	61	68	64
5	41	45	50	58	51	38	49	47	35	33	41	41	44	36	48	41	36
6	48	35	30	36	37	36	31	23	47	36	31	41	22	32	30	34	29
7	14	23	26	26	17	21	24	14	20	14	22	18	14	17	13	15	17
8	19	19	20	8	12	12	12	13	8	6	15	15	14	12	5	15	12
9	5	6	8	8	9	9	9	11	4	9	8	3	5	3	9	6	9
10	5	10	3	3	3	2	6	1	1	1	1	4	2	4	4	4	6
11	1	2	—	—	3	2	3	5	3	4	4	2	1	2	2	2	6
12	2	—	—	1	2	—	—	2	—	—	—	—	2	1	1	1	1
13	—	1	—	—	2	—	—	—	—	1	—	—	—	—	1	1	—
14	1	—	—	2	—	—	—	1	—	—	—	—	—	—	2	—	—
15	—	—	—	—	—	—	—	—	—	—	—	—	—	1	—	—	—
16	1	—	—	—	—	—	—	—	—	1	—	—	1	—	—	—	—
17	—	—	—	—	—	—	1	—	—	—	—	—	—	1	—	—	—
18	—	—	—	—	—	—	—	—	—	—	—	—	—	—	—	—	—
19	—	—	—	—	—	—	—	—	—	—	—	—	—	—	—	—	—

$r_i \mu$	Serial frequency															n_i
	86	87	88	89	90	91	92	93	94	95	96	97	98	99	100	
1	—	—	—	—	—	—	—	—	—	—	—	—	—	—	—	3409
2	31	44	36	40	43	36	23	37	22	29	34	26	20	34	43	6316
3	69	76	78	65	82	53	70	66	66	65	61	74	45	49	74	7460
4	66	69	70	68	69	69	70	67	79	76	71	68	93	63	66	4797
5	49	52	42	47	46	40	54	42	49	54	49	53	53	64	54	3442
6	29	21	31	36	24	39	38	35	36	41	42	33	37	41	17	1985
7	27	20	20	19	18	31	22	26	27	18	27	18	22	15	18	1192
8	15	9	13	15	10	12	14	17	9	8	8	12	10	19	10	654
9	7	3	4	5	4	11	6	4	5	2	3	4	13	6	10	341
10	3	4	4	1	—	3	2	3	2	2	3	8	4	4	4	207
11	2	2	2	—	1	2	1	2	3	2	1	2	2	2	3	106
12	—	—	—	1	1	—	—	1	—	1	—	—	1	1	1	43
13	1	—	—	2	1	1	—	—	—	1	—	2	—	—	—	27
14	—	—	—	—	—	1	—	—	1	—	—	—	—	1	—	9
15	1	—	—	1	1	1	—	—	1	—	—	—	—	—	—	7
16	—	—	—	—	—	—	—	—	—	—	—	—	—	—	—	3
17	—	—	—	—	—	—	—	—	—	—	—	—	—	—	—	1
18	—	—	—	—	—	—	—	—	—	—	1	—	—	—	—	1
19	—	—	—	—	—	—	—	—	—	—	—	—	—	—	—	1

$$\Sigma n_i = 30000$$

$$r_1 = 4,6 \mu$$

$$r_2 = 5,0 \mu$$

$$r_3 = 5,5 \mu$$

$$r_4 = 6,4 \mu$$

FTD-TT-62-500/1+2

1/XI 1946 г.

APPENDIX 2

r_{il}^{μ}	n_i
1	—
2	46
3	94
4	199
5	436
6	686
7	960
8	1362
9	1487
10	1391
11	1297
12	1141
13	996
14	790
15	701
16	528
17	480
18	345
19	313

r_{il}^{μ}	n_i
20	223
21	217
22	184
23	169
24	137
25	127
26	104
27	83
28	73
29	76
30	38
31	35
32	47
33	38
34	24
35	36
36	19
37	29
38	20

r_{il}^{μ}	n_i
39	25
40	11
41	8
42	10
43	3
44	5
45	2
46	1
47	1
48	—
49	1
50	2

$$\Sigma n_i = 15000$$

$$\bar{r}_1 = 12,6 \mu$$

$$\bar{r}_2 = 14,0 \mu$$

$$\bar{r}_3 = 15,6 \mu$$

$$\bar{r}_7 = 19,2 \mu$$

2/XI 1946 г.

APPENDIX 3

r_{il}^{μ}	n_i
1	—
2	407
3	675
4	874
5	1220
6	1311
7	1503
8	1453
9	1353
10	1142
11	1023
12	767
13	686
14	453
15	359
16	236

r_{il}^{μ}	n_i
17	276
18	192
19	189
20	101
21	131
22	111
23	87
24	43
25	73
26	48
27	48
28	19
29	37
30	24
31	15

r_{il}^{μ}	n_i
32	16
33	8
34	15
35	9
36	2
37	2
38	1
39	1

$$\Sigma n_i = 15000$$

$$\bar{r}_1 = 9,5 \mu$$

$$\bar{r}_2 = 10,8 \mu$$

$$\bar{r}_3 = 12,3 \mu$$

$$\bar{r}_7 = 15,6 \mu$$

12/VIII 1948 r.

$r_{1\mu}$	Serial frequency										n_i
	1	2	3	4	5	6	7	8	9	10	
1	—	—	—	—	—	—	—	—	—	—	—
2	1	4	5	1	3	1	—	—	5	5	25
3	2	1	8	—	3	2	1	2	4	7	30
4	4	4	4	7	1	3	2	4	1	7	37
5	3	6	3	5	3	2	3	4	6	10	45
6	4	2	7	3	1	2	3	5	7	4	38
7	8	11	8	5	6	3	7	6	3	5	62
8	8	7	6	6	7	14	9	8	11	2	78
9	7	6	8	13	18	15	12	10	3	4	96
10	8	11	9	4	11	14	8	7	5	3	80
11	5	4	4	5	4	12	5	10	13	8	70
12	5	5	6	8	4	2	14	7	10	12	73
13	6	4	4	10	6	5	10	6	5	7	63
14	3	6	5	7	3	2	10	5	8	6	55
15	6	1	3	5	5	2	4	9	6	4	45
16	5	5	5	5	1	4	4	6	1	4	40
17	3	7	3	6	4	1	2	3	5	4	38
18	6	3	6	1	4	3	1	3	3	4	34
19	3	3	—	—	6	2	3	1	1	1	20
20	4	3	1	1	2	—	—	1	1	—	13
21	4	2	1	2	3	5	1	1	—	—	19
22	2	1	1	2	2	—	—	—	1	—	9
23	2	2	—	1	1	3	—	—	1	2	12
24	1	2	1	1	2	1	1	2	—	—	11
25	—	—	1	2	—	1	—	—	—	—	4
26	—	—	—	—	—	1	—	—	—	—	1
27	—	—	—	—	—	—	—	—	—	—	—
28	—	—	1	—	—	—	—	—	—	1	2

$$\begin{aligned}\Sigma n_i &= 1000 \\ \overline{r_1} &= 11,3 \mu \\ \overline{r_2} &= 12,3 \mu \\ \overline{r_3} &= 13,3 \mu \\ \overline{r_4} &= 15,5 \mu\end{aligned}$$

FTD-TT-62-500/1+2

RESULTS OF AN ANALYSIS OF A WIND TUNNEL USED IN
A MAIN GEOPHYSICAL OBSERVATORY

By

P. V. D'yachenko and A. I. Kameneva

The data concerning the GGO wind tunnel, which is used as a calibrating device in the hydrometeorological service of the USSR, are explained in detail in this article.

The GGO wind tunnel occupies a special position in the hydrometeorological service. It has been used, and is being used, not only for the ordinary calibration of instruments, measurements of wind velocity, but also for various types of experimental investigations and scientific-method developments.

The tunnel was constructed in 1932 under the direction of M. A. Dement'ev¹. It was first analyzed by A. I. Chuvashov and Z. F. Val'ta. Subsequent analyses in 1935, 1937, and 1941 were performed by K. A. Auskulat, M. A. Agapitov, A. I. Kameneva, and M. M. Klestova. These periodic analyses were done in order to verify the invarialibility of its characteristics. In this instance, low velocities were not studied. Low velocities were included in the research program for 1952.

The results of the latter analysis of the GGO wind tunnel, which was conducted by the authors of this article, are briefly described below.

The results of the above-mentioned previous investigations are also cited below in order to provide a comparison of the

parameters of the tunnel. These results were taken from manuscripts and archive materials.

A Brief Description of the Wind Tunnel

The GGO wind tunnel, a schematic drawing of which is shown in Figure 1, is of the open tunnel type. It has an open working part, which is located in a closed chamber 1, the dimensions of which are 4.5 x 4.0 x 2.9 m. The tunnel is mounted in a larger casing, whose dimensions are 17 x 7 x 6 m. Its basic component parts are the tunnel collector or nozzle 2, which is the suction part, located before the working part; the working part 3, where the verifying and calibrating instruments are mounted; the duffusor cone 4, which is the intermediate part between the working part and the air screw, and with the wide part facing the air screw; a six-bladed air screw 5, producing a determined variation in the pressure necessary for the maintenance of the velocity in the tunnel; a return channel or tube 6 through the casing in which the tunnel is mounted; and an electric drive (converter, motor, and switch panel) safeguarding the spin of the air screw.

The collector, determining the form of the working cross section of the tunnel, has an octahedral cross section. The

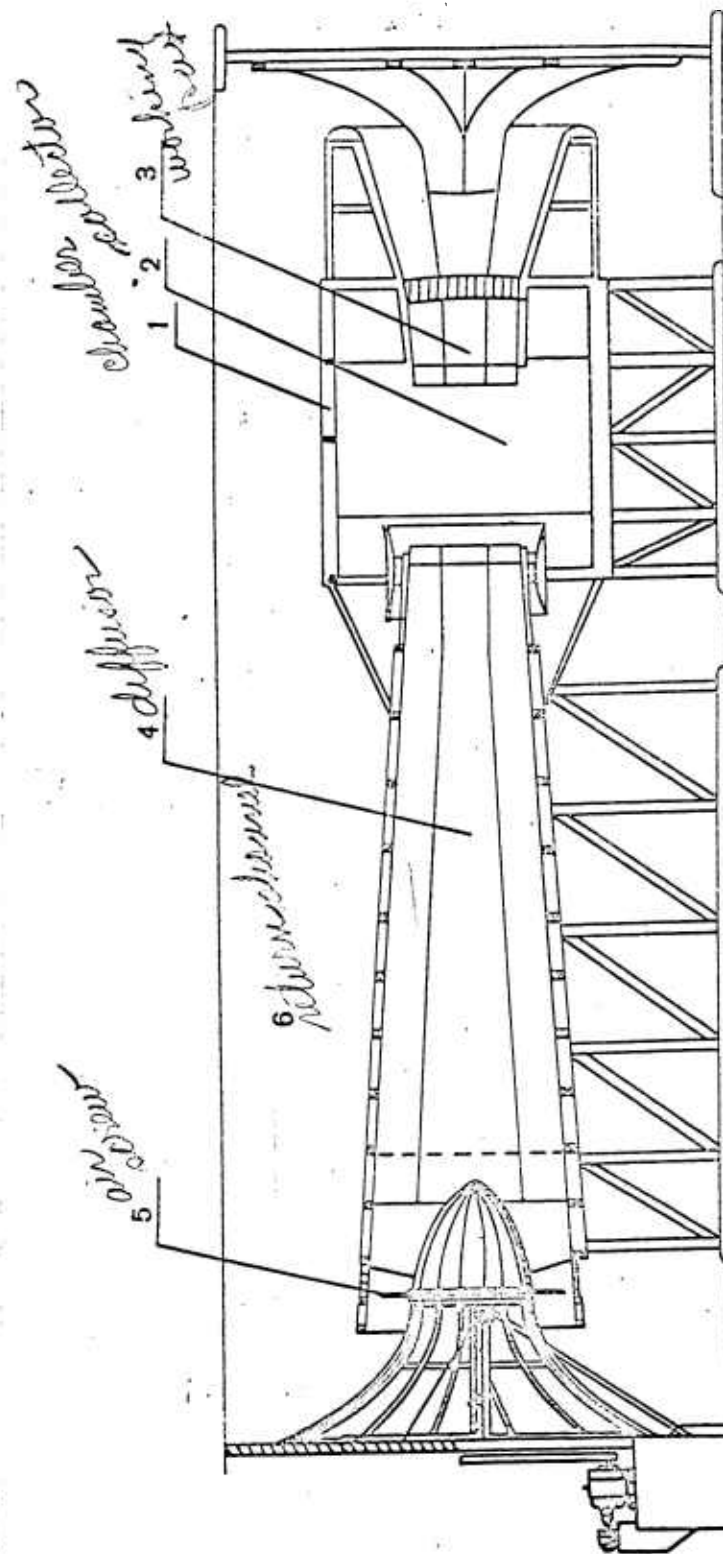


Figure 1. Schematic drawing of the GGO wind tunnel

diameter of the working cross section of the tunnel, measured along the circumference inscribed in the octahedron, is equal to 1 m.

The operation of the wind tunnel consists of the following. The air screw, when set in motion, sucks the air from the casing in which the wind tunnel is mounted. The air stream passes through the collector, containing the rectifying grid; enters the working part at first, then it goes into the diffuser cone, from where it is deflected by the air screw back into the same casing which serves, in this fashion, as a channel for the return of the air back into the collector.

The six-bladed air screw, which sets the air in motion, is powered by a direct-current 6.5 kilowatt (220 volt) electric motor. This electric motor is fed through a converter from a 220 volt, alternating current supply system. The electric supply is regulated through a special switch panel. The complete assembly makes it possible for the electric motor to operate in ~~in~~ very low revolutions, being decreased 2.5 times at the rotary drive of the screw. Owing to this, it is possible to obtain very low velocities in the tunnel.

The ability to obtain small air stream velocities, as well as even changes of velocity in the entire range, is also a basic feature of the GGO wind tunnel.

The ease of mounting the instruments in the air stream, the

ease of looking out after them, and the remote control through the air screw motor, which makes it possible to truthfully determine any velocity found in the closed chamber of the tunnel, should be added to the positive operation qualities of the wind tunnel.

The maximum velocity of the air stream produced in the tunnel consists of 20 m/sec.

The basic requirements for an artificial air stream in the tunnel, as concerns accuracy and reliability of experimental results, are a uniform distribution of the velocities in the working field of the tunnel with respect to different cross sections, and a preservation of the uniformity of the air stream, both in quantity as well as directional velocity.

The pressure and velocity are distributed uniformly with respect to magnitude in first-rate wind tunnels with any cross section, and should not deviate from the mean magnitude by more than $\pm 1\%$. With respect to direction, the air stream should be parallel to the axis of the tunnel. The maximum deviation of the angles of taper in the vertical plane should not be more than $0.25^{\circ(2)}$. A change of these parameters should bring about a zero value.

It is necessary to note, however, that an evaluation of the nature of the stream produced in the wind tunnel will be dependent

upon the accuracy of the instruments used for measuring the velocity. In our analysis, which was devoted to the measurement of velocity, we used the TsAGI micromanometer in pair, coupled with an air tube and an All-Union State Standard 6376-52, type B vane anemometer.

Analysis of the Field of Velocity in Average Velocities

The study of the field of velocity was conducted with steady, average (5, 10, 15 m/sec), and low (0.4, 0.6, 1.2, and 2.0 m/sec) velocities.

The working field of the channel in average velocities was studied by ordinary methods along the axis of both air tubes. One of them (cone shaped calibrating) was mounted securely in the center of the working field, and the second (spherical, Prandtl-type), located in a simplified coordinator, could be moved to any point in the selected cross section of the stream.

The readings of the velocity pressures in every individual point of the field were taken with the above-mentioned TsAGI micromanometer, which was connected to the movable tube at an angle of inclination of about 8° ($\sin \alpha = 0.125$). The readings of the velocity pressures in the center of the working field were taken simultaneously by the second calibrating micromanometer of the same type, which was connected to the stationary calibrating

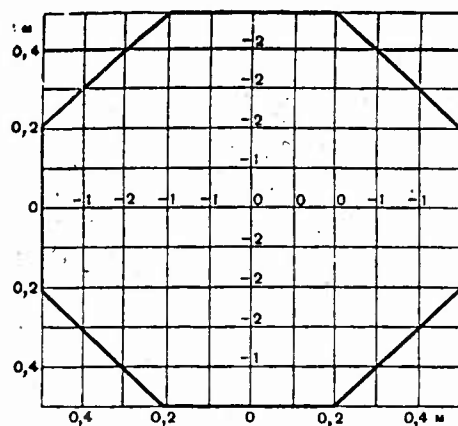


Figure 2. Deviations of the field's coefficients from the center (%), velocity 5 m/sec.

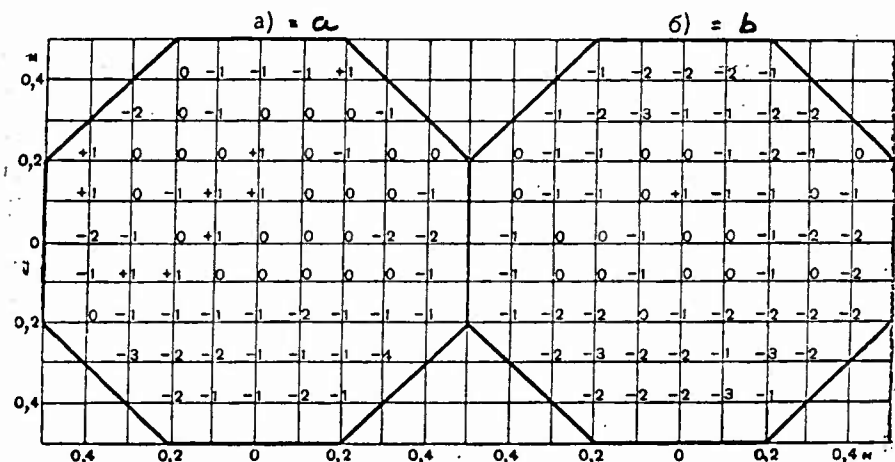


Figure 3. Deviations of the field's coefficients from the center (%)
Velocity: a = 10 m/sec; b = 15 m/sec.

Table 1

(A) Средняя скорость, м/сек.	(B) Среднее значение коэффициента	(C) Средняя квадратичная погрешность ($\pm \sigma$)		(F) Число случаев
		(D) абсолютная	(E) относительная	
6	0,991	0,009	0,9	80
10	0,993	0,006	0,6	80
15	0,996	0,008	0,8	80

A - average velocity, m/sec.
B - average value of coefficient
C - root mean square deviation ($\pm \sigma$)

D - absolute
E - relative
F - number of cases

tube.

During the processing, the readings of the movable tube were reduced to the readings of the calibrating tube, located in the center, with the help of a transfer coefficient, which was obtained, first of all, in the results of the movable tube with respect to the calibrating tube, and of verification of the micromanometers which were used in pair with the tubes.

The velocity distribution was analyzed in one cross section, going through the center of the working field of the tunnel, and along several contour lines spaced 10 cm from each other.

It is necessary to note that, during the measuring of the field along the vertical diameter below the center, an adverse effect of the stationary tube holder upon the readings of the movable tube was noticed. Therefore, instead of the stationary calibrating tube being used for the measuring of the velocity in the center of the field, the orifice in the collector, graduated according to the calibrating tube, was used. This method of measuring the velocity is used with the checking of meteorological instruments, and is mentioned in the pertinent handbook³.

The uniformity of the velocity fields was characterized by the values of the coefficients obtained as the ratio $\frac{v_n}{v_u}$, where

v_n is the velocity of the air stream at individual points of the field with respect to the movable tube, and where v_u is the simultaneously measured velocity in the center of the field with respect to the calibrating tube.

It is possible to visualize the accuracy of the analysis of the tunnel's field with given velocities by the root mean square deviation σ of a series of coefficients obtained in the center of the working field of the tunnel during the calibration of the movable tube by the calibrating tube, as is shown in Table I.

It can be seen from Table I that the root mean square deviation of the series of coefficients, characterizing the accuracy of the coefficients obtained through analysis of the field in given velocities, consists of from 0.6 to 0.9%.

The results of the analysis of the velocity field in average velocities are shown in Table II (see 1952), and are illustrated by the diagrams in Figures 2 and 3. These diagrams give the deviations of the coefficients for individual points of the field from the coefficient at the center, which was taken as unity, in percentages: $\left(\frac{v_n}{v_u} - 1 \right) 100\%$.

It follows from Table 2 and the diagrams, that the coefficients in the working part of the tunnel's field (in a girth of 40 x 80 cm) with given velocities are changed

Table 2

(A) Значения коэффициентов поля вдоль горизонтального диаметра

D Месяц и год	B Расстояние точек в потоке от оси трубы, м											
	C влево по потоку											
	0,4			0,3			0,2			0,1		
	E Скорость, м/сек.											
	5	10	15	5	10	15	5	10	15	5	10	15
XII 1937	—	—	1,00	—	—	1,00	—	—	1,01	—	—	1,00
IV 1941	1,00	1,01	1,00	1,00	1,01	1,00	1,02	1,02	1,02	1,00	1,00	1,01
X 1952	0,99	0,98	0,99	0,98	0,99	1,00	0,99	1,00	1,00	0,99	1,01	0,99

⑥ Месяц и год	⑤ Расстояние точек в потоке от оси трубы, м														
	④ центр						③ вправо по потоку								
	0,0			0,1			0,2			0,3			0,4		
	② Скорость, м/сек.														
	5	10	15	5	10	15	5	10	15	5	10	15	5	10	15
XII 1937	—	—	1,00	—	—	1,00	—	—	1,00	—	—	1,00	—	—	1,00
IV 1941	1,00	1,00	1,00	1,00	1,01	1,00	0,99	1,01	1,00	0,99	1,00	0,99	1,00	1,00	1,00
X 1952	1,00	1,00	1,00	1,00	1,00	1,00	1,00	1,00	0,99	0,99	0,98	0,98	0,99	0,98	0,98

(K) Значения коэффициентов поля вдоль вертикального диаметра

(N) Месяц и год	(L) Расстояние точек в потоке от оси трубы, м											
	(M) вверх от оси трубы											
	0,4			0,3			0,2			0,1		
	(O) Скорость, м/сек.											
	5	10	15	5	10	15	5	10	15	5	10	15
XII 1937	—	—	1,00	—	—	1,02	—	—	1,01	—	—	1,00
IV 1941	1,00	1,00	0,99	0,99	1,01	1,00	1,01	1,01	1,00	1,00	1,00	1,00
X 1952	0,98	0,99	0,98	0,98	1,00	0,99	0,98	1,01	1,00	0,99	1,01	1,01

(R) Месяц и год	(P) Расстояние точек в потоке от оси трубы, м														
	(Q) центр						(S) вниз от оси трубы								
	0,0			0,1			0,2			0,3			0,4		
	(T) Скорость, м/сек.														
	5	10	15	5	10	15	5	10	15	5	10	15	5	10	15
XII 1937	—	—	1,00	—	—	1,00	—	—	1,01	—	—	1,00	—	—	0,99
IV 1941	1,00	1,00	1,00	0,99	0,99	0,99	1,00	0,99	1,00	1,01	1,01	1,00	0,99	1,01	1,00
X 1952	1,00	1,00	1,00	0,98	1,00	1,00	0,98	0,99	0,99	0,98	0,98	0,98	0,99	0,99	0,98

Table 2

A	- value of the coefficients of the field along the horizontal diameter
B	- Spacing of the points in the stream from the axis of the tunnel, m.
C	- counterclockwise along the streams
D	- Month and Year
E	- Velocity, m/sec
F	- Spacing of the points in the stream from the axis of the tunnel, m.
G	- Month and Year
H	- Center
I	- Clockwise along the stream
J	- Velocity, m/sec
K	- Value of the coefficients of the field along the vertical diameter
L	- Spacing of the points in the stream from the axis of the tunnel, m.
M	- Upwards from the axis of the tunnel
N	- Month and Year
O	- Velocity, m/sec
P	- Spacing of the points in the stream from the axis of the tunnel, m.
Q	- Center
R	- Month and Year
S	- Downwards from the axis of the tunnel
T	- velocity, m/sec

insignificantly, within limits of 1%. Maximum deviations (3 to 4%) of the coefficients from the center are observed only at the extreme points of the field.

During the determination of the coefficients of the field with the help of the graduated orifice in the tunnel's collector, the uniformity of the velocities in the working field is maintained within the very same limits. This makes it possible to analyze the tunnel's field not by two air tubes, which causes a shading at certain points of the field, but by one tube, where this presents the possibility of using the calibrated orifice in the collector as a control point in the center of the working field.

The coefficients of the field, which were obtained during its analysis in 1937 and 1941, are shown in Table II as confirmation of the characteristic of the working field, obtained in 1952.

A relative comparison of the coefficients, obtained in different years, shows that these coefficients diverge among themselves by 1 to 2%. Divergences in 3% are single cases. This makes it possible to come to the conclusion that, for all practical purposes, the distribution of the velocities in the cross section of the channel, passing through the center of the working field, can be considered as constant in all examined velocities within the limits of accuracy of the experiment.

On the basis of such a conclusion, which was arrived at in 1952, other cross sections of the tunnel (at a distance of 0.3 m from the center plane and heading in the direction of the diffuser and collector) were not analyzed. They were examined in the preceding years, and, with respect to the uniformity of the distribution of the velocities, they differed very little from the cross section passing through the center of the tunnel.

An Analysis of the Tunnel's Field in Small Velocities

Two slide-wire axled vane anemometers from the Moscow hydrometric instrument factory were used for an analysis of the velocity field in low velocities. The anemometers made it possible to measure the mean velocity of a directed air stream. The sensitivity threshold of the anemometers consisted of 0.2 m/sec, and the upper limit of measurement consisted of 5 m/sec.

A simplified coordinator in the form of a rectangular frame with movable clamps, which was to be located outside of the tunnel's field, was needed. To fill this requirement, we strung out a copper wire at the necessary distances. The vanned anemometer, with its holding clamp loosened, could easily displace to various points of the tunnel's working field along this wire.

Because the size of the anemometer prevented the mounting of a second instrument as a regulating anemometer into the center of the working field, the velocity of the stream in the center was measured by one and the same anemometer - which was periodically placed in the center of the working field - through 2 to 3 measurements at individual points of the field.

The indications of the anemometer were read after holding it for 100 seconds at the examined point of the field.

In other respects, the measurements were conducted along the same plan which was used for the analysis of the field in average velocities. The coefficients were calculated in an analogous manner.

In view of the fact that the sensitivity threshold of the anemometers was close to 0.2 m/sec, it was safe to compute the measurements only from 0.4 m/sec. Therefore, the field was measured at velocities of 0.4, 0.7, 1.0, and 2.0 m/sec.

In order to control the results obtained at 0.4 m/sec, the measurements were made twice by two different anemometers.

The representation concerning the accuracy of measurement by vaned anemometers gives in Table III the root mean square deviation of a series of velocities, which were obtained by the readings of two anemometers periodically placed in the center of the working field of the tunnel during the process

Table 3

(A) Среднее значение скорости, м/сек.	(B) Средняя квадратичная погрешность (\pm)		(E) Число отсчетов
	(C) абсолютная, м/сек.	(D) относительная, %	
0,45	0,01	2,6	63
0,68	0,01	1,9	45

A - average magnitude of velocity, m/sec

B - root mean square deviation (+)

C - absolute, m/sec

D - relative, %

E - Number of readings

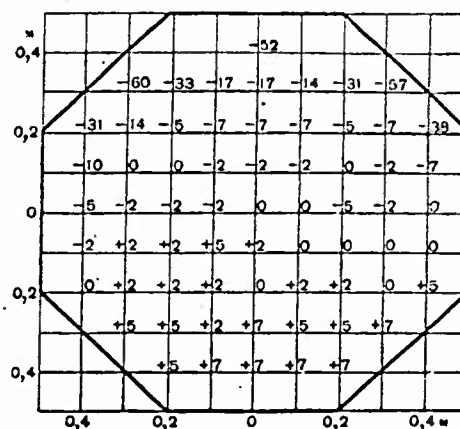


Figure 4. Deviations of the field's coefficients from the center (%), velocity 0.4 m/sec

of analysis.

In conformity with Table III, the root mean square deviation of the measurement of velocity by slide-wire axled anemometers does not exceed ± 0.01 m/sec in low velocities. Therefore, they are fully adequate for comparative measurements.

The results of the analysis of the field in low velocities are shown in Table IV and in the diagram of Figure 4.

From a comparison of the diagrams in Figures 3 and 4, it follows that in low velocities of the order of 0.4 /sec, the field of velocity in the center part (cross section 40 x 80 cm) is less uniform than at average velocities, particularly at the edges. There is a significant decrease of velocity in the upper part of the cross section. The deviations of the coefficients at individual points of the field away from the center amount to from 52 to 60%. Inversely, an increase in velocities can be observed in the lower part of the cross section.

In this particular case, the coefficients, as compared with the center, are greater by from 5 to 7%. A repeated examination of the field at a velocity of 0.4 m/sec by a second anemometer confirmed the results obtained the first time. The field gradually straightens out at velocities greater than 0.4 m/sec, and, as can be seen from Table IV, beginning with a velocity of 1.2 m/sec, the coefficients differ among themselves by no more

Table 4

Ⓐ Значения коэффициентов поля вдоль горизонтального диаметра

Ⓑ Скорость воздушного потока, м/сек.	Ⓒ Расстояние точек в потоке от оси трубы, м								
	Ⓓ влево по потоку				Ⓔ центр	Ⓕ вправо по потоку			
	0,4	0,3	0,2	0,1		0,1	0,2	0,3	0,4
0,4	0,95	0,98	0,98	0,98	1,00	1,00	0,95	0,98	1,00
0,6—0,7	0,97	0,98	0,97	0,98	1,00	0,98	0,97	1,00	0,98
1,2	0,99	0,99	1,00	1,00	1,00	0,99	0,99	0,98	0,98
2,0	1,01	1,01	1,00	1,00	1,00	1,00	1,00	1,00	0,98

Ⓔ Значения коэффициентов поля вдоль вертикального диаметра

Ⓗ Скорость воздушного потока, м/сек.	Ⓘ Расстояние точек в потоке от оси трубы, м								
	Ⓝ вверх от оси трубы				Ⓚ центр	Ⓛ вниз от оси трубы			
	0,4	0,3	0,2	0,1		0,1	0,2	0,3	0,4
0,4	0,48	0,83	0,93	0,98	1,00	1,02	1,00	1,07	1,07
0,6—0,7	0,82	0,96	0,96	0,97	1,00	1,00	1,04	1,04	1,05
1,2	0,94	0,99	0,99	1,00	1,00	1,00	1,00	1,01	1,01
2,0	0,95	0,99	1,00	1,00	1,00	1,00	1,00	0,99	0,99

A - values of the coefficients of the field along the horizontal diameter

B - velocity of air stream, m/sec

C - spacing of the points in the stream from the axis of the tunnel, m

D - counterclockwise along the stream

E - Center

F - clockwise along the stream

G - value of the coefficients of the field along the vertical diameter

H - velocity of air stream, m/sec

I - spacing of the points in the stream from the axis of the tunnel, m

J - upwards from the axis of the tunnel

K - center

L - Downwards from the axis of the tunnel

than 2%, which is within the limits of the accuracy of measurement of the velocity by a vane anemometer. Exceptions are the extreme points of the field up from the axis of the tunnel, where there is still a decrease of velocity in comparison with the center.

It can be assumed that the effect of a difference of temperatures in the closed chamber and in the casing of the tunnel manifests itself in low velocities. This difference of the air stream at low velocities produces an additional velocity field in the working volume, owing to the temperature heterogeneities, which bring about a different density of the air in the working field of the tunnel.

Hence follows the practical conclusion that the GGO wind tunnel cannot be suitable for the checking of vane anemometers at velocities below that of 0.4 m/sec, on account of the fact that the indicated difference of temperatures at these velocities will cause a still greater non-uniformity in their distribution.

Velocity Fluctuations of the Air Stream

Important characteristics of the nature of the air stream are the fluctuations of the velocity, which are always observed to a greater or lesser degree around a certain average value.

The inconstancy of the voltage in the network and the natural oscillations of the closed chamber under the influence

of the stream can be noted as causes of these fluctuations.

The magnitude of the fluctuation of the air stream was determined in the process of calibrating two air tubes, placed in the center of the working field of the tunnel, by the fluctuation of the alcohol column in a TsAGI micromanometer ($\sin \alpha = 0.125$) at various velocities of the stream - 6, 10, 12, and 15 m/sec. Ten instantaneous indications were read simultaneously by both micromanometers in each of the indicated velocities. A micromanometer was connected to each of the two air tubes.

The absolute value of the velocity fluctuation was characterized by the magnitude

$$\frac{v_{\max} - v_{\min}}{2} \text{ m/sec}$$

relative to

$$\frac{v_{\max} - v_{\min}}{v_{\max} + v_{\min}} 100\%$$

The results are shown in Table 5.

Due to the fact that the data cited in Table 5 includes the natural oscillations and inertia of the micromanometer, it is not sufficiently accurate, and can be used only for a qualitative judgement concerning the fluctuations of the air stream.

The velocity fluctuations of the air stream, as is evident from the table, do not exceed 0.1 m/sec in average velocities.

Table 5

(A)	Скорость, м/сек.		(B) Значение колебаний (\pm)		Число наблюдений (G)
	(C) максимальная	(D) минимальная	(E) абсолютное, м/сек.	(F) относительное, %	
5,92	5,96	5,84	0,06	1,0	160
9,81	9,87	9,71	0,08	0,8	160
11,84	11,93	11,77	0,08	0,7	160
14,96	15,06	14,84	0,11	0,7	160

A - velocity, m/sec

B - magnitude of fluctuation (\pm)

C - maximum

D - minimum

E - absolute, m/sec

F - relative, %

G - number of observations

If we are to take into consideration the fact that, in practice, it is proposed to take several readings by the micromanometer in order to eliminate random errors owing to these fluctuations, then it is possible to assume that the effect of the fluctuations upon the velocity measurement is insignificant.

Analysis of the Direction of the Stream

It was proposed to use a special cylindrical nozzle, which was produced by the "Etalon" factory, for an analysis of the direction of the air stream in the working field of the tunnel. However, this nozzle, in view of the insufficient length of its adapter, did not make it possible to measure the direction without disturbing the stream itself. Therefore, the analysis was limited only to the solution of the problem concerning the capability of applying the nozzle in low velocities, i.e., for a practical determination of its sensitivity.

This cylindrical nozzle, similar to the one described in Popov's work⁴, has three orifices, of which the two openings on the edges are symmetrically located at angles of 45° from the third, or center, orifice.

The direction of the stream is determined by the two outer openings, which are connected to the micromanometer. The operating principle of the nozzle is based on the fact that the pressures in the outer openings are equal if they are symmetrical with reference to the stream. The center orifice of the nozzle,

under conditions of its calibration by the calibrating air tube, serves for the determination of the stream velocity in that plane where the direction is also determined. For that reason, one of the outer orifices, after its orientation in the air stream, is connected to the micromanometer in addition to the center orifice. The orientation of the nozzles with respect to the air stream was done as follows: They were placed with the orifices facing against the stream, and rotated about their axis in one or the other direction until that time when the pressures in the outer points were not equal. The indicated position of the nozzle at the control point of the stream was taken as the origin (deflection angle of the nozzle $\alpha = 0^\circ$) and was fixed by a reading along the graduated circle of the nozzle. The deflection angle up to this position also determines the direction of the stream in the given points in relation to the direction at the control point, which was taken as the initial point.

In order to determine the sensitivity of the nozzle, the outer orifices were connected to the micromanometer at an angle of inclination $\alpha = 3^\circ$.

The nozzle, having been oriented in the stream with respect to direction, i.e., having attained equal pressures in the two outer openings, was turned at different angles of rotation in both directions, and the corresponding indications of the micromanometer were read in each instance. The results of the

Table 6

Скорость воздушного потока, м/сек. (A)	Среднее изменение показаний микроманометра при повороте насадки на 1° (B)		Число наблюдений (E)
	в делениях микроманометра (C)	в миллиметрах водяного столба (D)	
0,9	0,1	0,004	12
2,1	0,4	0,016	6
5,0	3,3	0,146	6
10,0	12,6	0,559	4

A - velocity of air stream, m/sec

B - average change of indication of micromanometer with a rotation of the nozzle by 1°

C - in micromanometer divisions

D - in mm of water column

E - number of observations

determination of the sensitivity of the nozzle are listed in Table VI.

It follows from Table VI that the micromanometer, with a rotation of the nozzle in 1^0 in low velocities, changes its indication in tenths on the scale of division. Therefore, the measurement of the direction at velocities below that of 2 m/sec will be accompanied by larger errors, and it is not appropriate to use the described method.

By generalizing the results of the analysis of the GGO wind tunnel in relation to the field of velocity and its operating characteristics, we may come to the conclusion that, regardless of its obsolete construction, it still belongs to that group of first-rate wind tunnels where it is possible, with the presence of appropriate measuring apparatus, to conduct accurate experiments and to conduct a checking of instruments in velocity limits from 0.5 to 20 m/sec. An intrinsic defect of the tunnel is the low upper limit of the produced velocities. This defect became particularly felt after the creation of new instruments during the past few years which can measure velocities up to 40 m/sec and above. In order to expand the capability of this wind tunnel, it is desirable to increase the upper velocity limit, or to construct a new tunnel.

References

1. Dement'ev, M. A. Aerodinamicheskaya truba Instituta Poverki. (Institute of Verification Wind Tunnel) Vestnik, Edinaya Gidrometeorologicheskaya Sluzhba (Periodical, United Hydrometeorological Service), 4, Sel'khozgiz, 1934.
2. Martynov, A. K. Eksperimental'naya aerodinamika. (Experimental aerodynamics) Oborongiz, M., 1950.
3. Rukovodstvo po poverke meteorologicheskikh priborov. (Handbook of meteorological instruments). Gidrometeoizdat, L., 1956.
4. Popov, S. G. Izmerenie Vozdushnykh Potokov. (Measurement of air streams). Gostekhizdat, 1947.

TESTING OF HAND ANEMOMETERS AT THE PLANT

This article discusses shortly the results of work which made it possible to produce hand cup anemometers GOST 6376-52, type A that are provided with a standard curve at the plant.

Until 1958, hand cup anemometers GOST 6376-52, type A manufactured at the Moscow Hydrometeorological Instrument Plant, before being shipped away, used to be tested in the wind tunnel of the plant. Four anemometers were mounted in the cross-section of the tunnel. As a result of the test for each anemometer, a calibration curve was plotted which made it possible to express the instrument's reading as an actual air stream velocity. Each anemometer to be shipped out was provided with such a calibration curve.

(Information on the anemometer as well as details on its conventional testing are set forth in the Specifications /1/ now in effect).

In view of the standardized manufacturing of hand anemometers and of the small difference between individual calibration curves, the Moscow Hydrometeorological Instrument Plant proposed that anemometers be produced that are provided with a single standard calibration curve.

In order to implement this proposal, this writer and plant workers conducted a special joint investigation in the plant control shop. It was revealed, first of all, that the most accurate standard calibration curve is obtainable by testing ^{the} anemometers in an UPAR -- an installation for the testing of hand anemometers -- which is also described in Specifications /1/. In the UPAR the test error is less than in the other aerodynamic installations of the plant. This is because in the UPAR, anemometers are tested singly and not in groups, the UPAR is little affected by changing external conditions (temperature and pressure), and a mechanical adjustment ensures uniform mounting of the hand

anemometers themselves.

These circumstances are dealt with in detail in the paper /2/.

To derive a standard calibration curve 129 calibration curves for standard anemometers manufactured before 1958 were used. All the curves were obtained from UPAR tests of these instruments.

Analysis of these curves showed that a single calibration curve will not suffice to produce accurate instruments, since test results of individual instruments may deviate substantially from this curve. Therefore, all the instruments were divided on a sensitivity basis into three groups according to the character of their curves. In the first group were placed 9 instruments whose highest readings (given 20 divisions per second) were 18.1 to 18.5 m/sec.; in the second group, 70 instruments with the maximum readings 18.6 to 19.0 m/sec.; and in the third group were placed 50 instruments with a maximum velocity reading of 19.1 to 19.5 m/sec.

Standard curves for each group were obtained by taking the arithmetic mean of the values read from the calibration curve of each anemometer for the actual air stream velocity; these values correspond to readings on the scale at every other division per second (1 to 20 divisions per second). Thus were obtained three standard curves. The mean maximum velocity proved to be 18.4 m/sec for the first standard curve, given anemometer readings of 20 divisions per second, 18.8 m/sec for the second, and 19.2 m/sec for the third.

To characterize a number of calibration curves which had been used for the plotting of individual standard curves, the root-mean-square error σ was calculated for the values read from the standard curve for the actual air stream velocities which correspond to readings on the anemometer scale of 1, 10, and 18 divisions per second. Table 1 gives the results obtained.

Table 1

Root-mean-square error for several calibration curves

Anemometer group	Anemometer readings, div/ sec									Number of instruments
	1			10			18			
	mean	$\pm \sigma$		mean	$\pm \sigma$		mean	$\pm \sigma$		
	velocity, m/sec	m/sec	%	velocity, m/sec	m/sec	%	velocity, m/sec	m/sec	%	
1	1,31	0,03	2,3	9,40	0,05	0,5	16,59	0,07	0,4	9
2	1,35	0,05	3,7	9,65	0,09	0,9	17,02	0,12	0,7	70
3	1,36	0,05	3,7	9,84	0,08	0,8	17,37	0,14	0,8	50

As Table 1 shows, the root-mean-square error of a number of calibration curves for individual anemometer groups does not exceed ± 0.14 m/sec or ± 0.8 % of the velocity in the vicinity of maximum velocities.

Table 2 shows the distribution of deviations of individual calibration curves from the mean (standard) curve which is characterized by the distribution of deviations of individual actual velocity values as read from individual calibration curves, from the arithmetic means for each group of instruments.

Table 2

Distribution of deviations of individual calibration curves from the mean (standard) curve in percents of the whole number

Anemometer group	Mean velocity, m/sec	Deviations not exceeding			Total number
		$\leq 1\sigma$	$\leq 2\sigma$	$\leq 3\sigma$	
1	1,31	78	100	100	9
	9,40	66	100	100	9
	16,59	78	89	100	9
2	1,35	76	96	100	70
	9,65	73	97	100	70
	17,02	68	99	100	70
3	1,36	78	92	100	50
	9,84	70	96	100	50
	17,37	68	94	100	50

From the data of Table 2, the overwhelming majority of deviations of individual curves from the standard curve fall within the range of twice the root-mean-square error and amounts to 89 to 99% for all the anemometer groups at velocities close to the upper limit.

In this context, anemometers whose individual test data will deviate from the standard calibration curve by more than 26 can be considered not to conform to our series, and cannot be provided with the standard curve that we obtained.

For any anemometer reading, the numerical expression for twice the root-mean-square error (we have in mind the highest error obtained for a group of 3 anemometers) will be approximately $(0.1 + 0.01 v)$ m/sec, where v is the actual air stream velocity.

The quantity $(0.1 + 0.01 v)$ m/sec is taken as a permissible variation of an individual calibration curve from the most suitable standard curve. This permissible variation is less than the error in a conventional wind tunnel group test of anemometers.

Evidently, when we arrange individual calibration curves between standard curves, and then substitute the most suitable standard curve for each individual curve, we are introducing an error not exceeding 0.2 m/sec.

It should be noted that by increasing the number of standard curves to five or more in lieu of the recommended three, it would seem at first glance that we should accomplish better conformity of the standard curve to the individual characteristic of an anemometer. Such a gain, however, would be but an apparent one. Actually the bringing closer together of velocity calibration curves through an increase in their number, is limited by the error magnitude of each individual anemometer. If this error exceeds deviations in velocity between selected standard curves, there will be no further gain in accuracy and there is no point in making use of such standard curves that are closer together. On the other hand, it follows from the data considered above

that a single standard curve is not enough.

In order to test whether the obtained standard curves agree with individual test data, the results of UPAR control tests of 412 hand anemometers, taken from the plant files were used. From readings taken on these instruments at the highest velocity at which maximum deviations from standard curves are most likely, the most suitable calibration curve was selected for each instrument. The deviations proved to be as follows: 115 anemometers (27.9%) fell along the selected standard curve, 216 (52.4%) showed deviations of 0.1 m/sec, 63 (15.3%) of 0.2 m/sec, 11 (2.7%) of 0.3 m/sec, and 7 (1.7%) of more than 0.3 m/sec.

Thus, the overwhelming majority of instruments could be provided with a standard curve.

Based on this work, a Procedure was written. In conformity with this Procedure, hand anemometers GOST 6376-52, type A are provided with a standard curve upon shipment.

All instruments produced are tested. The test includes an external examination, a determination of the sensitivity threshold, and a recording of two anemometer readings in the UPAR. Readings are checked at two velocities: at any speed within the range 1 to 5 m/sec and at 17 to 20 m/sec.

A anemometer which has met GOST specifications as to external examination and testing, is provided with the most suitable standard curve. Such a curve is selected from test data of anemometer readings by comparison^{of} these data with each of three standard curves. Readings should coincide with the selected curve or deviate from it by no more than $(0.1 + 0.1 v)$ m/sec.

Instruments which meet GOST specifications but deviate from standard curves by a value greater than indicated above, are provided with individual calibration curves obtained by the full testing of these instruments in conformity with the current Specifications for the Testing of Meteorological Instruments /1/.

The above-described production method for hand anemometers has been in effect at the Moscow Hydrometeorological Instrument Plant since 1958. The method makes

it possible to effect substantial savings,

and to produce instruments that are more comparable to each other, since the Control Bureau of UGMS (Local Administration of the Hydrometeorological Service) is also testing anemometers in UPAR's which have been calibrated in the GGO (Main Geophysical Observatory) wind tunnel.

Analysis and generalization of the results of this method at the plant will make possible the future control of output uniformity and quality from the distribution of anemometers among the standard curves, as well as the use of this method for testing other types of anemometers.

BIBLIOGRAPHY

1. Specifications for the Testing of Meteorological Instruments. Gidrometeoizdat, L., 1956.
2. D'yachenko, P. V. Installation for the Testing of Manual Anemometers. Trudy GGO, v. 61 (123), 1956.

ERRORS OF THERMOELECTRIC BALANCOMETER TESTING

This article contains the results of experimental investigations on errors with which the parameters of balancometers used in hydrometeorological network stations are determined in testing.

The investigation of error in testing thermoelectric balancometers, just as much similar work, being carried on by the Central Testing Laboratory, GGO, is intended to evaluate errors with which the parameters of balancometers used in hydrometeorological network stations are determined in testing. Accidental errors of the conversion factor, balancometer sensitivity and wind correction factors were evaluated. In addition, balancometer sensitivity dependance on the intensity and direction of incident radiation, on the temperature of the medium and on the direction of the air flow striking it was investigated.

Ten-battery balancometers, prepared in the GGO Experimental Workshop in 1951, 1956 and 1957, were studied. The balancometers satisfy the requirements imposed on them in testing with the exception of balancometer No. 3142; the sensitivities of its sides differ by 10% (permitted tolerance 5%).

The accidental errors were evaluated as the mean quadrantal error of a number of values obtained in repeated balancometer tests. Testing was carried out in conformity with the Manual on testing (1). By one testing the entire cycle of measurements carried out according to the Manual is understood.

ACCIDENTAL ERROR OF THE CONVERSION FACTOR AND SENSITIVITY

In order to evaluate accidental error in conversion factor and sensitivity determination, 6 balancometers were tested. 3 galvanometers, prepared by the GGO Experimental Workshop and the Leningrad

Hydrometeorological Device Factory, were used with the balancometers. A thermoelectric actinometer served as a model in testing. The tests were repeated ten times.

The conversion factors of balancometers coupled with galvanometers were determined by all the methods recommended in the Manual on testing, namely: (1) under laboratory conditions with radiation obtained from a lamp, (2) under natural conditions with an installation in which the detection surfaces of the balancometer are placed perpendicular to the incident radiation and protected from the action of scattered radiation and wind, and (3) under natural conditions without an installation with the detection surfaces of the balancometer placed horizontally just as when observations are made.

The sensitivity of balancometers (without coupled galvanometer) was determined only under laboratory conditions.

The conversion factors of the devices were determined under laboratory conditions at the installation TS.L.P. in November, 1957. The mean conversion factor values obtained for each device couple from ten testings and the mean quadrantal errors of a number of measurements for the sides of balancometer No. 1 are listed in Table 1. The mean quadrantal errors of the conversion factors calculated for each of the sides and for the mean values are given in Table 2.

The results given in Table 2 indicate that the mean quadrantal error of the conversion factor does not exceed 2.2%. The mean quadrantal error of the conversion factor (the average for two sides) calculated for all balancometers tested (repeated 60 times) is 1.2%.

Table 1

Mean conversion factor values a and mean quadrantal error σ (%)
obtained in testing under laboratory conditions

Instrument No.	$\frac{3413}{37}$	$\frac{3429}{37}$	$\frac{3142}{1178}$	$\frac{3324}{1178}$	$\frac{3136}{781}$	$\frac{3169}{781}$
a σ	0,0140 1,8	0,0138 1,2	0,0162 0,9	0,0150 1,2	0,0184 0,6	0,0166 1,2

Table 2

Mean quadrantal errors σ of the conversion factors of the balancometers %

Instrument No.	$\frac{3413}{37}$	$\frac{3429}{37}$	$\frac{3142}{1178}$	$\frac{3324}{1178}$	$\frac{3136}{781}$	$\frac{3169}{781}$	σ_{cp}
Side 1	1,8	1,2	0,9	1,2	0,6	1,2	1,2
Side 2	2,2	1,1	1,5	1,3	0,8	1,0	1,4
average	2,2	1,0	1,1	1,1	0,6	0,9	1,2

Table 3

Mean quadrantal error σ of balancometer sensitivity %

Instrument No.	3136	3159	3114	3142	3137	3169
Side 1	1,0	1,3	1,0	1,6	0,8	1,4
Side 2	1,0	1,0	1,5	2,1	1,2	1,7
average	0,8	0,9	1,1	1,8	1,0	1,4

The distribution of remaining errors is as follows: errors, not exceeding σ , constitute 70%, those not exceeding 2σ , 93% and those not exceeding 3σ , 100% of all the errors involved.

For evaluating errors in determination of balancometer sensitivity, the results of balancometer tests repeated ten times at the installation TS.B.P. in 1951 were used.

The mean quadrantal errors of sensitivity calculated for each of the sides and for the mean sensitivity values are given in Table 3.

It is evident from the data listed in Table 3 that the mean quadrantal error of sensitivity does not exceed 2.1%. The mean quadrantal error calculated for sensitivity values (the average for two sides) on all tested balancometers is 1.2%.

The distribution of remaining errors is as follows: errors not exceeding σ constitute 78%, those not exceeding 2σ , 95% and those not exceeding 3σ , 100% of all the errors involved.

Thus, accidental errors in determining conversion factors of balancometer-galvanometer couples and in determining balancometer sensitivity have one and the same order.

Balancometer conversion factors were determined for natural conditions during the expedition on Lake Sevan in September, 1957. The testing of the devices both with and without installations was repeated ten times. Because of the large amount of work involved in testing under natural conditions the conversion factors were determined for only one of the sides (No. 1) of each balancometer.

The mean conversion factor values obtained as a result of 10 tests in natural conditions in an installation and the mean quadran-

tal errors of a number of them are listed in Table 4.

From the data given in Table 4 it is evident that the mean quadrantal errors in the determination of conversion factors under natural conditions in an installation do not exceed 2.3%. The mean quadrantal error calculated from the results of tests on all balancometers (repeated 60 times) is 1.6%. The distribution of remaining errors is as follows: errors, not exceeding σ , constitute 82%, those not exceeding 2σ , 95% and those not exceeding 3σ , 100% of all the errors involved.

In determining balancometer conversion factors under natural conditions without an installation the test was conducted with the sun at an altitude of not less than 40° . The balancometers were placed so that their detection surfaces were horizontal and the handle would be directed toward the side away from the sun. The wind velocity during the test varied from 0 to 3 meters per second. The wind was intermittent.

From the data given in Table 5 it is evident that the mean quadrantal error does not exceed 2.3%. The mean quadrantal error calculated from the results of all balancometer tests is 1.7%. The distribution of remaining error is as follows: errors, not exceeding σ , constitute 80%, those not exceeding 2σ , 98% and those not exceeding 3σ , 100% of all the errors involved.

The mean conversion factor ^{VALUES} for side No. 1 and the mean quadrantal errors obtained in the determination of conversion factors by different methods are given in Table 6.

Table 4

Mean conversion factor a values and mean quadrantal errors σ (%) obtained in testing under natural conditions in an installation

Instrument No.	$\frac{3413}{37}$	$\frac{3429}{37}$	$\frac{3142}{1178}$	$\frac{3324}{1178}$	$\frac{3136}{781}$	$\frac{3169}{781}$
a	0,0140	0,0137	0,0164	0,0149	0,0181	0,0163
σ	1,1	0,9	2,3	1,0	1,6	2,0

Table 5

Mean conversion factor a values and mean quadrantal errors σ (%) obtained in testing under natural conditions without an installation

Instrument No.	$\frac{3413}{37}$	$\frac{3429}{37}$	$\frac{3142}{1178}$	$\frac{3324}{1178}$	$\frac{3136}{781}$	$\frac{3169}{781}$
a	0,0141	0,0137	0,0163	0,0149	0,0182	0,0162
σ	1,6	1,8	1,3	1,3	1,5	2,3

Table 6

Balancometer conversion factors obtained by various methods and the mean quadrantal errors σ , %

Method	Instrument No.						σ
	$\frac{3413}{37}$	$\frac{3429}{37}$	$\frac{3142}{1178}$	$\frac{3324}{1178}$	$\frac{3136}{781}$	$\frac{3169}{781}$	
In the laboratory	0,0140	0,0138	0,0162	0,0150	0,0184	0,0166	1,2
Under field conditions	0,0140	0,0137	0,0164	0,0149	0,0181	0,0163	1,6
{ in the in-	0,0141	0,0137	0,0163	0,0149	0,0182	0,0162	1,7
{ stallation							
{ without the							
{ installation							

The compounding of mean conversion factor values determined by different methods (Table 6) indicates that divergence between values determined by different methods is within the limits of accidental error and does not have a definite sign. This confirms the possibility of testing devices by any one of the demonstrated methods. The smallest accidental error value was obtained while testing under laboratory conditions as might be expected since radiation currents under laboratory conditions are more constant. It must be remembered that in testing in the laboratory 10 pair of comparative readings were taken, while under natural conditions 20 pair were taken. In testing under natural conditions without an installation one reading was understood as being the average of three readings taken one immediately after the other as is the custom in observation.

For evaluation of accidental error in the individual balancometer readings for each balancometer, the mean quadrantal error of the conversion factor determined by one pair of balancometer readings (in sun, in shade) is calculated. The values obtained are given in Table 7.

The distribution of remaining individual reading errors in conversion factor determination which were calculated from test results on all balancometers is given in Table 8.

The compounding of magnitudes of errors, given in Table 7, indicates that individual reading error in conversion factor determination under laboratory conditions is considerably less than individual reading error under natural conditions. Thus, it proves the necessity of taking a large number of readings in testing under natural conditions if an installation is not used for testing.

Table 7

Mean quadrantal errors of the individual reading in determining the conversion factor, %

Method	Instrument No.						σ_{cp}
	3413 37	3429 37	3142 1178	3324 1178	3136 781	3169 781	
In the laboratory	1,7	1,4	1,0	1,4	0,9	1,3	1,3
Under field conditions { in the installation	2,5	2,4	2,9	2,4	2,9	2,9	2,7
without the installation	3,2	3,4	3,8	3,2	3,3	4,3	3,5

Table 8

Distribution of remaining errors of the individual reading in determining the conversion factor, %

Method	Not exceeding			No. of cases
	σ	2σ	3σ	
In the laboratory	78	97	100	600
Under field conditions { in the installation	81	98	100	1200
without the installation	81	97	99	1203

The distribution of remaining errors given in Table 8 indicates that practically all deviations do not exceed double the mean quadrantal error which in testing under laboratory conditions is 2.6%, in testing under natural conditions in an installation, 5.4% and in testing under natural conditions without an installation, 7%. Thus, in determining balancometer conversion factors, values differing from the mean value by more than 26 should be disregarded.

BALANCOMETER SENSITIVITY DEPENDANCE ON RADIATION INTENSITY

In studying balancometer sensitivity dependance on radiation intensity for 4 balancometers, the sensitivity was determined at radiation intensities of 1.5, 0.75 and 0.15 cal/cm² per minute. The source of radiation was a 1000 kilowatt projector lamp and the flow of radiation was condensed by means of two lenses. The intensity of the radiation was varied by means of a rotating disc with sectors removed. This disc was proposed by B. A. Eisenstadt (2).

Balancometer sensitivity determination was carried out by the method ordinarily used in testing with one exception: that illumination of the devices was effected by means of a nonparallel beam. In the installation used in TS.L.P. for device testing, the intensity of parallel beams of radiation obtained from 1000 watt lamps is 0.6-0.7 cal/cm² per minute. In order to obtain larger radiation intensity values pencils of light were created. This led to the fact that surface illumination of the balancometer was uneven; the intensity diminished toward the edges. Because of this, the mean intensity values of the radiation striking the surface of the balancometer and actinometer are not identical and the absolute balancometer sensitivity values do not precisely correspond to the true values. However, since illumination distribution in a given experiment remains constant, it is possible to compound the sensitivity values

obtained with different radiation intensity values. With each radiation intensity value, the sensitivity of the balancometer was determined three times during which time the mounting of the balancometer and actinometer on the rotary table of the installation remained unchanged. The balancometer sensitivity values in millivolts at 1 cal/cm² per minute obtained with radiation intensities of 1.5, 0.75, and 0.15 cal/cm² per minute are given in Table 9..

It is evident from the data given in Table 9 that divergences in balancometer sensitivity values obtained with different radiation values are found to be within the limits of magnitude of accidental errors in measuring. Therefore, it can be assumed that within radiation intensity limits from 0.15 to 1.5 cal/cm² per minute, balancometer sensitivity does not depend on radiation intensity.

In addition, the sensitivities of three balancometers (No. 3324, 3142 and 3169) at radiation intensities of 0.3 and 3 cal/cm² per minute were compared. It appeared from this that with an increase of radiation intensity, balancometer sensitivity increases. If balancometer sensitivity at a radiation intensity of 0.3 cal/cm² per minute is taken to be 100%, the sensitivity of balancometer No. 3324 at a radiation of 3 cal/cm² per minute increased by 5%, of balancometer No. 3142, 2% and that of balancometer No. 3169, 6%. The results obtained contradict the theoretical calculations of K. Y. Kondratiev (3) according to which balancometer sensitivity diminishes with radiation balance increase.

Table 9

Balancometer sensitivity in millivolts at 1 cal/cm^2 per minute with different values of radiation intensity

Instrument No.	Radiation intensity, $\text{cal/cm}^2\text{-min}$		
	1,5	0,75	0,15
3324	7,04	6,94	6,93
	7,06	6,95	6,93
	7,04	6,96	6,88
	average 7,05	6,95	6,91
3142	6,81	6,78	6,92
	6,85	6,81	7,02
	6,86	6,84	6,88
	average 6,84	6,81	6,94
3169	9,32	9,16	9,14
	9,32	9,21	9,14
	9,30	9,20	9,15
	average 9,31	9,19	9,14
3429	6,70	6,67	6,71
	6,69	6,64	6,68
	6,68	6,58	6,72
	average 6,69	6,63	6,70

BALANCOMETER SENSITIVITY DEPENDANCE ON DIRECTION OF INCIDENTAL RADIATION

Balancometer sensitivity dependance on the direction of incidental radiation was investigated under laboratory conditions.

The correction factors for balancometer *INDICATIONS* at various angles of incidence were determined for 6 balancometers. In this case the balancometers were installed so that at an angle of incidence of 90° (at an elevation of the sun of 0°), the handle of the balancometer was directed toward the side opposite to the source of light. The correction factors were determined twice. In addition, for one of the balancometers (No. 3169), the correction factors for dependance on direction of incidental radiation were determined also by rotating the balancometer over the azimuth by 90° .

The correction factor values obtained for dependance on the elevation of the sun are given in Table 10. The correction factors for balancometer No. 3169, determined for two azimuths differing by 90°, are listed in the last two lines of Table 10.

From the data given in Table 10 it is evident that balancometer sensitivity depends on the direction of incidental radiation; here the correction factor for exposures of the balancometer is always greater than unity. Sensitivity dependance on the direction of incident radiation is given for elevations of the sun of 50° or less,

therefore, for all practical purposes, ^{INDICATIONS} of the balancometer are always somewhat ^{LOWERED}. The data obtained confirm the inexpediency of measurement with an unshaded balancometer, especially at small elevations of the sun.

Table 10

Correction factors for indications of the balancometer depending on the elevation of the sun

Instrument No.	Sun's altitude, degrees								Remarks
	2,5	5	10	20	30	40	50	70	
3413	1,86	1,17	1,15	1,09	1,06	1,05	1,03	1,00	
3429	1,20	1,18	1,11	1,06	1,02	1,02	1,02	1,00	
3142	1,19	1,16	1,08	1,04	1,03	1,02	1,02	1,01	
3324	1,26	1,20	1,17	1,08	1,06	1,04	1,02	1,00	
3136	1,73	1,28	1,12	1,05	1,03	1,02	1,01	1,00	
3169	1,45	1,28	1,18	1,08	1,04	1,02	1,01	1,00	
3169	1,50	1,41	1,17	1,06	1,02	1,01	1,00	1,00	Rotated along the azimuth by 90°

ERRORS IN WIND CORRECTION FACTOR DETERMINATION

For the evaluation of accidental errors of wind correction factors, The factors were determined in a wind tunnel ten times for 7 balanco-meters. In this case the correction factors were determined for each of the sides for two of the balancometers, for the others, over one side as required by the Manual.

The mean wind correction factor values at wind velocities of 1, 5, 10 and 15 meters per second are given in Table 11. In Table 12 the mean quadrantal error of correction factor determination at wind speeds of 5, 10 and 15 meter/second, expressed in percent of correc-tion factor size are listed.

Table 11

Mean values of wind correction factors

Instrument No.	Velocity, m/sec			
	1	5	10	15
3413	1,02	1,09	1,17	1,24
3429 (сторона 1)	1,02	1,06	1,11	1,16
3429 (" 2)	1,02	1,08	1,14	1,21
3142 (" 1)	1,04	1,16	1,28	1,38
3142 (" 2)	1,04	1,16	1,29	1,39
3324	1,02	1,08	1,15	1,22
3136	1,02	1,10	1,19	1,27
3169	1,02	1,11	1,20	1,27
3204	1,02	1,07	1,12	1,17

The mean quadrantal errors, calculated from all balancometer test results, are: 0.01 (1.3%) for a wind speed of 5 meters per second, 0.02 (1.7%) for a wind speed of 10 meters per second, and 0.2 (1.7%) for a wind speed of 15 meters per second.

The distribution of remaining errors is as follows: for a wind speed of 5 meters per second, the errors not exceeding σ constitute 73%, those not exceeding 2σ , 100%; for a wind speed of 10 meters per second, the errors not exceeding σ constitute 79% and those not exceeding 2σ , 100%; for a wind speed of 15 meters per second, errors

Table 12

Mean quadrantal errors of wind correction factors of balancometers (%) at
at wind speeds of 5, 10 and 15 meters per second

Instrument No.	velocity, m/sec		
	5	10	15
3413	1,3	1,8	1,9
3429	1,3	2,0	1,8
3142	1,3	1,7	1,8
3324	0,7	1,5	1,6
3136	1,8	2,1	2,0
3169	1,3	1,5	1,4
3204	1,2	1,5	1,5

not exceeding σ , constitute 80%, those not exceeding 2σ , 98% and those not exceeding 3σ , 100%.

The correction factors were determined for each of the sides for balancometers No. 3429 and 3142. According to the data listed in Table 11 it is evident that the correction factors for both sides of balancometer No. 3142 practically coincide while for balancometer No. 3429 they differ by 0.05 (4%) at a wind velocity of 15 meters per second. It must be noted that the sensitivities of the sides of balancometer No. 3142 differ by 10% while the sensitivities of the

sides of balancometer No. 3429 differ by no more than 1.5%.

The results outlined above were obtained for wind tunnel conditions in which the balancometer was installed (by eye) so that the detecting surfaces were parallel to the airflow; at the same time the detecting surfaces were located vertically and illuminated from the side.

As is known, balancometer ^{INDICATIONS} under natural wind conditions are very unstable and as a result it is possible to determine correction factors under natural conditions only from a large number of readings. The compounding of wind correction factors in determining them under natural conditions and in the wind tunnel (4) indicated that the mean correction factor values obtained from a large number of determinations made under natural conditions correspond well with the values obtained in wind tunnel testing. One of the causes of balancometer ^{INDICATION} inconstancy at the same wind velocity may be a difference in the degree of air turbulence and the fact that the air flow is not always directly parallelly to the detecting surfaces of the balancometer, but strikes them at different angles.

In order to evaluate the influence of the direction of the air flow striking the balancometer, wind correction factors were determined for three balancometers with different orientations of the balancometer in the air current of the wind tunnel. The detection surfaces of the balancometers were situated in the airflow at different angles of attack so that the current of air was directed first on the dark and then on the illuminated detection surface. The correction factors were determined at angles of incidence of 2, 5, 10 and 30°. In these experiments the balancometers No. 3413 and 3324 were arranged so that their detection surfaces were always situated

in vertical planes and illuminated from the side. However, balancometer No. 3572 was first situated horizontally and then tilted depending on the angle of incidence chosen. It was illuminated from above. In addition, the correction factors for balancometer No. 3572 at 0° angle of incidence were determined with the detection surfaces in a vertical position (as is done in ordinary testing).

Wind correction factors for balancometer ^{INDICATIONS} at different angles of incidence and with air current velocities of 2, 5, 10 and 15 meters per second are given in Table 13. On the last line of Table 13 the correction factors

for balancometer No. 3572 when the detection surfaces are placed vertically are given.

Graphs of wind correction factors for balancometer No. 3324 at different orientations in the air flow are given in Figure 1. For better visualization, the curves obtained with different angles of incidence are drawn on the general coordinates of the axis. The speed of the air flow in meters per second is drawn along the abscissa axis and the correction factors along the ordinate axis. The curves for cases where the air current was directed on the illuminated side of the balancometer are represented by broken lines. The curves for cases where the air flow was directed upon the nonilluminated side of the balancometer are represented by broken lines with dots. The curve for the case where the balancometer is located lengthwise with the flow is represented by a solid line (from the average value of ten testings)

The results given in Table 13 and in the graphs (Fig. 1) indicate

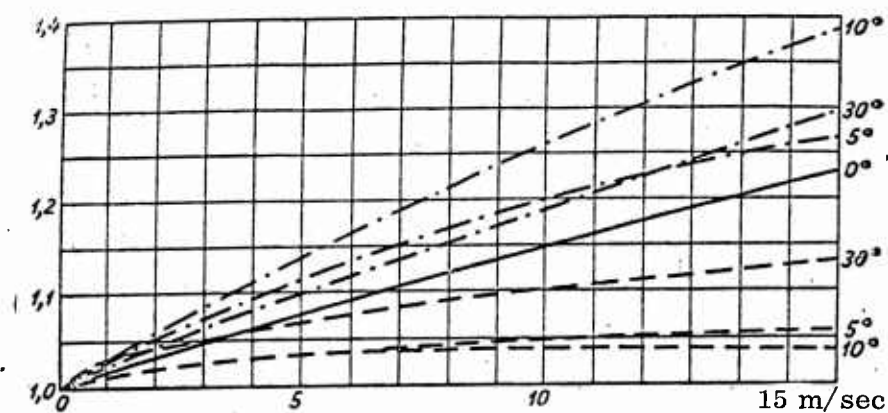


Fig. 1. The wind correction factors for balancometer No. 3324 at different orientations in the flow of air

Table 13

Wind correction factors of balancometers

Instrument No.	Incidence angle degrees	Stream velocity (m/sec), directed to the side							
		illuminated				dark			
		2	5	10	15	2	5	10	15
3413	0	1,04	1,09	1,17	1,24				
	2	1,04	1,09	1,16	1,21	1,03	1,07	1,12	1,16
	5	1,04	1,09	1,16	1,22	1,02	1,02	1,02	1,02
	10	1,06	1,14	1,26	1,35	1,02	1,05	1,08	1,09
	30	1,06	1,13	1,23	1,30	1,05	1,10	1,12	1,13
3324	0	1,03	1,08	1,15	1,22				
	5	1,05	1,12	1,20	1,26	1,02	1,04	1,05	1,06
	10	1,06	1,14	1,26	1,37	1,02	1,03	1,04	1,04
	30	1,04	1,10	1,19	1,28	1,05	1,08	1,11	1,13
3572	0	1,03	1,07	1,14	1,21				
	5	1,06	1,13	1,22	1,26	1,02	1,04	1,05	1,07
	10	1,08	1,16	1,28	1,36	1,03	1,06	1,09	1,11
	28	1,04	1,08	1,14	1,19	1,04	1,07	1,12	1,15
	0	1,04	1,09	1,17	1,23				

that wind correction factors depend essentially on the orientation of the balancometer in the air current.

The correction factors are decreased if the flow of air is directed on the illuminated side of the balancometer and are increased if it is directed upon the nonilluminated side. This indicates that the side opposite to the one upon which the flow of air is directed, i.e., the side upon which the turbulent air flow strikes is cooled to a greater degree. The maximum correction factor values were observed at angles of incidence of 10° , the minimum values at angles of incidence of 5° and 10° . At an angle of incidence of 10° depending on whether the air flow is directed on the illuminated or the non-illuminated side, the correction factors differ by 8 to 10% at an air current velocity of 5 meters per second and by 15 to 19% at an air current velocity of 10 meters per second. Thus, the large variations in balancometer **INDICATIONS** observed under natural conditions may be partially attributed to the fact that the balancometer is subjected to the action of randomly directed air currents. However, balancometer **INDICATION** variation may not be caused entirely by variance of the airflow striking the balancometer because, in testing with an installation where the balancometer is protected from wind influence, the mean quadrantal error of the individual reading (Table 7) also has a large value.

Correction factors obtained at angles of incidence of 2° differ only slightly from those obtained in an installation with the balancometer lengthwise to the current. It is possible by this to explain the comparatively small differences in correction factor values obtained

in repeated testing of balancometers installed along the current by sight.

The results given in Table 13 for balancometer No. 3572 for an angle of incidence of 0° indicate that the correction factors obtained with horizontal and vertical positioning of the detection surfaces practically coincide.

BALANCOMETER SENSITIVITY DEPENDANCE ON TEMPERATURE

Balancometer sensitivity dependance on the temperature of the medium has already been studied (5) for three balancometers in which the space between the detection plates and thermobattery was filled with rosin. It was established that balancometer sensitivity increases with a rise in temperature. At the present time, shellac instead of rosin is used in the manufacture of balancometers. It was useful to study these balancometers by the relationship of temperature coefficient of their sensitivities.

The temperature coefficients of balancometer sensitivities were determined within a temperature range of 3 to 48° according to the methods described in the treatise (5). Here two balancometers filled with rosin (Nos. 3136 and 3169), for which the temperature coefficients had been previously determined, and two balancometers filled with shellac (Nos. 3324 and 3429) were taken. The results of determinations on the temperature coefficients of sensitivity are given in Table 14.

The data given in Table 14 confirms the temperature coefficient values obtained previously for balancometers filled with rosin. For

Table 14

Results of determining the temperature coefficient of balancometer sensitivity

Date	Instrument No.			
	3136	3169	3324	3429
25 II	0,0009	0,0014	0,0008	-0,0001
26 III	0,0009	0,0014	0,0006	-0,0002
6 III	0,0013		0,0015	0,0000
18 III			0,0012	+0,0003
Average	0,0010	0,0014	0,0010	0,0000

balancometers filled with shellac, the temperature coefficient obtained for the sensitivity of balancometer No. 3324 is of the same order as that for balancometers filled with rosin. Balancometer No. 3429, on the other hand, does not have a temperature coefficient.

CONCLUSIONS

1. Balancometer conversion factors obtained by repeated testings under laboratory and natural conditions (by two methods) coincide very well. This confirms the possibility of conversion factor determination by any one of the three methods recommended by the Manual for testing meteorological devices.

2. It is suitable to test balancometers under laboratory conditions because here accidental errors of the conversion factor have a smaller value. This method also requires less work.

The mean quadrantal error in conversion factor determination is 1.2% in testing under laboratory conditions, 1.6% in testing under natural conditions with an installation and 1.7% in testing under natural conditions without an installation.

3. The mean quadrantal error of each individual reading in balancometer testing is 1.3% in testing under laboratory conditions, 2.7% under natural conditions with an installation and 3.5% under natural conditions without an installation.

The large accidental error values of individual readings in testing balancometers under natural conditions confirm the necessity of performing a large number of comparative readings (not less than 20 pair).

4. Within the limits of radiation balance magnitudes, encountered under natural conditions, balancometer sensitivity does not depend on the magnitude of measured radiation balance.

5. Balancometer sensitivity depends on the direction of the incident radiation: with increasing angle of incidence balancometer sensitivity decreases. In connection with this, the value of the radiation balance, measured by a balancometer, is always lowered. In measuring with unshaded balancometers it is necessary to introduce correction factors individual for each balancometer.

6. The mean quadrantal error in determining wind correction factors in a wind tunnel is 1.3% at an air flow velocity of 5 meters per second and 1.7% at an air flow velocity of 10 and 15 meters per second.

Balancometer ^{INDICATIONS} in wind depend essentially on the direction of the air currents striking the balancometer. Therefore, the correction factors obtained in the wind tunnel are applicable only for correcting averaged balancometer ^{INDICATIONS}

BIBLIOGRAPHY

1. MANUAL FOR TESTING METEOROLOGICAL DEVICES. Gidrometeoizdat, L. 1956
2. Eisenstadt, B. A., NEW METHOD OF MEASURING RADIATION BALANCE.

Transactions of T.G.O., 13th issue, 1957

3. Kondratiev, K. Y., RADIANT HEAT EXCHANGE IN THE ATMOSPHERE.

Gidrometeoizdat, L., 1956

4. Pokrovskaya, I. A., METHOD OF DETERMINING CORRECTION FACTORS TAKING INTO ACCOUNT WIND INFLUENCE ON THE EXPOSURES OF THERMO-ELECTRIC BALANCOMETERS AND EFFECTIVE PIRANOMETERS.

Transactions of GGO, 43rd issue, 1954.

5. Pokrovskaya, I. A., TEMPERATURE COEFFICIENTS OF NETWORK ACTINOMETRIC DEVICES.

Transactions of GGO, 46th issue, 1955.

FTD-TT-62-500/172

CONTENTS

P. V. Diachenko. EXPERIENCE IN APPLYING STATISTICAL MATHEMATICS
METHODS IN THE STUDY OF THE MICROSTRUCTURE OF FOGS, MISTS AND
CLOUDS.

P. V. Diachenko, A. I. Kamenieva. RESULTS OF WIND TUNNEL STUDIES
AT THE CHIEF GEOPHYSICAL OBSERVATORY.

A. I. Kamenieva. ON THE TESTING OF HAND ANEMOMETERS UNDER FACTORY
CONDITIONS.

I. A. Pokrovskaya. ERRORS IN TESTING THERMOELECTRIC BALANCOMETERS.

DISTRIBUTION LIST

DEPARTMENT OF DEFENSE	Nr. Copies	MAJOR AIR COMMANDS	Nr. Copies
		AFSC	
		SCFTR	1
		ARO	1
HEADQUARTERS USAF		ASTIA	10
		TD-B1a	3
AFCIN-3D2	1	TD-B1b	3
		AEDC (AEY)	1
		SSD (SSF)	2
OTHER AGENCIES		APGC (PGF)	1
		ESD (ESY)	1
		RADC (RAY)	1
CIA	1	AFSWC (SWF)	1
NSA	2	AFMTC (MTW)	1
AID	2	AFMDC (MDF)	1
OTS	2		
AEC	2		
PWS	1		
RAND	1		

UNCLASSIFIED

UNCLASSIFIED